The Paraventricular Nucleus of the Hypothalamus and its Role in Energy Homeostasis

by
Ian Enrique Gonzalez

A dissertation submitted in partial fulfilment
of the requirements for the degree of
Doctor of Philosophy
(Molecular and Integrative Physiology)
in the University of Michigan
2021

Doctoral Committee:

Professor David P. Olson (Co-chair)
Professor Martin G. Myers Jr. (Co-chair)
Professor Carol Elias
Professor Audrey Seasholtz
Professor Randy Seeley

Ian Enrique Gonzalez

igonzale@umich.edu

ORCID id: 0000-0002-4571-909X

Dedication

To my parents, Chantal and Jorge, for their loving support and my brother Lucas for his friendship and for keeping me motivated.

Acknowledgements

Thank you to my mentors Dave and Martin. David Olson has been incredibly supportive during my graduate training and instrumental in my development as a scientist. Whether it is designing an experiment or writing a grant, Dave has provided invaluable input and is largely responsible for my success. Thank you to my co-mentor Martin Myers Jr. who was influential in my becoming a research scientist. Martin's laboratory was the first laboratory I had joined and it has been thanks to his continuous support that I can confidently continue my career in the sciences.

I want to thank the current and past members of the Olson laboratory, whose support I would not have been successful without. Thank you Jessica Adams, Allen Zhu, Hongjuan Pei, Chunxia Lu, Latrice Falkner, Gizem Kurt and Aristides Diamant for your friendship and support during my graduate training. Thank you to Amy Sutton, who was a mentor early in my graduate career and continues to be a valuable collaborator in several of my projects. Thank you to Julliana Ramirez-Matias, who made a large contribution to and was crucial to the completion of several of my projects and whom I wish great success in their medical career.

Thank you to my collaborators in the Myers lab for your advice and expertise. A special thanks to Andrew Cheng for his collaboration on the CalcR project as well as his friendship and advice on navigating a graduate career. Thank you to Warren Pan for generating the CalcR-Cre mice used in many of my studies and for your help during my

prelims. Also thank you to Christa Patterson Polidori and Gina Leinninger for your mentorship and guidance during my undergraduate career.

Thank you to Melanie Schmitt, Lauren Benson, Zhe Wu and Nathan Qi of the Animal Phenotyping Core for the extensive collaborations on my projects. Without your work on the weekends and after hours, these projects could not have been completed.

I would like to thank my funding sources during my graduate training: Ruth L. Kirschstein National Research Service Award (F31-DK122753-01), National Institutes of Health; Systems and Integrative Biology Training Grant (T32-GM008322), National Institutes of Health.

Thank you to my committee members for your support and time: Dr. Audrey Seasholtz, Dr. Carol Elias, Dr. Randy Seeley as well as my co-chairs Dr. Martin Myers Jr. and Dr. David Olson.

Thank you to the Molecular and Integrative Physiology Department of the University of Michigan for your resources and time and making my graduate career possible. Thank you to Sue Mentor, Dan Michele and Susan Herzog for helping me navigate my graduate training and thank you to Michele Boggs for your administrative support.

Thank you to my MIP PhD cohort including Ally, Jon, Liz, Natalie and Thomas for your friendship and support both in and out of class. I greatly enjoyed hanging out after lab and I am proud to have marched with many of you for the several causes we believe in. Thank you to Diane Fingar and the Fingar lab for helping me towards my graduate

career. I also want to thank Malcolm Low and my friends of the Low Lab including Graham Jones, Zoe Thompson, Yusif Kunji and Kavaljit Chhabra.

Finally, I want to thank my family, Chantal, Jorge and Lucas for your unwavering support during my graduate career and beyond. I would also like to thank my friends JJ, Colin, Anabel, Jenny, Alyssa, Autumn, Mo, Stef, Andrew, and Lai, as well as many others. Many of you inspire me to strive for success and to constantly improve both as a scientist and as a person.

Table of Contents

List of Tables

Table:

List of Figures

Figure:

Abstract

Obesity and its comorbidities are a significant threat to public health, necessitating the development of new therapies to treat and prevent obesity. Body weight is maintained by balancing food intake and energy expenditure, a process mediated by the central nervous system (CNS). The paraventricular nucleus of the hypothalamus (PVH) is a crucial component of the CNS maintenance of energy balance; lesioning the PVH or disrupting its development produces hyperphagia and energy expenditure deficits in rodents and humans. The PVH is a heterogenous nucleus with many neuronal populations that may regulate energy homeostasis differently. To interrogate these neuronal populations, we used Cre-dependent viral tools to chemogenetically activate or to silence neuronal populations of the PVH. We used genetically engineered mice and immunohistochemistry to identify the overlap of subpopulations of the PVH as well as retrograde and anterograde tracing to determine the inputs and outputs of the PVH.

Insulin receptor substrate-4 (IRS4) and insulin receptor substrate-2 proteins act synergistically in the hypothalamus to maintain energy balance. Our in situ hybridization studies determined that IRS4 is expressed in the PVH, prompting us to investigate $IRS4^{PVH}$ neurons and their role in energy balance. The $IRS4^{PVH}$ neuronal population is distinct from oxytocin (OXT), nitric oxide synthase (NOS1), melanocortin 4-receptor

(MC4R) and prodynorphin (PDYN) neurons, all of which regulate energy balance. We found that activating IRS4^{PVH} neurons suppresses feeding and increases energy expenditure, while silencing IRS4^{PVH} neurons results in hyperphagic obesity. IRS4^{PVH} neurons project to regions of the hindbrain necessary for energy homeostasis such as the parabrachial nucleus (PBN), solitary nucleus (NTS), median eminence and the intermediolateral column of the spinal cord. The IRS4^{PVH} neurons are innervated by brain regions such as the lateral hypothalamic area, ventromedial hypothalamus, amygdala, supraoptic nucleus, bed nucleus of the stria terminalis, preoptic area, arcuate nucleus and PBN. We therefore determined that PVH and peri-PVH neurons expressing IRS4 regulate energy homeostasis.

Although we determined that calcitonin receptor (CalcR) expression in the PVH is not required for energy balance or the anorectic response to the salmon calcitonin ligand, we did find that CalcR^{PVH} neuron activity is important in energy homeostasis. Using chemogenetic activation and tetanus toxin mediated silencing of CalcR^{PVH} neurons, we determined that activating CalcR^{PVH} neurons suppresses feeding and increases ambulatory activity, while silencing CalcR^{PVH} neurons results in hyperphagic weight gain. CalcR^{PVH} neurons project to regions involved in regulating energy homeostasis such as the PBN, NTS and median eminence. CalcR^{PVH} neurons are distinct from many of the neuronal populations of the PVH that regulate energy balance such as those that express NOS1, arginine vasopressin, OXT and thyrotropin-releasing hormone with some overlap with corticotrophin-releasing hormone expressing PVH neurons. There is a notable overlap between the MC4R expressing PVH neurons and CalcR^{PVH} neurons, which may account for the hyperphagic obesity observed when

CalcR^{PVH} neurons are silenced. In addition, deleting MC4R from CalcR cells produced hyperphagic obesity in male and female mice. Lastly, we aimed to elucidate the roles that specific projection fields of PVH neurons play in energy homeostasis. Using a retrograde AAV-Cre and chemogenetics, we have begun to parse the energy balance roles of PVH neurons that project to the PBN and NTS specifically. Overall, our studies have improved our understanding of the roles specific PVH neurons play in energy homeostasis and the neuronal circuits in which they exert their effects.

Chapter 1

Introduction: Central Mechanisms of Energy Balance Control

The obesity epidemic is a growing problem in the United States, with 2013-2014 estimates indicating a prevalence of obesity of approximately 35% for adult males and 40.4% for adult females in the US. Comorbid diseases such as type 2 diabetes mellitus, hypertension, cardiovascular disease and stroke have seen significant increases as well.[1] Further, healthcare costs associated with obesity were estimated to be $149.4 billion in 2014.[2] To manage this widespread metabolic disease, anti-obesity agents have been developed and studied for their therapeutic value, many of them targeting the central nervous system (CNS), the gastrointestinal system and other systems that influence hormonal release and the resting metabolic rate.[3] A particular target of interest of the CNS is the hypothalamus, which is essential for the regulation of energy homeostasis and food intake through its interaction with peripheral signals such as leptin, insulin and ghrelin and its neural circuitry.[4,5] Therefore, several pharmacological agents have been developed to target signaling systems within the CNS, including those found within the hypothalamus.

There are currently many medications and treatments created for the purpose of managing obesity through the CNS. Lorcaserin was a weight loss drug that reduced appetite through the activation of the serotonin 2C ($5HT_{2C}$) receptor.[6-8] Although it was effective over long-term treatment, lorcaserin had several side effects including

headaches, fatigue, nausea and dizziness.[3,7,9,10] It was eventually removed from the market at the request of the FDA in February 2020 due to increased incidence of pancreatic, colorectal and lung cancers in clinical trials.[11]

Liraglutide is an injectable treatment that acts as a glucagon-like peptide-1 receptor agonist that increases insulin release from the pancreas and reduces glucagon release and serves as an anorectic as well as a treatment for type 2 diabetes.[12-14] This treatment is effective in producing sustained weight loss for about 2 years and is recommended for patients with at least a body mass index (BMI) of 30 kg/m^2 or in individuals with at least a BMI of 27kg/m^2 and another weight related comorbid disease.[13] In addition to causing abdominal pain, nausea, constipation, and diarrhea, liraglutide may increase chances of developing pancreatitis, gallbladder disease and potentially carcinoma of the thyroid.[13,15]

There are also several treatments that require a combination of drugs in order to improve their effectiveness as a weight loss treatment. One such combined treatment includes phentermine, which reduces appetite, and topiramate which is typically used to treat seizures and migraine headaches.[3,16,17] The phentermine/topiramate-extended release (ER) combined treatment functions as a noradrenergic and gamma aminobutyric acid (GABA) receptor activator and a kainite/α-amino-3-hydroxy-5-methyl-4-isoxazolepropionic acid glutamate receptor inhibitor to suppress appetite.[3,18,19] Aside from producing side effects such as constipation, dizziness and insomnia, this treatment is contraindicated for individuals with glaucoma or hyperthyroidism and can cause metabolic acidosis, hypokalemia and elevated creatinine levels.[3,20] Furthermore, women

who are pregnant run the risk of their child developing birth defects such as oral clefts if they take the phentermine/topiramate-ER combined treatment.[21]

Another obesity treatment combines naltrexone, which is typically used to treat alcohol and drug dependence and bupropion, which is used to treat depression.[22-24] Naltrexone is a competitive agonist of the μ-opioid receptor, the κ-opioid receptor and bupropion is a selective serotonin reuptake inhibitor.[25,26] Bupropion stimulates neurons that reduce appetite in the hypothalamus. These neurons release beta-endorphins, which reduce anorexigenic effects of bupropion. Naltrexone enhances the effects of bupropion, as it blocks beta-endorphin, producing a synergistic reduction in food intake.[27] Side effects for this treatment include nausea, constipation, diarrhea, increased blood pressure, heart rate and insomnia and possible liver damage, as well as a potential increase in suicidal thoughts.[25,26] Further, the effectiveness of this therapy appears to reduce after one year of treatment.[28]

Recombinant human leptin or metreleptin is an effective leptin replacement in the rare individuals that experience hyperphagic obesity due to leptin deficiency.[29-31] Metreleptin monotherapy for patients that exhibit non-leptin deficient obesity is ineffective for generating weight loss.[32] When metreleptin is combined with the amylin analog pramlintide, obese patients experience increased satiation, reduced feeding and a loss in body weight with only mild to moderate nausea.[33-37] However, the synergy between metreleptin and pramlintide loses efficiency in individuals that exceed a body mass index of 35 kg/m^2.[38] It is suggested through studies in rats that this may be the result of increased leptin resistance in obese individuals and that the threshold for amylin-induced leptin sensitization is greatly increased.[38]

While it would be ideal for treatments to engage with specific hypothalamic targets, most drugs act more broadly and current treatments are either ineffective for many patients or have several aversive side effects that interfere with patient compliance or pose a threat to the wellbeing of the patient. It is therefore necessary to continue to investigate hypothalamic nuclei and their related neurocircuitry to aid in the development of other possible therapeutics that more effectively maintain energy homeostasis without producing excessive or dangerous off target effects.

Role of the hypothalamic circuits and the regulation of energy homeostasis

Feeding behavior and energy expenditure is regulated through a variety of redundant neuronal systems within the hypothalamus and brainstem which serve to maintain energy homeostasis.[39] The hypothalamus receives and incorporates nutrient signals, satiety signals from the gut and signals from energy stores to balance food intake and energy expenditure in order to maintain sufficient body fat storage.[4] Overeating when energy stores are sufficient results in enhanced satiety and an inhibition of the food reward system, resulting in a reduction in feeding behavior. Conversely, when energy stores are insufficient, the hypothalamus responds by promoting the food reward system and decreasing the response to satiety signals, resulting in an increase in feeding behavior.[40,41] The energy homeostatic feeding mechanisms to maintain body weight have been evolutionarily conserved, as it is crucial to survival to sustain energy stores. In contrast, non-homeostatic feeding is driven by the consumption of palatable foods which is mediated by the midbrain dopamine and opioidergic food reward pathways. [42] Palatable foods are typically those that have a

preferred or desirable taste and are often high in fat or carbohydrate content, which can promote overconsumption due to activation of food reward pathways.[43,44] Systems have evolved to produce strong drives and a reward system in favor of food consumption, which can lead to excessive eating in environments with an abundant food source.[45] In addition to regulating feeding behavior, the hypothalamus regulates energy expenditure through influencing the autonomic nervous system and the endocrine system through the hindbrain, spinal cord and pituitary. The hypothalamus serves to modulate the basal metabolic rate, thermogenesis, spontaneous physical activity and exercise in order to counterbalance the intake of food.[39,46,47] In essence, the body is continuously working through the hypothalamus to balance energy intake against energy that is expended.

Energy homeostasis is achieved CNS monitoring of peripheral signals that inform the brain of current energy stores and in turn regulating feeding behavior as well as energy expenditure.[4,5] One of the best characterized peripheral energy status signals is the hormone leptin, which is released from adipose tissue in proportion to body fat and mediates energy homeostasis through the brain by regulating food intake and body weight.[48-53] This regulation based on current adiposity stores is called “adiposity negative feedback”.[48] Insulin, which is a hormone secreted from the pancreas, also regulates energy homeostasis.[54] It also participates in adiposity negative feedback and serves to reduce feeding behavior through targeting the brain, though to a lesser degree than leptin.[55] Gut peptides also regulate satiety through inducing meal termination, such as cholecystokinin (CCK) and glucagon-like peptide 1 (GLP-1).[56,57] CCK and GLP-1 are released from the gastrointestinal system due to food intake and communicate with the CNS through gut originating projections of the vagus nerve to the solitary tract (NTS) of

the hindbrain.[57-59] In contrast to CCK and GLP-1, ghrelin is a gastric hormone that is secreted prior to a meal that motivates food intake behavior.[60] High leptin concentrations function to improve the response to satiety signals such as CCK, resulting in a decrease in meal size, while the converse is true when leptin levels are low.[61-63] Leptin achieves this through activating leptin receptors in hindbrain regions such as the NTS and in the hypothalamus such as the arcuate nucleus (ARC).[64,65] Essentially, energy homeostasis is managed through the influence of peripheral signals and neurocircuitry related to satiety and food reward located in nuclei within the hypothalamus and hindbrain.

The paraventricular nucleus of the hypothalamus is essential to energy homeostasis

One hypothalamic region of crucial significance to energy homeostatic neurocircuitry is the paraventricular nucleus of the hypothalamus (PVH), which receives regulatory inputs from regions of the hypothalamus, including the ARC, as well as from the forebrain and hindbrain.[5] It has been found that lesions to the PVH or disruption of its development produces hyperphagic obesity and glucose dysregulation in humans and mice.[66-71] Normal development of the PVH requires the expression of the single-minded homolog 1 (Sim1) transcription factor as homozygous deficiency of Sim1 in mice is lethal. Loss of a single copy of Sim1 leads to abnormal PVH development with hyperphagic obesity as well as an increased sensitivity to high fat diet.[67,69,72-74] Similarly, ablation of Sim1 neurons produces obesity that is due to hyperphagia, although it should be noted that Sim1 is also expressed in other brain regions important to energy

balance, such as the supraoptic nucleus (SON), medial amygdala and the nucleus of the lateral olfactory tract (NLOT). [68,75] The PVH exerts its regulatory control on energy homeostasis by sending primarily glutamatergic projections to regions in the hindbrain and spinal cord which serve to regulate food intake and energy expenditure. Further, the PVH mediates neuroendocrine effects through projections to the median eminence (ME) to influence pituitary function.[5,76,77] In order to understand the regulatory role of the PVH in energy balance circuitry, it will be necessary to investigate the inputs and outputs of the PVH by analyzing the regions involved in energy homeostasis upstream and downstream of the nucleus.

Regions that receive outputs from the PVH

The Solitary Nucleus

Much of food intake behavior is influenced by peripheral signaling influencing circuitry within the CNS. The nucleus of the solitary tract (NTS) of the hindbrain serves as a gateway and integrator of these peripheral signals to the CNS.[78-80] The NTS is in direct contact with the area postrema (AP), a brain region that receives peripheral signal inputs through the fourth ventricle, which lacks the protection of the blood brain barrier.[81,82] Lesioning of the AP/NTS eliminates the anorexia induced by amylin, a known anorectic released from the pancreas following the ingestion of a meal, highlighting the role the AP and NTS play in responding to peripheral satiety signals.[83] The NTS is therefore the site at which input is received from both the AP and gut signals derived from the vagus that indicate acute and chronic states of

nutrition.[81,82,84,85] These signals are then passed to the dorsal motor nucleus of the vagus (DMV) to regulate vagal reflexes and gut motility.[81] In addition to receiving peripheral and vagal inputs following the ingestion of a meal, the NTS also serves to modulate the activity of neurons of the hypothalamus to produce a satiety response. [81] For example, cholecystokinin expressing NTS neurons that project to the parabrachial nucleus (PBN) suppress feeding with associated aversion while CCK^{NTS} neurons that project to the PVH produce feeding suppression that is non-aversive.[86-89]

Several neuronal subpopulations of the PVH found to be involved in food intake and energy expenditure regulation in mice such as those that express nitric oxide synthase 1 (NOS1), insulin receptor substrate 4 (IRS4) and calcitonin receptor (CalcR) send axonal projections to the NTS.[76,90-92] The NTS is also downstream of the ARC to PVH signaling pathway, as application of leptin activates oxytocin (OXT) neurons of the PVH that project to the NTS.[93] This potentially indicates projections from certain subpopulations of the PVH to the NTS could regulate satiety signaling. The NTS in turn relays satiety information to the PBN through glutamatergic projections.[94,95] In addition to potentially regulating food intake, projections from the PVH to the NTS may also influence energy expenditure through its interaction with the sympathetic nervous system. The PVH modulates sympathetic output through polysynaptic connections to the dorsal raphe, NTS and the spinal cord.[96,97] Further, the PVH and NTS have been found to be polysynaptically connected to brown adipose tissue (BAT), which is a tissue involved with thermogenesis.[98-102] Vagus nerve viscerosensory afferents synapse onto second order neurons in the NTS, which in turn mediate reflex changes in BAT energy expenditure and BAT sympathetic nerve activity due to visceral afferent

signaling.[98,103,104] The NTS receives inputs from regions of the forebrain and brainstem that may serve to integrate metabolic signals to regulate BAT thermogenesis.[78] Overall, given the known roles the NTS plays in regulating satiety and energy expenditure, it appears likely that PVH inputs to the NTS play at least a partial role in the regulation of energy homeostasis.

The Parabrachial Nucleus

The PBN of the hindbrain serves as an integrator of signals from the hypothalamus, brainstem and spinal column, and functions as a relay center that receives visceral and gustatory information.[5] The PBN modulates feeding behavior through projections to the hypothalamus, bed nucleus of the stria terminalis and the central nucleus of the amygdala (CeA).[105-107] The PVH is composed of several neuronal populations involved in energy homeostasis that send projections to the PBN. The $NOS1^{PVH}$, $IRS4^{PVH}$ and $CalcR^{PVH}$ neurons send projections to the medial (MPBN) and LPBN, all of which have been found to regulate feeding behavior and influence energy homeostasis.[76,90,92] Amylin and CCK activate a pathway involving the AP/NTS, lateral parabrachial nucleus (LPBN) and CeA, as lesioning of the LPBN reduces the ability of amylin and CCK to inhibit food intake and reduces activation in the LPBN and CeA.[108] This suggests that stimulation may begin in the NTS, travel to the LPBN and transmit to the CeA.[108-111] Calcitonin gene-related peptide (CGRP) expressing neurons of the PBN also project to the amygdala and are thought to mediate stress induced anorexia.[105]

The CGRP neuronal population of the PBN is a critical regulator of feeding behavior. $CGRP^{PBN}$ neurons receive stimulating inputs from ascending caudal hindbrain projections and remote activation of $CGRP^{PBN}$ neurons results in a reduction or complete cessation of feeding. [80,112] Chronic stimulation of $CGRP^{PBN}$ neurons can lead to death by starvation.[80,105,112] Further, agouti-related peptide (AgRP) expressing neurons of the ARC that project directly to the PBN play a role in regulating anorexia and activation of $CGRP^{PBN}$ neurons following the ablation of AGRP neurons will result in anorexia that can lead to starvation.[80,105] Inhibition of $CGRP^{PBN}$ neurons does not affect normal food intake, suggesting that these neurons are tonically inhibited by GABAergic inputs from AGRP neurons.[105] The PBN contains neurons with the function to protect rodents against ingesting substances that are unfamiliar or possibly toxic through fear of unfamiliar substances and conditioned taste aversion.[113] Rodents are apprehensive of consuming food with a novel taste and will only continue to eat if the food does not produce an aversive response.[113] Viral and genetic methods have demonstrated that neurons of the PBN such as the $CGRP^{PBN}$ neurons are activated by lithium chloride and lipopolysaccharide, both of which are toxic and lesioning the PBN disrupts conditioned taste aversion from developing. [105,114,115] These studies highlight the aversive nature in which certain neuronal populations of the PBN reduce feeding behavior when activated.

Melanocortin 4 receptor (MC4R) neurons of the PVH send dense projections to the PBN.[77] Optogenetic activation of $MC4R^{PVH}$ neuronal projections to the PBN suppresses food intake in a non-aversive manner, indicating that the PBN participates in ARC to PVH food intake circuitry.[116] Further, stimulating PVH^{MC4R} neurons that project to the PBN in hungry mice produces a place preference, indicating that

stimulation of this circuit produces feeding behavior that would be associated with a pleasant feeling of fullness.[116] This is in contrast to the $CGRP^{PBN}$ neurons, which are involved with producing an aversive response to feeding when activated.[113] This suggests that $MC4R^{PVH}$ neurons may engage with a different subpopulation of PBN neurons and indicates that the PBN is involved in regulating both aversive and non-aversive feeding behavior.

The Spinal Cord

The spinal cord is a site important for sympathetic output, and as such is a crucial component to regulating energy expenditure.[117] The PVH has been found to indirectly connect to brown adipose tissue (BAT), providing the potential to regulate thermogenesis and energy expenditure.[99-102,118] The raphe pallidus and NTS also receive projections from the PVH and have been implicated in regulating sympathetic outflow to BAT.[96,99] Further, the intermediolateral column of the spinal cord (IML) in the thoracic spinal cord receives direct projections from the PVH and regulates sympathetic activity.[97] Some of the PVH neurons project to cardiovascular responsive sites in the IML of the upper thoracic spinal cord.[119,120] $NOS1^{PVH}$, OXT^{PVH}, and $IRS4^{PVH}$ neurons project to the choline acetyltransferase (ChAT) preganglionic neurons of the IML, all of which have varying influence on energy expenditure regulation.[76,90] These PVH projections to the IML may regulate BAT mediated thermogenesis through direct projections to ChAT cells which also function to regulate the metabolic rate and locomotor activity.[76,90]

Pseudorabies viral tracing revealed that PVH neurons (more so from the posterior portion of the PVH) polysynaptically connect to the liver and epididymal white fat (eWAT) tissue in mice.[121] More specifically, arginine vasopressin (AVP), OXT, corticotropin-releasing hormone (CRH) and thyrotropin-releasing hormone (TRH) expressing neurons of the PVH sent polysynaptic projections to the eWAT tissue, while OXT and CRH polysynaptically projected to the liver.[121] Projections to the liver could influence hepatic glucose output and carbohydrate storage, while projections to eWAT tissue could influence lipolysis and glucose uptake.[122,123] Tracing further suggests that the lateral hypothalamus, ARC, NTS and noradrenergic cell group A5 were upstream of the PVH neurons that projected to the liver and eWAT, suggesting that the PVH serves as an integrator for this downstream signaling.[121] These studies serve to provide a possible avenue through which the PVH regulates the energy expenditure component of energy homeostasis using the sympathetic nervous system.

The Pituitary

The PVH contains neurons that are critical for neuroendocrine and autonomic regulation and is composed of magnocellular neurons and parvocellular neurons which have been characterized through immunohistochemical and anatomical labeling along with electrophysiological techniques.[124,125] The large magnocellular neurons project to the posterior pituitary gland and include vasopressin neurosecretory cells which regulate body fluid balance.[124-128] Magnocellular OXT^{PVH} neurons project to the median eminence and posterior pituitary to regulate the reproductive axis.[128-131]

Parvocellular neurons project to either the median eminence or the caudally projecting pre-autonomic cells, such as neurons that project to the medullary (NTS and rostral ventrolateral medulla) or spinal (such as the IML cell column) autonomic centers.[124] These include CRH^{PVH} neurons which are essential in controlling the hypothalamic-pituitary-adrenal (HPA) axis and project to the median eminence.[125,132-135] The TRH^{PVH} parvocellular neurons regulate the thyroid axis through projections to the median eminence.[136] Both the CRH and TRH parvocellular neurons release their contents into the median eminence for hypophysial portal circulation.[125,136] Growth and development are partially regulated by somatostatin neurons of the PVH that project to the median eminence.[129] There are also parvocellular AVP neurons, that release their contents in the median eminence, and those contents can then travel to the anterior pituitary through the hypophyseal portal system.[125,129] The released AVP works in synergy with released CRH to produce adrenocorticotropic hormone (ACTH).[125] The PVH is therefore an essential component of the neuroendocrine system through the HPA axis, providing many neuronal inputs to the pituitary to influence peripheral systems.

Regions that send inputs to the PVH

Local inputs to the PVH

Transynaptic labelling mediated by injecting a tracer into the adrenal medulla has found that the PVH is surrounded by GABAergic interneurons that connect to the parvocellular neurons of the dorsal and lateral regions of the of the PVH.[137] The PVH is

regularly active and the GABAergic neurons surrounding the PVH provide tonic inhibition to the neurons of the PVH. Further, these GABA expressing neurons surrounding the PVH are in turn surrounded by a population of neuronal nitric oxide synthase (nNOS) expressing neurons.[137] It is thought that the nNOS neurons surrounding the nucleus may enhance the synaptic function of GABAergic neurons and influence sympathetic outflow through the parvocellular sympathetic neurons of the PVH.[137,138] Therefore, with the direct application of NOS inhibitors or the GABA antagonist bicuculline to the PVH, sympathetic tone increase along with an increase in blood pressure.[139] In addition to inputs immediately surrounding the PVH, it is hypothesized that intra-PVH connections exist which allow for communication and modulation between neuronal subpopulations of the PVH.[140,141] This further complicates dissecting the function and mapping the neurocircuitry of the PVH, as it can be difficult to discern the influences of these intra-PVH neurons as opposed to inputs originating from regions external to the PVH.

The hindbrain

The PVH receives inputs from many regions of the brainstem which are primarily glutamatergic.[142] In addition to receiving vagal afferents to sense satiety peptides, the NTS receives information concerning volume, pressure and oxygen saturation from cardiovascular afferents. The NTS receives information from cardiovascular receptors such as chemoreceptors, arterial baroreceptors and venous volume receptors.[143-146] The NTS then transmits this cardiovascular information to the presympathetic neurons in the PVH.[147-150] Glutamatergic afferents from the NTS terminate in close proximity to

the presympathetic and magnocellular neurons of the PVH as well as the GABAergic and nNOS expressing neurons immediately surrounding the PVH.[142] Therefore, inputs from the NTS to the PVH may directly or indirectly influence the activity of sympathetic nerves along with regulating feeding behavior.

The lateral PBN is another region that provides substantial glutamatergic inputs to the PVH.[151] We have previously discussed the PBN and its role in regulating feeding behavior, meaning the PBN may modulate energy balance through its inputs to the PVH in addition to receiving modulatory inputs from the PVH. Further, activation of neurons in the PBN occurs following various stressors and may play a role in regulating the HPA axis, as stimulation of lateral PBN neurons induces the release of ACTH.[152-155] Additionally, the PBN is involved in LiCl mediated taste aversion.[113,115] This provides a possible means through which the PBN induces glucocorticoid mediated enhancement of aversive learning through the PVH.

The periaqueductal gray (PAG) rostral and caudal ventrolateral subdivisions send dense glutamatergic projections to the PVH.[151] The rostral subdivision of the PAG has been shown to respond to acute sources of stress and receives projections from regions found to regulate HPA function, such as the medial prefrontal cortex, lateral septum and other nuclei of the hypothalamus.[156-159] The rostral PAG also receives input dorsolateral column of the PAG, which associated with panic and escape behaviors and induces the corticosterone response.[160] This suggests that the PAG may activate neuroendocrine and stress responses in the PVH through rostral PAG outputs. The PVH also receives dense innervation from caudal ventrolateral subdivision of the PAG.[156,161] The caudal ventrolateral subdivision of the PAG responds to acute stressors

such as painful and noxious stimuli, swim stress and cold temperatures.[156,162-164] Further, the ventrolateral PAG receives inputs from regions that are HPA excitatory and inhibitory such as the prefrontal cortex and the amygdaloid nucleus.[151,159] Taken together, glutamatergic inputs from caudal ventrolateral PAG to the PVH may influence the stress response as well as the HPA axis.[151]

The Forebrain

In addition to receiving input from caudal brain regions, the PVH is also an integrator of signals from the hypothalamus and forebrain.[5,140,165] Tracing studies indicate that glutamatergic neurons from the ventromedial hypothalamic nucleus (VMH) project to the anterior portion of the PVH, while the posterior region of the PVH receives primarily glutamatergic inputs from the VMH, dorsomedial hypothalamus (DMH), lateral hypothalamus and posterior hypothalamus.[165] The medial preoptic nucleus also innervates the PVH, but does not do so with glutamatergic neurons.[165] Many of the hypothalamic and forebrain inputs received by the PVH are from regions that express receptors that are important for regulating energy balance aside from the previously mentioned ARC. The VMH contain neurons that express receptors for central and peripheral signals such as leptin receptor (LepRB), melanocortin 3 and 4 receptors, insulin receptor and cholecystokinin B receptor and the DMH expresses both LepRB and MC4R.[5,166-169]

The DMH has been implicated in regulating the stress response through inputs to the PVH, as stimulating the DMH enhances ACTH release.[170] The DMH is also thought

to be involved in the milk ejection reflex through excitatory projections to the PVH that induce activity in oxytocin expressing neurons during milk ejection.[140,171] Similarly, neurons in the bed nucleus of the stria terminalis (BNST) have been thought to be involved in regulating the milk ejection reflex through OXT^{PVH} neurons.[140,172] The BNST has been shown to interact with the HPA axis through the PVH, as lesioning studies of the BNST in regions that densely project to the PVH have been shown to increase CRH mRNA expression.[173]

The medial preoptic area (MPOA) potentially exerts influence over the magnocellular neurosecretory system through projections to oxytocin and vasopressin expressing neurons in the PVH.[174,175] The MPOA may also provide excitatory and inhibitory inputs to parvocellular neurons of the PVH and could influence the HPA stress response.[176] Finally, the PVH receives moderate direct input from the amygdala and appear to have excitatory influences on the HPA axis and play a role in responding to emotional stressors.[138,177,178]

Role of the melanocortin system and energy balance through the PVH

One area of primary importance to the regulation of feeding behavior through the PVH is the ARC. The ARC is in direct contact with the median eminence, which exposes the nucleus to peripheral circulating peptides in the 3rd ventricle. This allows for hormones such as insulin, leptin and ghrelin to regulate energy homeostasis through cells in the ARC.[179] The ARC is composed of subpopulations that respond to these signals through the expression of insulin receptors (INSR), leptin receptors (ObR) and

ghrelin receptors (GHSR) to then stimulate or suppress feeding.[180-182] Among these ARC neurons are the pro-opiomelanocortin (POMC) cells, which release α-melanocyte stimulating hormone (α-MSH) and functions to inhibit food intake and regulate body weight through binding with melanocortin receptors such as the melanocortin-4 receptors (MC4R) in the PVH and activating the $MC4R^{PVH}$ neuron. These POMC neurons are activated by leptin and are inhibited when leptin levels are deficient.[183,184] POMC neurons are also activated by insulin, while ghrelin inhibits them.[180-182] Counter to the POMC neurons are those that co-express AgRP, neuropeptide Y (NPY) and GABA.[50,185] AgRP neurons function as an antagonist to the MC4R receptor, blocking α-MSH from inducing anorectic behavior through the receptor, while NPY interacts with Y1 and Y5 receptors on neurons in the PVH to increase food intake behavior. AgRP/NPY neurons also produce the GABA neurotransmitter, which suppresses α-MSH secretion from POMC neurons through inhibiting $POMC^{ARC}$ neurons.[180,181] These AgRP/NPY/GABA neurons function to stimulate feeding when activated by signals such as ghrelin and are conversely inhibited when exposed to leptin and insulin.[181,182,186-189] This produces a bimodal system that contains these two non-overlapping $AgRP^{ARC}$ and $POMC^{ARC}$ neuronal populations that work antagonistically, with $AgRP^{ARC}$ neurons inhibiting satiety promoting postsynaptic neurons (Figure 1.1). Optogenetic and chemogenetic activation of $POMC^{ARC}$ produces hypophagia and weight loss.[190,191] Converse to this, optogenetic and chemogenetic stimulation of $AgRP^{ARC}$ neurons result in hyperphagia and an increase in weight gain.[190-192] This is due to the interaction of $POMC^{ARC}$ and $AgRP^{ARC}$ with MC4R expressing neurons in the PVH.[190-194]

The cellular heterogeneity of the PVH

Pharmacological and genetic studies have demonstrated that MC4R neurons play a role in promoting satiety and weight loss when activated.[75,77,184,195-198] Germline loss of MC4R expression in mice and humans produces extreme hyperphagic obesity and shows similar phenotypes to deficiencies in the Sim1 gene.[199,200] These phenotypes include early onset hyperphagia, increased sensitivity to a high fat diet and an overall increase in growth.[75,195,201] In wildtype mice, applying melanocortin agonists results in a reduction in feeding and meal size.[202] In an experiment, MC4Rs were re-expressed in Sim1 neurons of mice that previously lacked MC4R expression, and this resulted in the rescue of normal, non-hyperphagic feeding.[75] Sim1 expression is abundant in the PVH as well as the amygdala, but it was found that re-expressing MC4Rs in the PVH of mice with previously deleted MC4R expression was both necessary and sufficient to regulate feeding behavior.[75,77] These $MC4R^{PVH}$ neurons expressed Sim1, were glutamatergic and not GABAergic, and were distinct from prodynorphin, corticotropin-releasing hormone, vasopressin and oxytocin expressing neurons in the PVH.[77] Further, $MC4R^{PVH}$ neurons make synaptic connections to neurons of the parabrachial nucleus, a region known to relay visceral information to the forebrain.[77,88,116] While appetite regulation through MC4R expression has been found to be primarily due to the $MC4R^{PVH}$ expressing neurons, regulation of energy expenditure and glucose is a quality of MC4R expressing neurons in the brainstem and spinal cord.[75,77,117]

While $MC4R^{PVH}$ neurons are critical for the regulation of feeding, they alone do not account for all the energy homeostatic qualities attributed to $Sim1^{PVH}$ neurons. For example, $MC4R^{PVH}$ neurons alone do not account for PVH mediated food intake

regulation entirely, as inhibiting MC4R^{PVH} neurons using chemogenetics results in a hyperphagia that is only about half of what is produced by chemogenetic inhibition of Sim1^{PVH} neurons. This suggests that there are other neuronal populations of the PVH that contribute to the regulation of feeding behavior along with the MC4R^{PVH} neuronal population.[116,191] Further, AgRP^{ARC} neurons GABAergically inhibit non-MC4R neurons of the PVH and optogenetic experiments suggest that AgRP^{ARC} neurons may also drive food intake through non-MC4R neurons.[116,191] There are several neuronal populations in the PVH that project to hindbrain and spinal cord regions that could potentially influence energy expenditure through the sympathetic nervous system.[76,90] Further, the PVH is composed of several neurons that project to the median eminence, suggesting interaction with the pituitary and metabolic regulation through neuroendocrine control.[76,136,203] It is due to the heterogeneity of the PVH and the many possible ways in which it regulates energy homeostasis that researchers aim to identify and characterize the various subpopulations of the PVH and their role in maintaining energy balance. The following is a non-exhaustive examination of the PVH neurons that have been identified to influence energy homeostasis.

Nitric oxide synthase 1

NOS1 neurons of the PVH are a large subset of Sim1^{PVH} neurons, which send projections to regions of the hindbrain including the PBN and NTS which are known to be important for regulating food intake.[76,93,204,205] NOS1^{PVH} neurons also project to the upper thoracic spinal cord, including the ChAT expressing region of the IML, suggesting potential connections with and regulation of preganglionic sympathetic neurons and

thus energy expenditure regulation.[76,99] These neurons send projections to the median eminence (ME), indicating that they contain parvocellular neurons that influence the function of the pituitary and magnocellular projections that release signals into the systemic circulation directly through the posterior pituitary.[76] $NOS1^{PVH}$ neurons were found to suppress feeding in a similar manner to $Sim1^{PVH}$ neurons when chemogenetically activated.[76] Further, activation of these neurons led to modest increases in energy expenditure and activity level. A subpopulation of the $NOS1^{PVH}$ neurons are the oxytocin (OXT) expressing neurons of the PVH.[76] As the $NOS1^{PVH}$ neurons are a very large population in the PVH, it is unclear if the suppression of food intake due to activating these neurons is the result of activating a yet undiscovered subpopulation of these neurons, necessitating further investigation of PVH populations that overlap with the $NOS1^{PVH}$ neuronal population.

Oxytocin

In the PVH, oxytocin (OXT) is produced in magnocellular neurons that primarily project to the posterior lobe of the pituitary gland, where it is released into the blood.[128] OXT release into the neurohypophysial system has been thought to play a role in the regulation of mammalian reproduction physiology such as milk ejection during lactation and uterine contractions during the birthing process.[130,131] OXT also initiates maternal responses and bonding following birth and may influence social cognition such as social bonding, facial recognition and the ability to assess emotional states of others through facial cues.[130,206-211] OXT is also produced in parvocellular PVH neurons, which project to the median eminence as well as regions of the forebrain.[212,213]

Retrograde tracing using cholera toxin B demonstrated that OXT^{PVH} neurons project to the NTS of rats.[91] OXT^{PVH} neurons that project to the NTS may participate in ARC to PVH signaling to the NTS due to their activation following leptin administration, suggesting potential regulation of feeding.[93] Further, Sim1 haploinsufficient mice have decreased expression of OXT and are obese.[74] Ablation of OXT or OXT receptors from mice however, does not strongly influence the regulation of body weight unless given a high-fat diet. This only promotes a diet induced obesity that is not due to hyperphagia, rather due to a decrease in energy expenditure.[214,215] Ablation of OXT neurons through Cre-dependent diphtheria toxin in adult mice also does not promote hyperphagic obesity.[216] Tracing studies using synaptic terminal-specific retrobeads and viral vectors on transgenic mice have revealed that OXT^{PVH} neurons send few projections to the NTS or PBN.[76,217] Further, chemogenetic activation of OXT^{PVH} neurons does not influence food intake, suggesting that OXT^{PVH} neurons are not responsible for the feeding behavior regulation attributed to the PVH.[76] OXT^{PVH} neurons do not express significant MC4R and attempting to selectively re-express MC4R in OXT neurons in MC4R-null mice does not reverse the hyperphagic obesity phenotype seen in MC4R-null mice.[77] Activating OXT^{PVH} neurons does not suppress food intake initiated by activating PVH-projecting AgRP neurons, which contrasts with the activation of $MC4R^{PVH}$ neurons that results in the inhibition of hyperphagia facilitated by AgRP.[116] These findings suggest that OXT^{PVH} neurons do not influence the melanocortin signaling system. Activating OXT^{PVH} neurons does have a modest influence on energy expenditure, as chemogenetic activation of these neurons increases oxygen consumption and activity levels.[76] This regulation of energy expenditure may be due to the OXT^{PVH} neurons

found within the NOS1^{PVH} field of neurons, which project to sympathetic preganglionic neurons in the thoracic spinal cord and regulate ChAT neurons in the IML.[76]

Glucagon like peptide receptor

GLP-1 is a post-translational cleavage product of preproglucagon which is encoded by the *Gcg* gene. It as an incretin hormone that is produced primarily in L-cells of the intestine as well as a subpopulation of neurons in the NTS.[218,219] GLP-1 promotes weight loss and augments glucose dependent insulin secretion through the pancreas.[220] GLP-1 receptor (GLP1R) expression is essential in the CNS, more specifically in glutamatergic rather than GABAergic neurons, for GLP1R agonists such as liraglutide to produce its physiological effects such as reduced food intake and body weight.[56,221-226] It is thought that liraglutide exerts its anorectic effects through GLP1R neurons in the ARC and liraglutide applied to the VMH activates brown adipose tissue thermogenesis, suggesting that GLP1R signaling may influence energy expenditure regulation as well.[222,227,228] The GLP-1 producing neurons in the NTS send projections to hypothalamic regions including the PVH, a region that expresses GLP1R.[229-232] Direct application of GLP-1 to the PVH suppresses food intake behavior and administration of a GLP-1 antagonist increases food intake.[233] It has also been determined that endogenous GLP-1 regulates food intake through the PVH, and that this may be due to the activation of CRH and nesfatin-1 neurons.[229] Ablation of GLP1R in Sim1 neurons in mice has negligible effects on food intake and body weight and a minor influence on energy expenditure, suggesting that alternate neuronal circuits may compensate for the deletion of GLP1R in Sim1 neurons early in development.[234-236]

Through the use of Gcg-Cre transgenic mice, researchers investigated these neurons using chemogenetic and optogenetic methods. They determined that NTS to PVH GLP-1 signaling sufficiently suppresses food intake and does so independently of glutamate co-released from GCG neurons.[237] GLP1R activation has been determined to increase excitatory synaptic strength to CRH neurons through enhancing subunit membrane trafficking of the AMPA receptor.[237] While ablation of GLP1R expression from Sim1 neurons early in development does not show strong effects on food intake, post-natal ablation of GLP1R from the PVH results in an increase in body weight gain and food intake, suggesting that GLP1R signaling is necessary for the regulation of energy homeostasis when compensation early in development is not allowed to occur.[234,237] Further, chronic perturbation of $GLP1R^{PVH}$ neurons using virally delivered tetanus toxin in mice resulted in hyperphagic obesity. Chemogenetic inhibition of $GLP1R^{PVH}$ neurons produced enhanced feeding behavior, while acute activation of these neurons suppresses appetite without influencing energy expenditure.[238]

Arginine Vasopressin

Arginine Vasopressin (AVP) expression in the PVH is found in both parvocellular and magnocellular neurons.[239] Magnocellular AVP neurons regulate osmotic balance regulation and the secretion of AVP from these neurons is regulated by selective osmoreceptors, with AVP concentrations increasing as plasma osmolarity increases.[240,241]. Further, baroreceptors modulate the release of AVP in response to arterial volume changes and physiological stress has also shown to increase the release of AVP.[242-245] The AVP expressing parvocellular cells send their terminals to the

external zone of the median eminence near the capillaries of the hypophyseal portal, allowing them to secrete AVP into the portal blood.[239] AVP has been shown to work synergistically with corticotropin releasing hormone (CRH) to influence the secretion of ACTH.[246,247]

AVP synthesized in the parvocellular neurons of the PVH has been implicated in the regulation of blood glucose, feeding and locomotor activity.[248-252] Studies have found that AVP stimulates glycogen phosphorylation to break down glycogen and increase the concentration of glucose.[250] Infusion of AVP in humans has resulted in increases of plasma glucose and glucagon concentrations.[250] It has been found that chemogenetically activating AVP^{PVH} neurons acutely reduces feeding behavior and the anorectic melanocortin agonist MTII activates AVP^{PVH} neurons. Further, AVP^{PVH} neurons may serve as a regulatory node for melanocortin mediated feeding circuitry, as their ablation partially reverses melanocortin induced anorexia.[253]

Thyrotropin-releasing hormone

Thyrotropin-releasing hormone (TRH) is both a neurotransmitter and neurohormone that is critical in the regulation of the hypothalamic-pituitary-thyroid (HPT) axis.[136] The parvocellular TRH^{PVH} neurons that participate in the neuroendocrine system release TRH into the pericapillary space of the external zone of the median eminence and communicate with the anterior pituitary, inducing the synthesis and release of TSH.[136,254] In turn, the TSH induces the secretion of thyroid hormones thyroxine (T_4) and triiodothyronine (T_3), which signal peripheral tissues to promote

cellular metabolism and energy expenditure.[136,255,256] This results in the control of the basal metabolic rate through the regulation of metabolism in most tissues in the body including heart and skeletal muscle.[257] Cold exposure results in the release of TRH, which in turn releases thyroid hormones to promote thermogenesis in thermogenic organs including brown adipose tissue (BAT), white adipose tissue and skeletal muscle.[257-262] Non-hypophysiotropic TRH^{PVH} neurons also promote thermoregulation through neural connections with BAT, likely contributing to the regulation of thermogenesis through the autonomic nervous system.[262,263] ICV administration of TRH in Syrian hamsters resulted in an increase in BAT activity and an increase in core temperature without influencing thyroid hormone levels, suggesting a central effect mediated through the sympathetic nervous system.[262,264]

Under normal circumstances, thyroid hormones are typically maintained at a constant level in order to maintain an appropriate metabolic rate.[265-267] Under conditions of starvation, energy stores are preserved through the suppression of T_4 and T_3 which in turn induces an increase in the biosynthesis and secretion of hypophysiotropic TRH.[268] This raises the threshold for feedback inhibition of the thyroid hormones and results in an increase in the secretion of TSH.[269] Increased plasma concentrations of thyroid hormones, however, suppress synthesis and release of TRH, resulting in a reduction in the threshold for feedback regulation of thyroid hormones and therefore a suppression in TSH secretion, causing a reduced release of thyroid hormones.[269] Additionally, leptin released by adipocytes increases TRH levels when in a fed state. Leptin directly stimulates TRH in the PVH through inducing the phosphorylation of signal transducer and activator of transcription 3 (STAT3) in TRH neurons, while fasting inhibits TRH

neurons.[270-272] The phospho-STAT3 regulates prepro-TRH transcription through binding to the prepro-TRH promoter.[270,273,274] Leptin indirectly stimulates TRH neurons through upregulating POMC expression and inhibition both AgRP and NPY expression in the ARC.[187,275-278] Leptin resistance in rats as a result of diet-induced obesity inactivates the indirect pathway, however the HPT axis activity is maintained in obese rodents and humans.[268,279,280] It was found that increased thyroid hormone levels in obese rats was due primarily to central leptin activity and that T_3 feedback inhibition of prepro-TRH gene is a result of leptin induced pSTAT3 signaling.[268] It is because of this relationship between T_3 and pSTAT3 signaling that the HPT axis can maintain its normal activities during an obese state.[268] Interestingly, chemogenetic activation of TRH^{PVH} neurons promotes food intake, which contrasts with the food intake suppression observed following the activation of other studied PVH neuronal populations such as the $NOS1^{PVH}$ neurons.[76,281] This may be due to the excitatory inputs TRH^{PVH} neurons provide to the AgRP neurons in the ARC that promote feeding behavior.[281]

Corticotropin releasing hormone

The corticotropin releasing hormone (CRH) system mediates the behavioral and endocrine response to stress through the hypothalamic-pituitary-adrenal axis.[203] CRH is produced by parvocellular neurons of the PVH and is released in the median eminence into the primary capillary plexus of the hypophyseal portal system.[282,283] The CRH is then transported to the anterior lobe of the pituitary, where corticotropes are stimulated to release ACTH, which in turn stimulates the release of hormones such as glucocorticoids.[246,284,285] ICV injections of CRH in genetically obese and lean mice

results in decreased feeding, oxygen consumption and activity level, however the role CRH^{PVH} neurons play in feeding when interrogated directly is not clearly understood.[286-289] Other sources have suppressed feeding behavior through chemogenetic activation of CRH^{PVH} neurons.[237] It has been proposed through combined chemogenetic/optogenetic studies, that activation of CRH^{PVH} neurons by glucagon-like peptide-1 expressing neurons of the NTS contributes to food intake suppression.[237] However, another study counters this, as it finds that there is very little overlap between CRH and GLP1R neurons in the PVH.[238] In addition, CRH^{PVH} neuron activity is rapidly reduced following refeeding after a fast indicating that CRH^{PVH} neuron activity may be more responsive to alterations in stress than feeding directly.[238] Finally, chronic silencing of CRH^{PVH} neurons failed to produce the hyperphagic obesity observed in silencing $GLP1R^{PVH}$ neurons.[238]

Prodynorphin

Prodynorphin (PDYN)-expressing neurons of the PVH are a subpopulation of $Sim1^{PVH}$ neurons that receive projections from $AGRP^{ARC}$ neurons but are distinct from the MC4R neurons of the PVH.[290] The summation of the contributions of the $PDYN^{PVH}$ and $MC4R^{PVH}$ neurons to the regulation of body weight account for the majority of the obesity prevention attributed to the $SIM1^{PVH}$ neurons. $PDYN^{PVH}$ neurons are independent from $MC4R^{PVH}$ neurons but are necessary to maintain normal body weight and energy balance.[290] Inhibition of both $PDYN^{PVH}$ and $MC4R^{PVH}$ neurons results in a hyperphagia that is similar to the activation of $AgRP^{ARC}$ neurons.[190,192,290] This suggests that the $PDYN^{PVH}$ and $MC4R^{PVH}$ neurons are primarily engaged by $AgRP^{ARC}$ neurons

that project to the PVH to regulate feeding. Silencing $PDYN^{PVH}$ neurons results in increased food intake in mice to a similar extent as mice with $MC4R^{PVH}$ neurons inhibited. Inhibition of both neuronal populations of the PVH results in a hyperphagia that is similar to that which results from inhibition of $Sim1^{PVH}$ neurons, which supports that the $PDYN^{PVH}$ and $MC4R^{PVH}$ neurons make up the majority of satiety neurons of the PVH.[68,290] Further, chronic inhibition of both neuronal populations result in an additive increase in body weight. The majority of the satiety phenotype of the $PDYN^{PVH}$ neurons is a result of its projections to the PBN, as optogenetic inhibition of the terminals of $PDYN^{PVH}$ neurons in the PBN results in a similar hyperphagic phenotype to the chemogenetic inhibition of all $PDYN^{PVH}$ neurons.[290] Channelrhodopsin-2-assisted circuit mapping reveals that $PDYN^{PVH}$ and $MC4R^{PVH}$ neurons project to the parabrachial complex, but the $PDYN^{PVH}$ neurons synapse onto the pre-locus coeruleus and the $MC4R^{PVH}$ neurons synapse onto the central lateral parabrachial nucleus, indicating they are two non-overlapping glutamatergic circuits.[116,290] $PDYN^{PVH}$ neurons are therefore responsive to caloric need and are both necessary and sufficient to regulate feeding.

Future Directions:

Numerous studies have demonstrated that the PVH is essential for the regulation of energy homeostasis through its regulation of food intake and energy expenditure.[4,5,291] Disruption of the PVH either through developmental or mechanical lesions result in hyperphagic obesity and glucose dysregulation in both humans and rodents.[66-71] The PVH is composed of diverse cell populations that are defined by their expression of neuropeptides, enzymes and cell surface receptors.[5,217] Although many

neuronal populations of the PVH have been identified as contributors to feeding and energy balance regulation through cell specific manipulations, there is still much to learn about the different ways in which subpopulations of the PVH participate in energy homeostatic neurocircuitry. This therefore necessitates further investigation of the significant neuronal subpopulations within the PVH and how they differentially influence energy balance through physiological processes such as the regulation of feeding behavior, energy expenditure and the neuroendocrine system.

In pursuit of this goal, we investigated neuronal populations of the PVH for their energy homeostatic properties. We studied the insulin receptor substrate-4 (IRS4) expressing neurons of the PVH, as previous studies showed that insulin receptor substrate-2 (IRS2) and IRS4 work synergistically to maintain energy balance and our in situ hybridization studies showed an abundance of IRS4 expression in the PVH.[90,292] We utilized viral tools to acutely activate and chronically silence IRS4^{PVH} neurons to determine the necessity and sufficiency of IRS4^{PVH} neurons in regulating energy balance as well as retrograde and anterograde tracers to determine which regions are upstream and downstream of the IRS4^{PVH} neurons.[90] We also studied the calcitonin receptor (CalcR) expressing neurons of the PVH, as direct application of the anorectic salmon calcitonin (sCT) to the PVH of rats suppresses feeding behavior and CalcR is highly expressed in the PVH.[293] We then conducted studies in which we deleted CalcR expression in Sim1 expressing neurons in order to determine if CalcR expression in these neurons is necessary for the anorectic response of sCT as well as whether it was necessary to maintain energy homeostasis.[294] Following these experiments, we investigated CalcR expressing neurons as a population of the PVH. Similarly to the

previous project, we us activation and inhibition techniques to investigated the sufficiency and necessity of CalcR^{PVH} neurons to regulate energy homeostasis, as well as conducted anterograde tracing using viral tools. As the MC4R^{PVH} neuronal population was found to overlap with CalcR^{PVH} neurons, we also silenced MC4R^{PVH} neurons for the purposes of comparison.[92] Further, as MC4R expression in the PVH is crucial for maintaining normal feeding behavior and body weight, we deleted MC4R expression from CalcR neurons to study the importance of MC4R expression in CalcR neurons in energy balance and their responsiveness to the anorectic melanotan II (MTII).[77] While these studies identify novel PVH neuronal populations which are involved in energy balance, they do not demonstrate the role the downstream projection targets of these PVH neurons play in energy homeostatic circuitry.

The PVH is thought to regulate food intake through projections to hindbrain regions such as the PBN and NTS, two regions that are known integrators of satiety signals.[76-78,295] The PVH is also thought to regulate energy expenditure through the modulation of sympathetic outputs through polysynaptic connections through the dorsal raphe, the NTS and spinal cord.[96,97,99,296,297] While we have identified several neuronal subpopulations of the PVH that project to both regions, we have yet to confirm their specific roles in the regulation of food intake and energy expenditure. For example, chemogenetic activation of NOS1^{PVH} neurons suppresses food intake and promotes energy expenditure and projects to both the PBN and NTS. This method indicates the summation of the physiological effects produced by NOS1^{PVH} neurons interacting with brain regions downstream but fails to discern the physiological effects attributed to projections to the PBN or NTS specifically.[76] We therefore need to utilize methods that

allow us to specifically manipulate neuronal cells of the PVH based on their downstream targeted regions. Optogenetics has been an effective tool for this sort of investigation, demonstrating that optogenetic stimulation of PBN projection terminals of $MC4R^{PVH}$ neurons results in a non-aversive suppression in feeding behavior as an example.[116] This method, however, is not effective for investigating PVH neurons that project to the NTS, as it is not feasible to implant optic fibers in such caudal regions without a skull for stabilization. Therefore, we have developed methods using retrograde viral vectors that will allow us to investigate the contribution of specific PVH neuronal circuits in the regulation of energy balance. This method will allow us to use specific manipulations in order to determine the energy homeostatic roles of PVH neurons that project to PBN and NTS. These studies will improve our understanding of how the PVH regulates energy balance through its projections to specific downstream regions.

References:

1. Flegal KM, Kruszon-Moran D, Carroll MD, Fryar CD, Ogden CL. Trends in Obesity Among Adults in the United States, 2005 to 2014. *JAMA.* 2016;315(21):2284-2291.
2. Kim DD, Basu A. Estimating the Medical Care Costs of Obesity in the United States: Systematic Review, Meta-Analysis, and Empirical Analysis. *Value Health.* 2016;19(5):602-613.
3. Yanovski SZ, Yanovski JA. Long-term drug treatment for obesity: a systematic and clinical review. *JAMA.* 2014;311(1):74-86.
4. Morton GJ, Meek TH, Schwartz MW. Neurobiology of food intake in health and disease. *Nat Rev Neurosci.* 2014;15(6):367-378.
5. Sutton AK, Myers MG, Jr., Olson DP. The Role of PVH Circuits in Leptin Action and Energy Balance. *Annu Rev Physiol.* 2016;78:207-221.
6. Connolly HM, Crary JL, McGoon MD, et al. Valvular heart disease associated with fenfluramine-phentermine. *N Engl J Med.* 1997;337(9):581-588.
7. Fidler MC, Sanchez M, Raether B, et al. A one-year randomized trial of lorcaserin for weight loss in obese and overweight adults: the BLOSSOM trial. *J Clin Endocrinol Metab.* 2011;96(10):3067-3077.
8. Chan EW, He Y, Chui CS, Wong AY, Lau WC, Wong IC. Efficacy and safety of lorcaserin in obese adults: a meta-analysis of 1-year randomized controlled trials (RCTs) and narrative review on short-term RCTs. *Obes Rev.* 2013;14(5):383-392.
9. Smith SR, Weissman NJ, Anderson CM, et al. Multicenter, placebo-controlled trial of lorcaserin for weight management. *N Engl J Med.* 2010;363(3):245-256.
10. O'Neil PM, Smith SR, Weissman NJ, et al. Randomized placebo-controlled clinical trial of lorcaserin for weight loss in type 2 diabetes mellitus: the BLOOM-DM study. *Obesity (Silver Spring).* 2012;20(7):1426-1436.
11. Drug Safety Communications. FDA requests the withdrawal of the weight-loss drug Belviq, Belviq XR (lorcaserin) from the market: Potential risk of cancer outweighs the benefits. U.S. Food and Drug Administration. https://www.fda.gov/drugs/drug-safety-and-availability/fda-requests-withdrawal-weight-loss-drug-belviq-belviq-xr-lorcaserin-market. Published February 13, 2020. Accessed April 17, 2021. .
12. Monami M, Dicembrini I, Marchionni N, Rotella CM, Mannucci E. Effects of glucagon-like peptide-1 receptor agonists on body weight: a meta-analysis. *Exp Diabetes Res.* 2012;2012:672658.
13. Astrup A, Carraro R, Finer N, et al. Safety, tolerability and sustained weight loss over 2 years with the once-daily human GLP-1 analog, liraglutide. *Int J Obes (Lond).* 2012;36(6):843-854.
14. Wadden TA, Hollander P, Klein S, et al. Weight maintenance and additional weight loss with liraglutide after low-calorie-diet-induced weight loss: The SCALE Maintenance randomized study. *Int J Obes (Lond).* 2015;39(1):187.
15. Drucker DJ, Sherman SI, Bergenstal RM, Buse JB. The safety of incretin-based therapies--review of the scientific evidence. *J Clin Endocrinol Metab.* 2011;96(7):2027-2031.

16. Hendricks EJ, Greenway FL, Westman EC, Gupta AK. Blood pressure and heart rate effects, weight loss and maintenance during long-term phentermine pharmacotherapy for obesity. *Obesity (Silver Spring).* 2011;19(12):2351-2360.
17. Hampp C, Kang EM, Borders-Hemphill V. Use of prescription antiobesity drugs in the United States. *Pharmacotherapy.* 2013;33(12):1299-1307.
18. Allison DB, Gadde KM, Garvey WT, et al. Controlled-release phentermine/topiramate in severely obese adults: a randomized controlled trial (EQUIP). *Obesity (Silver Spring).* 2012;20(2):330-342.
19. Gadde KM, Allison DB, Ryan DH, et al. Effects of low-dose, controlled-release, phentermine plus topiramate combination on weight and associated comorbidities in overweight and obese adults (CONQUER): a randomised, placebo-controlled, phase 3 trial. *Lancet.* 2011;377(9774):1341-1352.
20. Smith SM, Meyer M, Trinkley KE. Phentermine/topiramate for the treatment of obesity. *Ann Pharmacother.* 2013;47(3):340-349.
21. Margulis AV, Mitchell AA, Gilboa SM, et al. Use of topiramate in pregnancy and risk of oral clefts. *Am J Obstet Gynecol.* 2012;207(5):405 e401-407.
22. Greenway FL, Fujioka K, Plodkowski RA, et al. Effect of naltrexone plus bupropion on weight loss in overweight and obese adults (COR-I): a multicentre, randomised, double-blind, placebo-controlled, phase 3 trial. *Lancet.* 2010;376(9741):595-605.
23. Apovian CM, Aronne L, Rubino D, et al. A randomized, phase 3 trial of naltrexone SR/bupropion SR on weight and obesity-related risk factors (COR-II). *Obesity (Silver Spring).* 2013;21(5):935-943.
24. Wadden TA, Foreyt JP, Foster GD, et al. Weight loss with naltrexone SR/bupropion SR combination therapy as an adjunct to behavior modification: the COR-BMOD trial. *Obesity (Silver Spring).* 2011;19(1):110-120.
25. Niciu MJ, Arias AJ. Targeted opioid receptor antagonists in the treatment of alcohol use disorders. *CNS Drugs.* 2013;27(10):777-787.
26. Li Z, Maglione M, Tu W, et al. Meta-analysis: pharmacologic treatment of obesity. *Ann Intern Med.* 2005;142(7):532-546.
27. Caixas A, Albert L, Capel I, Rigla M. Naltrexone sustained-release/bupropion sustained-release for the management of obesity: review of the data to date. *Drug Des Devel Ther.* 2014;8:1419-1427.
28. Mordes JP, Liu C, Xu S. Medications for weight loss. *Curr Opin Endocrinol Diabetes Obes.* 2015;22(2):91-97.
29. Farooqi IS, Jebb SA, Langmack G, et al. Effects of recombinant leptin therapy in a child with congenital leptin deficiency. *N Engl J Med.* 1999;341(12):879-884.
30. Farooqi IS, Matarese G, Lord GM, et al. Beneficial effects of leptin on obesity, T cell hyporesponsiveness, and neuroendocrine/metabolic dysfunction of human congenital leptin deficiency. *J Clin Invest.* 2002;110(8):1093-1103.
31. Montague CT, Farooqi IS, Whitehead JP, et al. Congenital leptin deficiency is associated with severe early-onset obesity in humans. *Nature.* 1997;387(6636):903-908.
32. Heymsfield SB, Greenberg AS, Fujioka K, et al. Recombinant leptin for weight loss in obese and lean adults: a randomized, controlled, dose-escalation trial. *JAMA.* 1999;282(16):1568-1575.

33. Roth JD, Roland BL, Cole RL, et al. Leptin responsiveness restored by amylin agonism in diet-induced obesity: evidence from nonclinical and clinical studies. *Proc Natl Acad Sci U S A.* 2008;105(20):7257-7262.
34. Trevaskis JL, Coffey T, Cole R, et al. Amylin-mediated restoration of leptin responsiveness in diet-induced obesity: magnitude and mechanisms. *Endocrinology.* 2008;149(11):5679-5687.
35. Turek VF, Trevaskis JL, Levin BE, et al. Mechanisms of amylin/leptin synergy in rodent models. *Endocrinology.* 2010;151(1):143-152.
36. Osto M, Wielinga PY, Alder B, Walser N, Lutz TA. Modulation of the satiating effect of amylin by central ghrelin, leptin and insulin. *Physiol Behav.* 2007;91(5):566-572.
37. Ravussin E, Smith SR, Mitchell JA, et al. Enhanced weight loss with pramlintide/metreleptin: an integrated neurohormonal approach to obesity pharmacotherapy. *Obesity (Silver Spring).* 2009;17(9):1736-1743.
38. Trevaskis JL, Wittmer C, Athanacio J, Griffin PS, Parkes DG, Roth JD. Amylin/leptin synergy is absent in extreme obesity and not restored by calorie restriction-induced weight loss in rats. *Obes Sci Pract.* 2016;2(4):385-391.
39. Berthoud HR, Lenard NR, Shin AC. Food reward, hyperphagia, and obesity. *Am J Physiol Regul Integr Comp Physiol.* 2011;300(6):R1266-1277.
40. Berthoud HR. Multiple neural systems controlling food intake and body weight. *Neurosci Biobehav Rev.* 2002;26(4):393-428.
41. Lenard NR, Berthoud HR. Central and peripheral regulation of food intake and physical activity: pathways and genes. *Obesity (Silver Spring).* 2008;16 Suppl 3:S11-22.
42. Figlewicz DP, Sipols AJ. Energy regulatory signals and food reward. *Pharmacol Biochem Behav.* 2010;97(1):15-24.
43. Berthoud HR. Neural control of appetite: cross-talk between homeostatic and non-homeostatic systems. *Appetite.* 2004;43(3):315-317.
44. Berthoud HR. Interactions between the "cognitive" and "metabolic" brain in the control of food intake. *Physiol Behav.* 2007;91(5):486-498.
45. Speakman JR. A nonadaptive scenario explaining the genetic predisposition to obesity: the "predation release" hypothesis. *Cell Metab.* 2007;6(1):5-12.
46. Elmquist JK. Hypothalamic pathways underlying the endocrine, autonomic, and behavioral effects of leptin. *Int J Obes Relat Metab Disord.* 2001;25 Suppl 5:S78-82.
47. Schwartz MW. Brain pathways controlling food intake and body weight. *Exp Biol Med (Maywood).* 2001;226(11):978-981.
48. Zhang Y, Proenca R, Maffei M, Barone M, Leopold L, Friedman JM. Positional cloning of the mouse obese gene and its human homologue. *Nature.* 1994;372(6505):425-432.
49. Considine RV, Sinha MK, Heiman ML, et al. Serum immunoreactive-leptin concentrations in normal-weight and obese humans. *N Engl J Med.* 1996;334(5):292-295.
50. Baskin DG, Breininger JF, Schwartz MW. Leptin receptor mRNA identifies a subpopulation of neuropeptide Y neurons activated by fasting in rat hypothalamus. *Diabetes.* 1999;48(4):828-833.

51. Elmquist JK, Bjorbaek C, Ahima RS, Flier JS, Saper CB. Distributions of leptin receptor mRNA isoforms in the rat brain. *J Comp Neurol.* 1998;395(4):535-547.
52. Campfield LA, Smith FJ, Guisez Y, Devos R, Burn P. Recombinant mouse OB protein: evidence for a peripheral signal linking adiposity and central neural networks. *Science.* 1995;269(5223):546-549.
53. Halaas JL, Boozer C, Blair-West J, Fidahusein N, Denton DA, Friedman JM. Physiological response to long-term peripheral and central leptin infusion in lean and obese mice. *Proc Natl Acad Sci U S A.* 1997;94(16):8878-8883.
54. Woods SC, Lotter EC, McKay LD, Porte D, Jr. Chronic intracerebroventricular infusion of insulin reduces food intake and body weight of baboons. *Nature.* 1979;282(5738):503-505.
55. Bagdade JD, Bierman EL, Porte D, Jr. The significance of basal insulin levels in the evaluation of the insulin response to glucose in diabetic and nondiabetic subjects. *J Clin Invest.* 1967;46(10):1549-1557.
56. Turton MD, O'Shea D, Gunn I, et al. A role for glucagon-like peptide-1 in the central regulation of feeding. *Nature.* 1996;379(6560):69-72.
57. Gibbs J, Young RC, Smith GP. Cholecystokinin decreases food intake in rats. *J Comp Physiol Psychol.* 1973;84(3):488-495.
58. Strubbe JH, Woods SC. The timing of meals. *Psychol Rev.* 2004;111(1):128-141.
59. West DB, Fey D, Woods SC. Cholecystokinin persistently suppresses meal size but not food intake in free-feeding rats. *Am J Physiol.* 1984;246(5 Pt 2):R776-787.
60. Tschop M, Smiley DL, Heiman ML. Ghrelin induces adiposity in rodents. *Nature.* 2000;407(6806):908-913.
61. McMinn JE, Sindelar DK, Havel PJ, Schwartz MW. Leptin deficiency induced by fasting impairs the satiety response to cholecystokinin. *Endocrinology.* 2000;141(12):4442-4448.
62. McLaughlin CL, Baile CA. Decreased sensitivity of Zucker obese rats to the putative satiety agent cholecystokinin. *Physiol Behav.* 1980;25(4):543-548.
63. Morton GJ, Gelling RW, Niswender KD, Morrison CD, Rhodes CJ, Schwartz MW. Leptin regulates insulin sensitivity via phosphatidylinositol-3-OH kinase signaling in mediobasal hypothalamic neurons. *Cell Metab.* 2005;2(6):411-420.
64. Grill HJ, Schwartz MW, Kaplan JM, Foxhall JS, Breininger J, Baskin DG. Evidence that the caudal brainstem is a target for the inhibitory effect of leptin on food intake. *Endocrinology.* 2002;143(1):239-246.
65. Morton GJ, Blevins JE, Williams DL, et al. Leptin action in the forebrain regulates the hindbrain response to satiety signals. *J Clin Invest.* 2005;115(3):703-710.
66. Sims JS, Lorden JF. Effect of paraventricular nucleus lesions on body weight, food intake and insulin levels. *Behav Brain Res.* 1986;22(3):265-281.
67. Tolson KP, Gemelli T, Gautron L, Elmquist JK, Zinn AR, Kublaoui BM. Postnatal Sim1 deficiency causes hyperphagic obesity and reduced Mc4r and oxytocin expression. *J Neurosci.* 2010;30(10):3803-3812.
68. Xi D, Gandhi N, Lai M, Kublaoui BM. Ablation of Sim1 neurons causes obesity through hyperphagia and reduced energy expenditure. *PLoS One.* 2012;7(4):e36453.

69. Michaud JL, Rosenquist T, May NR, Fan CM. Development of neuroendocrine lineages requires the bHLH-PAS transcription factor SIM1. *Genes Dev.* 1998;12(20):3264-3275.
70. Holder JL, Jr., Butte NF, Zinn AR. Profound obesity associated with a balanced translocation that disrupts the SIM1 gene. *Hum Mol Genet.* 2000;9(1):101-108.
71. Leibowitz SF, Hammer NJ, Chang K. Hypothalamic paraventricular nucleus lesions produce overeating and obesity in the rat. *Physiol Behav.* 1981;27(6):1031-1040.
72. Holder JL, Jr., Zhang L, Kublaoui BM, et al. Sim1 gene dosage modulates the homeostatic feeding response to increased dietary fat in mice. *Am J Physiol Endocrinol Metab.* 2004;287(1):E105-113.
73. Kublaoui BM, Holder JL, Jr., Gemelli T, Zinn AR. Sim1 haploinsufficiency impairs melanocortin-mediated anorexia and activation of paraventricular nucleus neurons. *Mol Endocrinol.* 2006;20(10):2483-2492.
74. Kublaoui BM, Gemelli T, Tolson KP, Wang Y, Zinn AR. Oxytocin deficiency mediates hyperphagic obesity of Sim1 haploinsufficient mice. *Mol Endocrinol.* 2008;22(7):1723-1734.
75. Balthasar N, Dalgaard LT, Lee CE, et al. Divergence of melanocortin pathways in the control of food intake and energy expenditure. *Cell.* 2005;123(3):493-505.
76. Sutton AK, Pei H, Burnett KH, Myers MG, Jr., Rhodes CJ, Olson DP. Control of food intake and energy expenditure by Nos1 neurons of the paraventricular hypothalamus. *J Neurosci.* 2014;34(46):15306-15318.
77. Shah BP, Vong L, Olson DP, et al. MC4R-expressing glutamatergic neurons in the paraventricular hypothalamus regulate feeding and are synaptically connected to the parabrachial nucleus. *Proc Natl Acad Sci U S A.* 2014;111(36):13193-13198.
78. Grill HJ, Hayes MR. Hindbrain neurons as an essential hub in the neuroanatomically distributed control of energy balance. *Cell Metab.* 2012;16(3):296-309.
79. Rinaman L. Ascending projections from the caudal visceral nucleus of the solitary tract to brain regions involved in food intake and energy expenditure. *Brain Res.* 2010;1350:18-34.
80. Wu Q, Clark MS, Palmiter RD. Deciphering a neuronal circuit that mediates appetite. *Nature.* 2012;483(7391):594-597.
81. Berthoud HR, Blackshaw LA, Brookes SJ, Grundy D. Neuroanatomy of extrinsic afferents supplying the gastrointestinal tract. *Neurogastroenterol Motil.* 2004;16 Suppl 1:28-33.
82. Hyde TM, Miselis RR. Effects of area postrema/caudal medial nucleus of solitary tract lesions on food intake and body weight. *Am J Physiol.* 1983;244(4):R577-587.
83. Rowland NE, Richmond RM. Area postrema and the anorectic actions of dexfenfluramine and amylin. *Brain Res.* 1999;820(1-2):86-91.
84. Wislocki GB, Leduc EH. Vital staining of the hematoencephalic barrier by silver nitrate and trypan blue, and cytological comparisons of the neurohypophysis, pineal body, area postrema, intercolumnar tubercle and supraoptic crest. *J Comp Neurol.* 1952;96(3):371-413.

85. Eng R, Miselis RR. Polydipsia and abolition of angiotensin-induced drinking after transections of subfornical organ efferent projections in the rat. *Brain Res.* 1981;225(1):200-206.
86. D'Agostino G, Lyons DJ, Cristiano C, et al. Appetite controlled by a cholecystokinin nucleus of the solitary tract to hypothalamus neurocircuit. *Elife.* 2016;5.
87. Roman CW, Sloat SR, Palmiter RD. A tale of two circuits: CCK(NTS) neuron stimulation controls appetite and induces opposing motivational states by projections to distinct brain regions. *Neuroscience.* 2017;358:316-324.
88. Herbert H, Saper CB. Cholecystokinin-, galanin-, and corticotropin-releasing factor-like immunoreactive projections from the nucleus of the solitary tract to the parabrachial nucleus in the rat. *J Comp Neurol.* 1990;293(4):581-598.
89. Vitale M, Vashishtha A, Linzer E, Powell DJ, Friedman JM. Molecular cloning of the mouse CCK gene: expression in different brain regions and during cortical development. *Nucleic Acids Res.* 1991;19(1):169-177.
90. Sutton AK, Gonzalez IE, Sadagurski M, et al. Paraventricular, subparaventricular and periventricular hypothalamic IRS4-expressing neurons are required for normal energy balance. *Sci Rep.* 2020;10(1):5546.
91. Blevins JE, Eakin TJ, Murphy JA, Schwartz MW, Baskin DG. Oxytocin innervation of caudal brainstem nuclei activated by cholecystokinin. *Brain Res.* 2003;993(1-2):30-41.
92. Gonzalez IE, Ramirez-Matias J, Lu C, et al. Paraventricular Calcitonin Receptor-Expressing Neurons Modulate Energy Homeostasis in Male Mice. *Endocrinology.* 2021;162(6).
93. Blevins JE, Schwartz MW, Baskin DG. Evidence that paraventricular nucleus oxytocin neurons link hypothalamic leptin action to caudal brain stem nuclei controlling meal size. *Am J Physiol Regul Integr Comp Physiol.* 2004;287(1):R87-96.
94. Norgren R. Projections from the nucleus of the solitary tract in the rat. *Neuroscience.* 1978;3(2):207-218.
95. Herbert H, Moga MM, Saper CB. Connections of the parabrachial nucleus with the nucleus of the solitary tract and the medullary reticular formation in the rat. *J Comp Neurol.* 1990;293(4):540-580.
96. Madden CJ, Morrison SF. Neurons in the paraventricular nucleus of the hypothalamus inhibit sympathetic outflow to brown adipose tissue. *Am J Physiol Regul Integr Comp Physiol.* 2009;296(3):R831-843.
97. Caverson MM, Ciriello J, Calaresu FR. Paraventricular nucleus of the hypothalamus: an electrophysiological investigation of neurons projecting directly to intermediolateral nucleus in the cat. *Brain Res.* 1984;305(2):380-383.
98. Szekely M. The vagus nerve in thermoregulation and energy metabolism. *Auton Neurosci.* 2000;85(1-3):26-38.
99. Bamshad M, Song CK, Bartness TJ. CNS origins of the sympathetic nervous system outflow to brown adipose tissue. *Am J Physiol.* 1999;276(6):R1569-1578.
100. Cano G, Passerin AM, Schiltz JC, Card JP, Morrison SF, Sved AF. Anatomical substrates for the central control of sympathetic outflow to interscapular adipose tissue during cold exposure. *J Comp Neurol.* 2003;460(3):303-326.

101. Oldfield BJ, Giles ME, Watson A, Anderson C, Colvill LM, McKinley MJ. The neurochemical characterisation of hypothalamic pathways projecting polysynaptically to brown adipose tissue in the rat. *Neuroscience.* 2002;110(3):515-526.
102. Yoshida K, Nakamura K, Matsumura K, et al. Neurons of the rat preoptic area and the raphe pallidus nucleus innervating the brown adipose tissue express the prostaglandin E receptor subtype EP3. *Eur J Neurosci.* 2003;18(7):1848-1860.
103. Blouet C, Schwartz GJ. Duodenal lipid sensing activates vagal afferents to regulate non-shivering brown fat thermogenesis in rats. *PLoS One.* 2012;7(12):e51898.
104. Ono K, Tsukamoto-Yasui M, Hara-Kimura Y, et al. Intragastric administration of capsiate, a transient receptor potential channel agonist, triggers thermogenic sympathetic responses. *J Appl Physiol (1985).* 2011;110(3):789-798.
105. Carter ME, Soden ME, Zweifel LS, Palmiter RD. Genetic identification of a neural circuit that suppresses appetite. *Nature.* 2013;503(7474):111-114.
106. D'Hanis W, Linke R, Yilmazer-Hanke DM. Topography of thalamic and parabrachial calcitonin gene-related peptide (CGRP) immunoreactive neurons projecting to subnuclei of the amygdala and extended amygdala. *J Comp Neurol.* 2007;505(3):268-291.
107. Schwaber JS, Sternini C, Brecha NC, Rogers WT, Card JP. Neurons containing calcitonin gene-related peptide in the parabrachial nucleus project to the central nucleus of the amygdala. *J Comp Neurol.* 1988;270(3):416-426, 398-419.
108. Becskei C, Grabler V, Edwards GL, Riediger T, Lutz TA. Lesion of the lateral parabrachial nucleus attenuates the anorectic effect of peripheral amylin and CCK. *Brain Res.* 2007;1162:76-84.
109. Voshart K, van der Kooy D. The organization of the efferent projections of the parabrachial nucleus of the forebrain in the rat: a retrograde fluorescent double-labeling study. *Brain Res.* 1981;212(2):271-286.
110. Hermann GE, Rogers RC. Convergence of vagal and gustatory afferent input within the parabrachial nucleus of the rat. *J Auton Nerv Syst.* 1985;13(1):1-17.
111. Block CH, Hoffman G, Kapp BS. Peptide-containing pathways from the parabrachial complex to the central nucleus of the amygdala. *Peptides.* 1989;10(2):465-471.
112. Wu Q, Boyle MP, Palmiter RD. Loss of GABAergic signaling by AgRP neurons to the parabrachial nucleus leads to starvation. *Cell.* 2009;137(7):1225-1234.
113. Reilly S. The parabrachial nucleus and conditioned taste aversion. *Brain Res Bull.* 1999;48(3):239-254.
114. Reilly S, Trifunovic R. Lateral parabrachial nucleus lesions in the rat: aversive and appetitive gustatory conditioning. *Brain Res Bull.* 2000;52(4):269-278.
115. Reilly S, Trifunovic R. Lateral parabrachial nucleus lesions in the rat: neophobia and conditioned taste aversion. *Brain Res Bull.* 2001;55(3):359-366.
116. Garfield AS, Li C, Madara JC, et al. A neural basis for melanocortin-4 receptor-regulated appetite. *Nat Neurosci.* 2015;18(6):863-871.
117. Rossi J, Balthasar N, Olson D, et al. Melanocortin-4 receptors expressed by cholinergic neurons regulate energy balance and glucose homeostasis. *Cell Metab.* 2011;13(2):195-204.

118. Morrison SF, Madden CJ. Central nervous system regulation of brown adipose tissue. *Compr Physiol.* 2014;4(4):1677-1713.
119. Badoer E. Hypothalamic paraventricular nucleus and cardiovascular regulation. *Clin Exp Pharmacol Physiol.* 2001;28(1-2):95-99.
120. Ramchandra R, Hood SG, Frithiof R, McKinley MJ, May CN. The role of the paraventricular nucleus of the hypothalamus in the regulation of cardiac and renal sympathetic nerve activity in conscious normal and heart failure sheep. *J Physiol.* 2013;591(1):93-107.
121. Stanley S, Pinto S, Segal J, et al. Identification of neuronal subpopulations that project from hypothalamus to both liver and adipose tissue polysynaptically. *Proc Natl Acad Sci U S A.* 2010;107(15):7024-7029.
122. Puschel GP. Control of hepatocyte metabolism by sympathetic and parasympathetic hepatic nerves. *Anat Rec A Discov Mol Cell Evol Biol.* 2004;280(1):854-867.
123. Fredholm BB, Karlsson J. Metabolic effects of prolonged sympathetic nerve stimulation in canine subcutaneous adipose tissue. *Acta Physiol Scand.* 1970;80(4):567-576.
124. Tasker JG, Dudek FE. Electrophysiological properties of neurones in the region of the paraventricular nucleus in slices of rat hypothalamus. *J Physiol.* 1991;434:271-293.
125. Scott LV, Dinan TG. Vasopressin and the regulation of hypothalamic-pituitary-adrenal axis function: implications for the pathophysiology of depression. *Life Sci.* 1998;62(22):1985-1998.
126. Brody MJ. Central nervous system and mechanisms of hypertension. *Clin Physiol Biochem.* 1988;6(3-4):230-239.
127. Gimpl G, Fahrenholz F. The oxytocin receptor system: structure, function, and regulation. *Physiol Rev.* 2001;81(2):629-683.
128. Bargmann W. [The neurosecretory connection between the hypothalamus and the neurohypophysis]. *Z Zellforsch Mikrosk Anat.* 1949;34(5):610-634.
129. Ferguson AV, Latchford KJ, Samson WK. The paraventricular nucleus of the hypothalamus - a potential target for integrative treatment of autonomic dysfunction. *Expert Opin Ther Targets.* 2008;12(6):717-727.
130. Ross HE, Cole CD, Smith Y, et al. Characterization of the oxytocin system regulating affiliative behavior in female prairie voles. *Neuroscience.* 2009;162(4):892-903.
131. Burbach JP, Luckman SM, Murphy D, Gainer H. Gene regulation in the magnocellular hypothalamo-neurohypophysial system. *Physiol Rev.* 2001;81(3):1197-1267.
132. Dallman MF, Strack AM, Akana SF, et al. Feast and famine: critical role of glucocorticoids with insulin in daily energy flow. *Front Neuroendocrinol.* 1993;14(4):303-347.
133. Antoni FA. Hypothalamic control of adrenocorticotropin secretion: advances since the discovery of 41-residue corticotropin-releasing factor. *Endocr Rev.* 1986;7(4):351-378.
134. Jones MT, Gillham B. Factors involved in the regulation of adrenocorticotropic hormone/beta-lipotropic hormone. *Physiol Rev.* 1988;68(3):743-818.

135. Kalra SP, Dube MG, Pu S, Xu B, Horvath TL, Kalra PS. Interacting appetite-regulating pathways in the hypothalamic regulation of body weight. *Endocr Rev.* 1999;20(1):68-100.
136. Fekete C, Lechan RM. Central regulation of hypothalamic-pituitary-thyroid axis under physiological and pathophysiological conditions. *Endocr Rev.* 2014;35(2):159-194.
137. Watkins ND, Cork SC, Pyner S. An immunohistochemical investigation of the relationship between neuronal nitric oxide synthase, GABA and presympathetic paraventricular neurons in the hypothalamus. *Neuroscience.* 2009;159(3):1079-1088.
138. Herman JP, Tasker JG, Ziegler DR, Cullinan WE. Local circuit regulation of paraventricular nucleus stress integration: glutamate-GABA connections. *Pharmacol Biochem Behav.* 2002;71(3):457-468.
139. Zhang K, Patel KP. Effect of nitric oxide within the paraventricular nucleus on renal sympathetic nerve discharge: role of GABA. *Am J Physiol.* 1998;275(3):R728-734.
140. Boudaba C, Schrader LA, Tasker JG. Physiological evidence for local excitatory synaptic circuits in the rat hypothalamus. *J Neurophysiol.* 1997;77(6):3396-3400.
141. Ziegler DR, Herman JP. Local integration of glutamate signaling in the hypothalamic paraventricular region: regulation of glucocorticoid stress responses. *Endocrinology.* 2000;141(12):4801-4804.
142. Affleck VS, Coote JH, Pyner S. The projection and synaptic organisation of NTS afferent connections with presympathetic neurons, GABA and nNOS neurons in the paraventricular nucleus of the hypothalamus. *Neuroscience.* 2012;219:48-61.
143. Lovick TA, Coote JH. Effects of volume loading on paraventriculo-spinal neurones in the rat. *J Auton Nerv Syst.* 1988;25(2-3):135-140.
144. Lovick TA, Coote JH. Circulating atrial natriuretic factor activates vagal afferent inputs to paraventriculo-spinal neurones in the rat. *J Auton Nerv Syst.* 1989;26(2):129-134.
145. Reddy MK, Patel KP, Schultz HD. Differential role of the paraventricular nucleus of the hypothalamus in modulating the sympathoexcitatory component of peripheral and central chemoreflexes. *Am J Physiol Regul Integr Comp Physiol.* 2005;289(3):R789-797.
146. Reddy MK, Schultz HD, Zheng H, Patel KP. Altered nitric oxide mechanism within the paraventricular nucleus contributes to the augmented carotid body chemoreflex in heart failure. *Am J Physiol Heart Circ Physiol.* 2007;292(1):H149-157.
147. Clement DL, Pelletier CL, Shepherd JT. Role of vagal afferents in the control of renal sympathetic nerve activity in the rabbit. *Circ Res.* 1972;31(6):824-830.
148. Karim F, Kidd C, Malpus CM, Penna PE. The effects of stimulation of the left atrial receptors on sympathetic efferent nerve activity. *J Physiol.* 1972;227(1):243-260.
149. Kappagoda CT, Linden RJ, Snow HM. Effect of stimulating right atrial receptors on urine flow in the dog. *J Physiol.* 1973;235(2):493-502.
150. Spyer KM. Annual review prize lecture. Central nervous mechanisms contributing to cardiovascular control. *J Physiol.* 1994;474(1):1-19.

151. Ziegler DR, Edwards MR, Ulrich-Lai YM, Herman JP, Cullinan WE. Brainstem origins of glutamatergic innervation of the rat hypothalamic paraventricular nucleus. *J Comp Neurol.* 2012;520(11):2369-2394.
152. Chan RK, Sawchenko PE. Spatially and temporally differentiated patterns of c-fos expression in brainstem catecholaminergic cell groups induced by cardiovascular challenges in the rat. *J Comp Neurol.* 1994;348(3):433-460.
153. Kainu T, Honkaniemi J, Gustafsson JA, Rechardt L, Pelto-Huikko M. Co-localization of peptide-like immunoreactivities with glucocorticoid receptor- and Fos-like immunoreactivities in the rat parabrachial nucleus. *Brain Res.* 1993;615(2):245-251.
154. Li HY, Sawchenko PE. Hypothalamic effector neurons and extended circuitries activated in "neurogenic" stress: a comparison of footshock effects exerted acutely, chronically, and in animals with controlled glucocorticoid levels. *J Comp Neurol.* 1998;393(2):244-266.
155. Carlson DE, Nabavian AM, Gann DS. Corticotropin-releasing hormone but not glutamate elicits hormonal responses from the parabrachial region in cats. *Am J Physiol.* 1994;267(1 Pt 2):R337-348.
156. Canteras NS, Goto M. Fos-like immunoreactivity in the periaqueductal gray of rats exposed to a natural predator. *Neuroreport.* 1999;10(2):413-418.
157. Kollack-Walker S, Don C, Watson SJ, Akil H. Differential expression of c-fos mRNA within neurocircuits of male hamsters exposed to acute or chronic defeat. *J Neuroendocrinol.* 1999;11(7):547-559.
158. Silveira MC, Sandner G, Graeff FG. Induction of Fos immunoreactivity in the brain by exposure to the elevated plus-maze. *Behav Brain Res.* 1993;56(1):115-118.
159. Bandler R, Shipley MT. Columnar organization in the midbrain periaqueductal gray: modules for emotional expression? *Trends Neurosci.* 1994;17(9):379-389.
160. Lim LW, Blokland A, van Duinen M, et al. Increased plasma corticosterone levels after periaqueductal gray stimulation-induced escape reaction or panic attacks in rats. *Behav Brain Res.* 2011;218(2):301-307.
161. Krout KE, Loewy AD. Periaqueductal gray matter projections to midline and intralaminar thalamic nuclei of the rat. *J Comp Neurol.* 2000;424(1):111-141.
162. Bellchambers CE, Chieng B, Keay KA, Christie MJ. Swim-stress but not opioid withdrawal increases expression of c-fos immunoreactivity in rat periaqueductal gray neurons which project to the rostral ventromedial medulla. *Neuroscience.* 1998;83(2):517-524.
163. Keay KA, Bandler R. Deep and superficial noxious stimulation increases Fos-like immunoreactivity in different regions of the midbrain periaqueductal grey of the rat. *Neurosci Lett.* 1993;154(1-2):23-26.
164. Yoshida K, Konishi M, Nagashima K, Saper CB, Kanosue K. Fos activation in hypothalamic neurons during cold or warm exposure: projections to periaqueductal gray matter. *Neuroscience.* 2005;133(4):1039-1046.
165. Ulrich-Lai YM, Jones KR, Ziegler DR, Cullinan WE, Herman JP. Forebrain origins of glutamatergic innervation to the rat paraventricular nucleus of the hypothalamus: differential inputs to the anterior versus posterior subregions. *J Comp Neurol.* 2011;519(7):1301-1319.

166. Elmquist JK, Ahima RS, Elias CF, Flier JS, Saper CB. Leptin activates distinct projections from the dorsomedial and ventromedial hypothalamic nuclei. *Proc Natl Acad Sci U S A.* 1998;95(2):741-746.
167. Girardet C, Butler AA. Neural melanocortin receptors in obesity and related metabolic disorders. *Biochim Biophys Acta.* 2014;1842(3):482-494.
168. Flak JN, Goforth PB, Dell'Orco J, et al. Ventromedial hypothalamic nucleus neuronal subset regulates blood glucose independently of insulin. *J Clin Invest.* 2020;130(6):2943-2952.
169. Paranjape SA, Chan O, Zhu W, et al. Influence of insulin in the ventromedial hypothalamus on pancreatic glucagon secretion in vivo. *Diabetes.* 2010;59(6):1521-1527.
170. Bailey TW, Dimicco JA. Chemical stimulation of the dorsomedial hypothalamus elevates plasma ACTH in conscious rats. *Am J Physiol Regul Integr Comp Physiol.* 2001;280(1):R8-15.
171. Takano S, Negoro H, Honda K, Higuchi T. Lesion and electrophysiological studies on the hypothalamic afferent pathway of the milk ejection reflex in the rat. *Neuroscience.* 1992;50(4):877-883.
172. Ingram CD, Adams TS, Jiang QB, et al. Mortyn Jones Memorial Lecture. Limbic regions mediating central actions of oxytocin on the milk-ejection reflex in the rat. *J Neuroendocrinol.* 1995;7(1):1-13.
173. Herman JP, Cullinan WE, Watson SJ. Involvement of the bed nucleus of the stria terminalis in tonic regulation of paraventricular hypothalamic CRH and AVP mRNA expression. *J Neuroendocrinol.* 1994;6(4):433-442.
174. Miselis RR. The efferent projections of the subfornical organ of the rat: a circumventricular organ within a neural network subserving water balance. *Brain Res.* 1981;230(1-2):1-23.
175. Sawchenko PE, Swanson LW. The organization of forebrain afferents to the paraventricular and supraoptic nuclei of the rat. *J Comp Neurol.* 1983;218(2):121-144.
176. Viau V, Meaney MJ. The inhibitory effect of testosterone on hypothalamic-pituitary-adrenal responses to stress is mediated by the medial preoptic area. *J Neurosci.* 1996;16(5):1866-1876.
177. Dayas CV, Buller KM, Day TA. Neuroendocrine responses to an emotional stressor: evidence for involvement of the medial but not the central amygdala. *Eur J Neurosci.* 1999;11(7):2312-2322.
178. Herman JP, Cullinan WE. Neurocircuitry of stress: central control of the hypothalamo-pituitary-adrenocortical axis. *Trends Neurosci.* 1997;20(2):78-84.
179. Yeo GS, Heisler LK. Unraveling the brain regulation of appetite: lessons from genetics. *Nat Neurosci.* 2012;15(10):1343-1349.
180. Andrews ZB, Liu ZW, Walllingford N, et al. UCP2 mediates ghrelin's action on NPY/AgRP neurons by lowering free radicals. *Nature.* 2008;454(7206):846-851.
181. Cowley MA, Smith RG, Diano S, et al. The distribution and mechanism of action of ghrelin in the CNS demonstrates a novel hypothalamic circuit regulating energy homeostasis. *Neuron.* 2003;37(4):649-661.
182. Briggs DI, Andrews ZB. Metabolic status regulates ghrelin function on energy homeostasis. *Neuroendocrinology.* 2011;93(1):48-57.

183. Schwartz MW, Seeley RJ, Woods SC, et al. Leptin increases hypothalamic pro-opiomelanocortin mRNA expression in the rostral arcuate nucleus. *Diabetes.* 1997;46(12):2119-2123.
184. Fan W, Boston BA, Kesterson RA, Hruby VJ, Cone RD. Role of melanocortinergic neurons in feeding and the agouti obesity syndrome. *Nature.* 1997;385(6612):165-168.
185. Hahn TM, Breininger JF, Baskin DG, Schwartz MW. Coexpression of Agrp and NPY in fasting-activated hypothalamic neurons. *Nat Neurosci.* 1998;1(4):271-272.
186. Hagan MM, Rushing PA, Pritchard LM, et al. Long-term orexigenic effects of AgRP-(83---132) involve mechanisms other than melanocortin receptor blockade. *Am J Physiol Regul Integr Comp Physiol.* 2000;279(1):R47-52.
187. Cowley MA, Smart JL, Rubinstein M, et al. Leptin activates anorexigenic POMC neurons through a neural network in the arcuate nucleus. *Nature.* 2001;411(6836):480-484.
188. Spanswick D, Smith MA, Mirshamsi S, Routh VH, Ashford ML. Insulin activates ATP-sensitive K+ channels in hypothalamic neurons of lean, but not obese rats. *Nat Neurosci.* 2000;3(8):757-758.
189. Spanswick D, Smith MA, Groppi VE, Logan SD, Ashford ML. Leptin inhibits hypothalamic neurons by activation of ATP-sensitive potassium channels. *Nature.* 1997;390(6659):521-525.
190. Aponte Y, Atasoy D, Sternson SM. AGRP neurons are sufficient to orchestrate feeding behavior rapidly and without training. *Nat Neurosci.* 2011;14(3):351-355.
191. Atasoy D, Betley JN, Su HH, Sternson SM. Deconstruction of a neural circuit for hunger. *Nature.* 2012;488(7410):172-177.
192. Krashes MJ, Koda S, Ye C, et al. Rapid, reversible activation of AgRP neurons drives feeding behavior in mice. *J Clin Invest.* 2011;121(4):1424-1428.
193. Krashes MJ, Shah BP, Koda S, Lowell BB. Rapid versus delayed stimulation of feeding by the endogenously released AgRP neuron mediators GABA, NPY, and AgRP. *Cell Metab.* 2013;18(4):588-595.
194. Zhan C, Zhou J, Feng Q, et al. Acute and long-term suppression of feeding behavior by POMC neurons in the brainstem and hypothalamus, respectively. *J Neurosci.* 2013;33(8):3624-3632.
195. Huszar D, Lynch CA, Fairchild-Huntress V, et al. Targeted disruption of the melanocortin-4 receptor results in obesity in mice. *Cell.* 1997;88(1):131-141.
196. Rossi M, Kim MS, Morgan DG, et al. A C-terminal fragment of Agouti-related protein increases feeding and antagonizes the effect of alpha-melanocyte stimulating hormone in vivo. *Endocrinology.* 1998;139(10):4428-4431.
197. Small CJ, Kim MS, Stanley SA, et al. Effects of chronic central nervous system administration of agouti-related protein in pair-fed animals. *Diabetes.* 2001;50(2):248-254.
198. Yaswen L, Diehl N, Brennan MB, Hochgeschwender U. Obesity in the mouse model of pro-opiomelanocortin deficiency responds to peripheral melanocortin. *Nat Med.* 1999;5(9):1066-1070.

199. Vaisse C, Clement K, Guy-Grand B, Froguel P. A frameshift mutation in human MC4R is associated with a dominant form of obesity. *Nat Genet.* 1998;20(2):113-114.
200. Yeo GS, Farooqi IS, Aminian S, Halsall DJ, Stanhope RG, O'Rahilly S. A frameshift mutation in MC4R associated with dominantly inherited human obesity. *Nat Genet.* 1998;20(2):111-112.
201. Itoh M, Suganami T, Nakagawa N, et al. Melanocortin 4 receptor-deficient mice as a novel mouse model of nonalcoholic steatohepatitis. *Am J Pathol.* 2011;179(5):2454-2463.
202. Azzara AV, Sokolnicki JP, Schwartz GJ. Central melanocortin receptor agonist reduces spontaneous and scheduled meal size but does not augment duodenal preload-induced feeding inhibition. *Physiol Behav.* 2002;77(2-3):411-416.
203. Smith SM, Vale WW. The role of the hypothalamic-pituitary-adrenal axis in neuroendocrine responses to stress. *Dialogues Clin Neurosci.* 2006;8(4):383-395.
204. Sawchenko PE, Swanson LW. The organization of noradrenergic pathways from the brainstem to the paraventricular and supraoptic nuclei in the rat. *Brain Res.* 1982;257(3):275-325.
205. Fulwiler CE, Saper CB. Cholecystokinin-immunoreactive innervation of the ventromedial hypothalamus in the rat: possible substrate for autonomic regulation of feeding. *Neurosci Lett.* 1985;53(3):289-296.
206. Kendrick KM, Keverne EB, Baldwin BA. Intracerebroventricular oxytocin stimulates maternal behaviour in the sheep. *Neuroendocrinology.* 1987;46(1):56-61.
207. Kosfeld M, Heinrichs M, Zak PJ, Fischbacher U, Fehr E. Oxytocin increases trust in humans. *Nature.* 2005;435(7042):673-676.
208. Domes G, Heinrichs M, Michel A, Berger C, Herpertz SC. Oxytocin improves "mind-reading" in humans. *Biol Psychiatry.* 2007;61(6):731-733.
209. Donaldson ZR, Young LJ. Oxytocin, vasopressin, and the neurogenetics of sociality. *Science.* 2008;322(5903):900-904.
210. Guastella AJ, Mitchell PB, Dadds MR. Oxytocin increases gaze to the eye region of human faces. *Biol Psychiatry.* 2008;63(1):3-5.
211. Savaskan E, Ehrhardt R, Schulz A, Walter M, Schachinger H. Post-learning intranasal oxytocin modulates human memory for facial identity. *Psychoneuroendocrinology.* 2008;33(3):368-374.
212. Silverman AJ, Witkin JW, Silverman RC, Gibson MJ. Modulation of gonadotropin-releasing hormone neuronal activity as evidenced by uptake of fluorogold from the vasculature. *Synapse.* 1990;6(2):154-160.
213. Landgraf R, Neumann ID. Vasopressin and oxytocin release within the brain: a dynamic concept of multiple and variable modes of neuropeptide communication. *Front Neuroendocrinol.* 2004;25(3-4):150-176.
214. Takayanagi Y, Kasahara Y, Onaka T, Takahashi N, Kawada T, Nishimori K. Oxytocin receptor-deficient mice developed late-onset obesity. *Neuroreport.* 2008;19(9):951-955.
215. Camerino C. Low sympathetic tone and obese phenotype in oxytocin-deficient mice. *Obesity (Silver Spring).* 2009;17(5):980-984.

216. Wu Z, Xu Y, Zhu Y, et al. An obligate role of oxytocin neurons in diet induced energy expenditure. *PLoS One.* 2012;7(9):e45167.
217. Biag J, Huang Y, Gou L, et al. Cyto- and chemoarchitecture of the hypothalamic paraventricular nucleus in the C57BL/6J male mouse: a study of immunostaining and multiple fluorescent tract tracing. *J Comp Neurol.* 2012;520(1):6-33.
218. Holst JJ. The physiology of glucagon-like peptide 1. *Physiol Rev.* 2007;87(4):1409-1439.
219. Larsen PJ, Tang-Christensen M, Holst JJ, Orskov C. Distribution of glucagon-like peptide-1 and other preproglucagon-derived peptides in the rat hypothalamus and brainstem. *Neuroscience.* 1997;77(1):257-270.
220. Baggio LL, Drucker DJ. Biology of incretins: GLP-1 and GIP. *Gastroenterology.* 2007;132(6):2131-2157.
221. Fonseca VA, Zinman B, Nauck MA, Goldfine AB, Plutzky J. Confronting the type 2 diabetes epidemic: the emerging role of incretin-based therapies. *Am J Med.* 2010;123(7):S2-S10.
222. Sisley S, Gutierrez-Aguilar R, Scott M, D'Alessio DA, Sandoval DA, Seeley RJ. Neuronal GLP1R mediates liraglutide's anorectic but not glucose-lowering effect. *J Clin Invest.* 2014;124(6):2456-2463.
223. Burmeister MA, Ayala J, Drucker DJ, Ayala JE. Central glucagon-like peptide 1 receptor-induced anorexia requires glucose metabolism-mediated suppression of AMPK and is impaired by central fructose. *Am J Physiol Endocrinol Metab.* 2013;304(7):E677-685.
224. Schick RR, Zimmermann JP, vorm Walde T, Schusdziarra V. Peptides that regulate food intake: glucagon-like peptide 1-(7-36) amide acts at lateral and medial hypothalamic sites to suppress feeding in rats. *Am J Physiol Regul Integr Comp Physiol.* 2003;284(6):R1427-1435.
225. Donahey JC, van Dijk G, Woods SC, Seeley RJ. Intraventricular GLP-1 reduces short- but not long-term food intake or body weight in lean and obese rats. *Brain Res.* 1998;779(1-2):75-83.
226. Adams JM, Pei H, Sandoval DA, et al. Liraglutide Modulates Appetite and Body Weight Through Glucagon-Like Peptide 1 Receptor-Expressing Glutamatergic Neurons. *Diabetes.* 2018;67(8):1538-1548.
227. Beiroa D, Imbernon M, Gallego R, et al. GLP-1 agonism stimulates brown adipose tissue thermogenesis and browning through hypothalamic AMPK. *Diabetes.* 2014;63(10):3346-3358.
228. Secher A, Jelsing J, Baquero AF, et al. The arcuate nucleus mediates GLP-1 receptor agonist liraglutide-dependent weight loss. *J Clin Invest.* 2014;124(10):4473-4488.
229. Katsurada K, Maejima Y, Nakata M, et al. Endogenous GLP-1 acts on paraventricular nucleus to suppress feeding: projection from nucleus tractus solitarius and activation of corticotropin-releasing hormone, nesfatin-1 and oxytocin neurons. *Biochem Biophys Res Commun.* 2014;451(2):276-281.
230. Gaykema RP, Newmyer BA, Ottolini M, et al. Activation of murine pre-proglucagon-producing neurons reduces food intake and body weight. *J Clin Invest.* 2017;127(3):1031-1045.

231. Gu G, Roland B, Tomaselli K, Dolman CS, Lowe C, Heilig JS. Glucagon-like peptide-1 in the rat brain: distribution of expression and functional implication. *J Comp Neurol.* 2013;521(10):2235-2261.
232. Cork SC, Richards JE, Holt MK, Gribble FM, Reimann F, Trapp S. Distribution and characterisation of Glucagon-like peptide-1 receptor expressing cells in the mouse brain. *Mol Metab.* 2015;4(10):718-731.
233. McMahon LR, Wellman PJ. PVN infusion of GLP-1-(7-36) amide suppresses feeding but does not induce aversion or alter locomotion in rats. *Am J Physiol.* 1998;274(1):R23-29.
234. Ghosal S, Packard AEB, Mahbod P, et al. Disruption of Glucagon-Like Peptide 1 Signaling in Sim1 Neurons Reduces Physiological and Behavioral Reactivity to Acute and Chronic Stress. *J Neurosci.* 2017;37(1):184-193.
235. Fan CM, Kuwana E, Bulfone A, et al. Expression patterns of two murine homologs of Drosophila single-minded suggest possible roles in embryonic patterning and in the pathogenesis of Down syndrome. *Mol Cell Neurosci.* 1996;7(1):1-16.
236. Burmeister MA, Ayala JE, Smouse H, et al. The Hypothalamic Glucagon-Like Peptide 1 Receptor Is Sufficient but Not Necessary for the Regulation of Energy Balance and Glucose Homeostasis in Mice. *Diabetes.* 2017;66(2):372-384.
237. Liu J, Conde K, Zhang P, et al. Enhanced AMPA Receptor Trafficking Mediates the Anorexigenic Effect of Endogenous Glucagon-like Peptide-1 in the Paraventricular Hypothalamus. *Neuron.* 2017;96(4):897-909 e895.
238. Li C, Navarrete J, Liang-Guallpa J, et al. Defined Paraventricular Hypothalamic Populations Exhibit Differential Responses to Food Contingent on Caloric State. *Cell Metab.* 2019;29(3):681-694 e685.
239. Antoni FA. Vasopressinergic control of pituitary adrenocorticotropin secretion comes of age. *Front Neuroendocrinol.* 1993;14(2):76-122.
240. Leng G, Brown CH, Russell JA. Physiological pathways regulating the activity of magnocellular neurosecretory cells. *Prog Neurobiol.* 1999;57(6):625-655.
241. Stricker EM, Sved AF. Controls of vasopressin secretion and thirst: similarities and dissimilarities in signals. *Physiol Behav.* 2002;77(4-5):731-736.
242. Aguilera G, Pham Q, Rabadan-Diehl C. Regulation of pituitary vasopressin receptors during chronic stress: relationship to corticotroph responsiveness. *J Neuroendocrinol.* 1994;6(3):299-304.
243. Aguilera G, Rabadan-Diehl C. Vasopressinergic regulation of the hypothalamic-pituitary-adrenal axis: implications for stress adaptation. *Regul Pept.* 2000;96(1-2):23-29.
244. Aguilera G, Subburaju S, Young S, Chen J. The parvocellular vasopressinergic system and responsiveness of the hypothalamic pituitary adrenal axis during chronic stress. *Prog Brain Res.* 2008;170:29-39.
245. Thrasher TN. Baroreceptor regulation of vasopressin and renin secretion: low-pressure versus high-pressure receptors. *Front Neuroendocrinol.* 1994;15(2):157-196.
246. Salata RA, Jarrett DB, Verbalis JG, Robinson AG. Vasopressin stimulation of adrenocorticotropin hormone (ACTH) in humans. In vivo bioassay of

corticotropin-releasing factor (CRF) which provides evidence for CRF mediation of the diurnal rhythm of ACTH. *J Clin Invest.* 1988;81(3):766-774.
247. Gillies GE, Linton EA, Lowry PJ. Corticotropin releasing activity of the new CRF is potentiated several times by vasopressin. *Nature.* 1982;299(5881):355-357.
248. Benarroch EE. Oxytocin and vasopressin: social neuropeptides with complex neuromodulatory functions. *Neurology.* 2013;80(16):1521-1528.
249. Meyer AH, Langhans W, Scharrer E. Vasopressin reduces food intake in goats. *Q J Exp Physiol.* 1989;74(4):465-473.
250. Spruce BA, McCulloch AJ, Burd J, et al. The effect of vasopressin infusion on glucose metabolism in man. *Clin Endocrinol (Oxf).* 1985;22(4):463-468.
251. Wideman CH, Murphy HM. Modulatory effects of vasopressin on glucose and protein metabolism during food-restriction stress. *Peptides.* 1993;14(2):259-261.
252. Tsunematsu T, Fu LY, Yamanaka A, et al. Vasopressin increases locomotion through a V1a receptor in orexin/hypocretin neurons: implications for water homeostasis. *J Neurosci.* 2008;28(1):228-238.
253. Pei H, Sutton AK, Burnett KH, Fuller PM, Olson DP. AVP neurons in the paraventricular nucleus of the hypothalamus regulate feeding. *Mol Metab.* 2014;3(2):209-215.
254. Lechan RM, Fekete C. The TRH neuron: a hypothalamic integrator of energy metabolism. *Prog Brain Res.* 2006;153:209-235.
255. Joseph-Bravo P, Jaimes-Hoy L, Uribe RM, Charli JL. 60 YEARS OF NEUROENDOCRINOLOGY: TRH, the first hypophysiotropic releasing hormone isolated: control of the pituitary-thyroid axis. *J Endocrinol.* 2015;227(3):X3.
256. Joseph-Bravo P, Jaimes-Hoy L, Charli JL. Advances in TRH signaling. *Rev Endocr Metab Disord.* 2016;17(4):545-558.
257. Bianco AC, Salvatore D, Gereben B, Berry MJ, Larsen PR. Biochemistry, cellular and molecular biology, and physiological roles of the iodothyronine selenodeiodinases. *Endocr Rev.* 2002;23(1):38-89.
258. Zoeller RT, Kabeer N, Albers HE. Cold exposure elevates cellular levels of messenger ribonucleic acid encoding thyrotropin-releasing hormone in paraventricular nucleus despite elevated levels of thyroid hormones. *Endocrinology.* 1990;127(6):2955-2962.
259. Sanchez E, Uribe RM, Corkidi G, et al. Differential responses of thyrotropin-releasing hormone (TRH) neurons to cold exposure or suckling indicate functional heterogeneity of the TRH system in the paraventricular nucleus of the rat hypothalamus. *Neuroendocrinology.* 2001;74(6):407-422.
260. Uribe RM, Redondo JL, Charli JL, Joseph-Bravo P. Suckling and cold stress rapidly and transiently increase TRH mRNA in the paraventricular nucleus. *Neuroendocrinology.* 1993;58(1):140-145.
261. Cabral A, Valdivia S, Reynaldo M, Cyr NE, Nillni EA, Perello M. Short-term cold exposure activates TRH neurons exclusively in the hypothalamic paraventricular nucleus and raphe pallidus. *Neurosci Lett.* 2012;518(2):86-91.
262. Zhang Z, Boelen A, Kalsbeek A, Fliers E. TRH Neurons and Thyroid Hormone Coordinate the Hypothalamic Response to Cold. *Eur Thyroid J.* 2018;7(6):279-288.

263. Munzberg H, Qualls-Creekmore E, Berthoud HR, Morrison CD, Yu S. Neural Control of Energy Expenditure. *Handb Exp Pharmacol.* 2016;233:173-194.
264. Shintani M, Tamura Y, Monden M, Shiomi H. Thyrotropin-releasing hormone induced thermogenesis in Syrian hamsters: site of action and receptor subtype. *Brain Res.* 2005;1039(1-2):22-29.
265. Flier JS, Harris M, Hollenberg AN. Leptin, nutrition, and the thyroid: the why, the wherefore, and the wiring. *J Clin Invest.* 2000;105(7):859-861.
266. Nillni EA. Regulation of the hypothalamic thyrotropin releasing hormone (TRH) neuron by neuronal and peripheral inputs. *Front Neuroendocrinol.* 2010;31(2):134-156.
267. Nillni EA, Sevarino KA. The biology of pro-thyrotropin-releasing hormone-derived peptides. *Endocr Rev.* 1999;20(5):599-648.
268. Perello M, Cakir I, Cyr NE, et al. Maintenance of the thyroid axis during diet-induced obesity in rodents is controlled at the central level. *Am J Physiol Endocrinol Metab.* 2010;299(6):E976-989.
269. Toni R, Lechan RM. Neuroendocrine regulation of thyrotropin-releasing hormone (TRH) in the tuberoinfundibular system. *J Endocrinol Invest.* 1993;16(9):715-753.
270. Huo L, Munzberg H, Nillni EA, Bjorbaek C. Role of signal transducer and activator of transcription 3 in regulation of hypothalamic trh gene expression by leptin. *Endocrinology.* 2004;145(5):2516-2523.
271. Legradi G, Emerson CH, Ahima RS, Flier JS, Lechan RM. Leptin prevents fasting-induced suppression of prothyrotropin-releasing hormone messenger ribonucleic acid in neurons of the hypothalamic paraventricular nucleus. *Endocrinology.* 1997;138(6):2569-2576.
272. Legradi G, Emerson CH, Ahima RS, Rand WM, Flier JS, Lechan RM. Arcuate nucleus ablation prevents fasting-induced suppression of ProTRH mRNA in the hypothalamic paraventricular nucleus. *Neuroendocrinology.* 1998;68(2):89-97.
273. Guo F, Bakal K, Minokoshi Y, Hollenberg AN. Leptin signaling targets the thyrotropin-releasing hormone gene promoter in vivo. *Endocrinology.* 2004;145(5):2221-2227.
274. Nillni EA, Vaslet C, Harris M, Hollenberg A, Bjorbak C, Flier JS. Leptin regulates prothyrotropin-releasing hormone biosynthesis. Evidence for direct and indirect pathways. *J Biol Chem.* 2000;275(46):36124-36133.
275. Fekete C, Mihaly E, Luo LG, et al. Association of cocaine- and amphetamine-regulated transcript-immunoreactive elements with thyrotropin-releasing hormone-synthesizing neurons in the hypothalamic paraventricular nucleus and its role in the regulation of the hypothalamic-pituitary-thyroid axis during fasting. *J Neurosci.* 2000;20(24):9224-9234.
276. Fekete C, Sarkar S, Rand WM, et al. Neuropeptide Y1 and Y5 receptors mediate the effects of neuropeptide Y on the hypothalamic-pituitary-thyroid axis. *Endocrinology.* 2002;143(12):4513-4519.
277. Harris M, Aschkenasi C, Elias CF, et al. Transcriptional regulation of the thyrotropin-releasing hormone gene by leptin and melanocortin signaling. *J Clin Invest.* 2001;107(1):111-120.

278. Perello M, Stuart RC, Nillni EA. The role of intracerebroventricular administration of leptin in the stimulation of prothyrotropin releasing hormone neurons in the hypothalamic paraventricular nucleus. *Endocrinology.* 2006;147(7):3296-3306.
279. Enriori PJ, Evans AE, Sinnayah P, et al. Diet-induced obesity causes severe but reversible leptin resistance in arcuate melanocortin neurons. *Cell Metab.* 2007;5(3):181-194.
280. Munzberg H, Flier JS, Bjorbaek C. Region-specific leptin resistance within the hypothalamus of diet-induced obese mice. *Endocrinology.* 2004;145(11):4880-4889.
281. Krashes MJ, Shah BP, Madara JC, et al. An excitatory paraventricular nucleus to AgRP neuron circuit that drives hunger. *Nature.* 2014;507(7491):238-242.
282. Vale W, Spiess J, Rivier C, Rivier J. Characterization of a 41-residue ovine hypothalamic peptide that stimulates secretion of corticotropin and beta-endorphin. *Science.* 1981;213(4514):1394-1397.
283. Rivier C, Vale W. Modulation of stress-induced ACTH release by corticotropin-releasing factor, catecholamines and vasopressin. *Nature.* 1983;305(5932):325-327.
284. Munck A, Guyre PM, Holbrook NJ. Physiological functions of glucocorticoids in stress and their relation to pharmacological actions. *Endocr Rev.* 1984;5(1):25-44.
285. Bamberger CM, Schulte HM, Chrousos GP. Molecular determinants of glucocorticoid receptor function and tissue sensitivity to glucocorticoids. *Endocr Rev.* 1996;17(3):245-261.
286. Drescher VS, Chen HL, Romsos DR. Corticotropin-releasing hormone decreases feeding, oxygen consumption and activity of genetically obese (ob/ob) and lean mice. *J Nutr.* 1994;124(4):524-530.
287. McGill BE, Bundle SF, Yaylaoglu MB, Carson JP, Thaller C, Zoghbi HY. Enhanced anxiety and stress-induced corticosterone release are associated with increased Crh expression in a mouse model of Rett syndrome. *Proc Natl Acad Sci U S A.* 2006;103(48):18267-18272.
288. Bruhn TO, Plotsky PM, Vale WW. Effect of paraventricular lesions on corticotropin-releasing factor (CRF)-like immunoreactivity in the stalk-median eminence: studies on the adrenocorticotropin response to ether stress and exogenous CRF. *Endocrinology.* 1984;114(1):57-62.
289. Bale TL, Vale WW. CRF and CRF receptors: role in stress responsivity and other behaviors. *Annu Rev Pharmacol Toxicol.* 2004;44:525-557.
290. Li MM, Madara JC, Steger JS, et al. The Paraventricular Hypothalamus Regulates Satiety and Prevents Obesity via Two Genetically Distinct Circuits. *Neuron.* 2019;102(3):653-667 e656.
291. Duplan SM, Boucher F, Alexandrov L, Michaud JL. Impact of Sim1 gene dosage on the development of the paraventricular and supraoptic nuclei of the hypothalamus. *Eur J Neurosci.* 2009;30(12):2239-2249.
292. Sadagurski M, Dong XC, Myers MG, Jr., White MF. Irs2 and Irs4 synergize in non-LepRb neurons to control energy balance and glucose homeostasis. *Mol Metab.* 2014;3(1):55-63.

293. Chait A, Suaudeau C, De Beaurepaire R. Extensive brain mapping of calcitonin-induced anorexia. *Brain Res Bull.* 1995;36(5):467-472.
294. Cheng W, Gonzalez I, Pan W, et al. Calcitonin Receptor Neurons in the Mouse Nucleus Tractus Solitarius Control Energy Balance via the Non-aversive Suppression of Feeding. *Cell Metab.* 2020;31(2):301-312 e305.
295. Geerling JC, Shin JW, Chimenti PC, Loewy AD. Paraventricular hypothalamic nucleus: axonal projections to the brainstem. *J Comp Neurol.* 2010;518(9):1460-1499.
296. Cao WH, Madden CJ, Morrison SF. Inhibition of brown adipose tissue thermogenesis by neurons in the ventrolateral medulla and in the nucleus tractus solitarius. *Am J Physiol Regul Integr Comp Physiol.* 2010;299(1):R277-290.
297. Fyda DM, Cooper KE, Veale WL. Modulation of brown adipose tissue-mediated thermogenesis by lesions to the nucleus tractus solitarius in the rat. *Brain Res.* 1991;546(2):203-210.

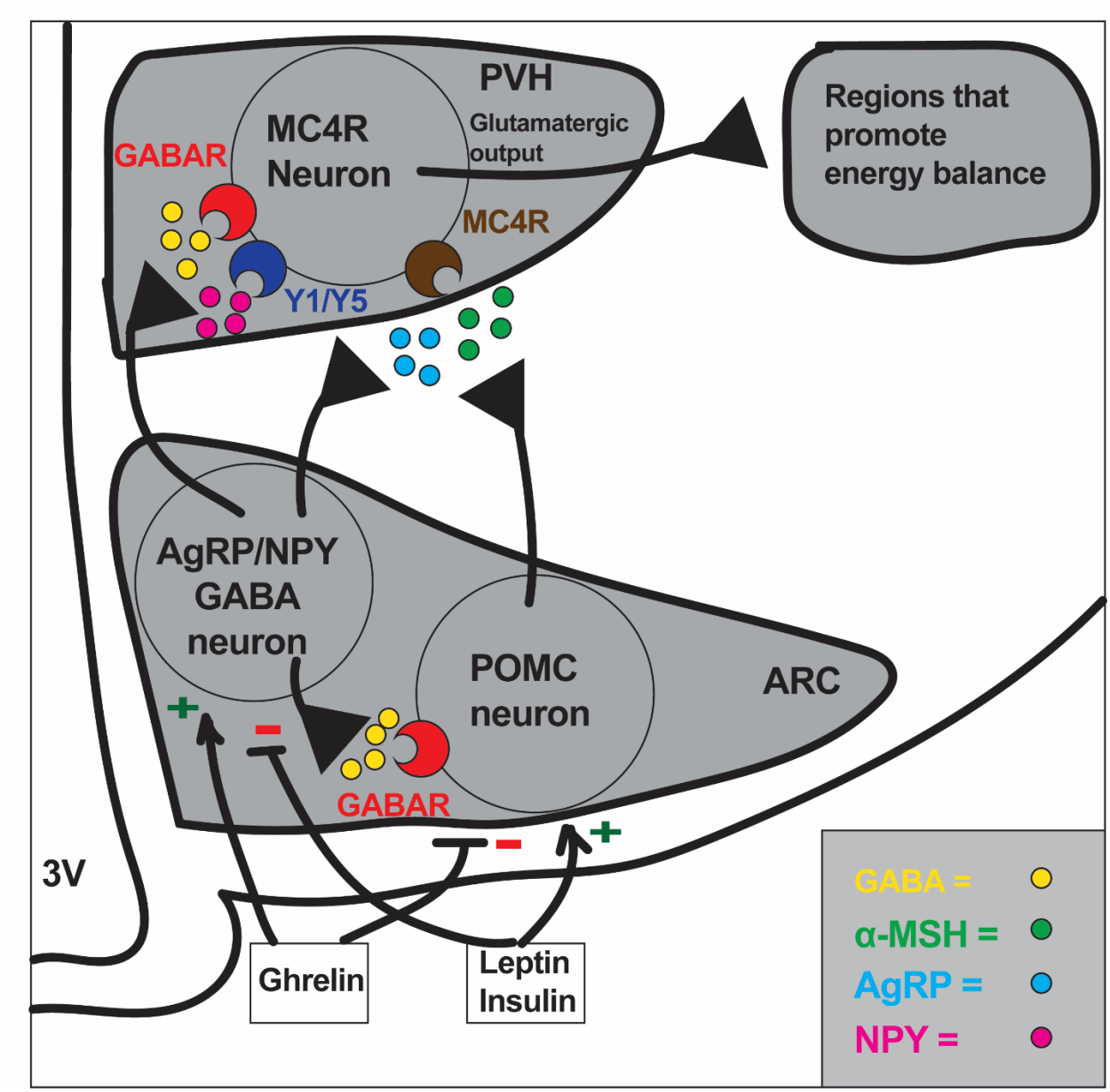

Figure 1.1: Melanocortin signaling through the ARC to PVH circuit. The ARC contains neurons that co-express AgRP, NPY and GABA as well as POMC neurons. The AgRP/NPY/GABA neurons promote food intake through downstream receptors in the PVH, while the POMC neurons generate the anorectic α-MSH to suppress food

intake through interaction through activation of the MC4R expressing neurons in the PVH. AgRP acts as an antagonist for the MC4R receptor, blocking the activities of α-MSH while NPY increases feeding through interaction with Y1 and Y5 receptors in the PVH. Stimulation of the $MC4R^{PVH}$ neurons with α-MSH activates efferent outputs to regions in the hypothalamus and hindbrain to mediate food intake behavior and the regulation of body weight. AgRP/NPY neurons also produce the neurotransmitter GABA, which inhibits $POMC^{ARC}$ neurons to suppress α-MSH secretion from POMC neurons. AgRP/NPY/GABA neurons of the ARC and $MC4R^{PVH}$ neurons express GHSR, ObR and INSR. Ghrelin functions to stimulate AgRP/NPY/GABA neurons, while it inhibits the activities of POMC neurons in the ARC. Conversely, insulin and leptin promote POMC activity and inhibit AgRP/NPY/GABA neurons. 3V= third ventricle, ARC= arcuate nucleus, PVH= paraventricular nucleus of the hypothalamus.

Chapter 2

Paraventricular, Subparaventricular and Periventricular Hypothalamic IRS4-Expressing Neurons are Required for Normal Energy Balance[1]

Abstract

Understanding the neural components modulating feeding-related behavior and energy expenditure is crucial to combating obesity and its comorbidities. Neurons within the paraventricular nucleus of the hypothalamus (PVH) are a key component of the satiety response; activation of the PVH decreases feeding and increases energy expenditure, thereby promoting negative energy balance. In contrast, PVH ablation or silencing in both rodents and humans leads to substantial obesity. Recent studies have identified genetically-defined PVH subpopulations that control discrete aspects of energy balance (e.g. oxytocin (OXT), neuronal nitric oxide synthase 1 (NOS1), melanocortin 4-receptor (MC4R), prodynorphin (PDYN)). We previously demonstrated that non-OXT $NOS1^{PVH}$ neurons contribute to PVH-mediated feeding suppression. Here, we identify and characterize a non-OXT, non-NOS1 subpopulation of PVH and peri-PVH neurons expressing insulin-receptor substrate 4 ($IRS4^{PVH}$) involved in energy balance control.

[1] Chapter 2 was previously published in Scientific Reports – Nature: Sutton AK, **Gonzalez IE**, Sadagurski M, et al. Paraventricular, subparaventricular and periventricular hypothalamic IRS4-expressing neurons are required for normal energy balance. Sci Rep. 2020;10(1):5546.

Using Cre-dependent viral tools to activate, trace and silence these neurons, we highlight the sufficiency and necessity of IRS4^{PVH} neurons in normal feeding and energy expenditure regulation. Furthermore, we demonstrate that IRS4^{PVH} neurons lie within a complex hypothalamic circuitry that engages distinct hindbrain regions and is innervated by discrete upstream hypothalamic sites. Overall, we reveal a requisite role for IRS4^{PVH} neurons in PVH-mediated energy balance which raises the possibility of developing novel approaches targeting IRS4^{PVH} neurons for anti-obesity therapies.

Introduction

Genetic polymorphisms associated with obesity are disproportionately clustered in pathways affecting neural function and architecture in the central nervous system (CNS).[1] Within the brain, the paraventricular nucleus of the hypothalamus (PVH) is a primary hypothalamic node that integrates neural and humoral information regarding energy balance and sends output signals to structures in the hindbrain and spinal cord to control satiety and energy expenditure.[2-4] Dysregulation of the entire PVH with site-directed lesions or inhibition of PVH melanocortin-4 receptor (MC4R) action produce profound obesity.[5-7] However, while disruption of MC4R^{PVH} activity leads to obesity due to hyperphagia, lesions of the entire PVH are associated with both feeding and energy expenditure dysregulation.[7-9] While MC4R^{PVH} activity is necessary and sufficient to alter feeding behavior, MC4R action in the PVH cannot be ascribed to neural populations expressing oxytocin (OXT), vasopressin (AVP), or corticotropin-releasing hormone (CRH).[7] Manipulation of other PVH populations, such as neuronal nitric oxide synthase

1 ($NOS1^{PVH}$) neurons, is sufficient to alter both feeding and energy expenditure.[10] This raises the possibility that distinct PVH cell types might independently or coordinately regulate feeding and/or energy expenditure. Even though substantial efforts have been made to define PVH neuronal populations and their distinct roles in energy balance control, few studies have revealed PVH populations that are capable of regulating multiple aspects of energy balance (i.e. energy expenditure and feeding), apart from the $NOS1^{PVH}$ population.

Nos1 expression marks a relatively large percentage of PVH neurons that send projections to hindbrain and spinal cord sites. Chemogenetic activation of $NOS1^{PVH}$ neurons suppresses feeding and increases energy expenditure by promoting both increased physical activity and thermogenesis.[10] OXT^{PVH} neurons are almost entirely contained within the $NOS1^{PVH}$ field, yet their activation drives only small changes in energy expenditure and does not suppress feeding.[10] $NOS1^{PVH}$-dependent changes in energy expenditure are likely independent of MC4R-signaling in the PVH, since activation of $MC4R^{PVH}$ neurons suppresses feeding but does not affect energy expenditure and selective PVH expression of Mc4R in an otherwise Mc4R-null background has little impact on energy expenditure.[8,11] Given the important contribution of both energy expenditure and feeding dysregulation in the development of obesity, the identification of distinct targets that have the capability to modulate both aspects of energy balance is particularly pertinent.

Recent reports indicate that insulin receptor substrate-4 (IRS4) acts in synergy with insulin receptor substrate-2 (IRS2) in the hypothalamus to maintain normal bodyweight.[12] We discovered that Irs4 is expressed in and adjacent to the PVH and that

the paraventricular and periventricular IRS4-expressing cell population (referred to as IRS4^{PVH}) is both necessary and sufficient for normal feeding and bodyweight, suggesting a functional role for PVH and peri-PVH Irs4-expressing neurons in the control of energy homeostasis. Additionally, we find that NTS-projecting and PBN-projecting IRS4^{PVH} neurons are densely innervated by local PVH neurons, supporting a role for an intra-PVH network in the regulation of energy balance. Monosynaptic afferent neural tracing suggests that the inputs to IRS4^{PVH} neurons vary depending on the brain regions to which an IRS4^{PVH} subset projects. Overall, our study proposes a novel framework for the regulation of bodyweight consisting of multiple interconnected PVH populations that are potentially under independent control to modulate distinct energy balance parameters including feeding and energy expenditure.

Results

Irs4 expression marks a distinct PVH subpopulation

Hypothalamic IRS4 and IRS2 synergistically contribute to body weight maintenance.[12] Since in situ hybridization (Allen Mouse Brain Atlas[13]) reveals dense Irs4 expression in and adjacent to the PVH, we sought to determine the role of IRS4^{PVH} neurons in energy homeostasis using Cre-dependent technologies in combination with a novel IRS4-iCre knock-in mouse model in which Cre recombinase expression is tethered to Irs4 (Figure 2.1 A). The Irs4 gene is located on the X chromosome. Since random X inactivation may lead to variable Cre activity in female mice, male mice were used exclusively in all studies. In situ hybridization of both Cre and Irs4 mRNA in the PVH of IRS4-iCre mice

was used to verify the appropriate expression of Cre recombinase in the IRS4-iCre mouse line and demonstrated substantial overlap of Irs4 and Cre mRNA transcripts in the PVH (Figure 2.1 B). To investigate $IRS4^{PVH}$ neuron overlap with other known PVH populations, $IRS4^{PVH}$ neurons were labeled by injection of a Cre-dependent GFP reporter virus into the PVH of IRS4-iCre mice (Figure 2.1 C). This approach eliminates the possibility of overrepresentation of the $IRS4^{PVH}$ reporter population due to developmental Irs4 expression and aligns with subsequent Cre-dependent viral technologies used to manipulate $IRS4^{PVH}$ neurons in adult mice. Brains stained for GFP (indicating IRS4-iCre activity) and neurophysin I, the carrier protein for oxytocin, indicate that adult $IRS4^{PVH}$ neurons do not substantially overlap with OXT^{PVH} neurons (Figure 2.1 D). To determine if $IRS4^{PVH}$ neurons are contained within the $NOS1^{PVH}$ population, we stained brain slices from IRS4-iCre mice injected with AAV-Flex-GFP for NOS1 peptide and GFP and found that $IRS4^{PVH}$ neurons are a separate population from $NOS1^{PVH}$ cells (Figure 2.1 E). As AVP^{PVH} neurons are also able to modestly control feeding, we examined the overlap of AVP and IRS4 within the PVH.[14] Indeed, GFP-identified PVH neurons representing IRS4-iCre activity do not overlap substantially with immunoreactivity for copeptin, the carrier molecule for AVP (Figure 2.1 F). To investigate the potential overlap between $IRS4^{PVH}$ neurons and other subpopulations of the PVH recently reported to contribute to energy homeostasis, we conducted in situ hybridization for Irs4 mRNA in combination with Crh, Pdyn, and thyrotropin-releasing hormone (Trh) mRNAs (Figure 2.2). The majority of $IRS4^{PVH}$ neurons do not express Crh (9.76 + 2.94% of $IRS4^{PVH}$ with Crh, n = 3 mice) or Pdyn (15.77 + 1.19% of $IRS4^{PVH}$ with Pdyn, n = 3 mice), and a modest fraction of CRH^{PVH} and $PDYN^{PVH}$ neurons express

Irs4 mRNA (26.08 + 2.38% and 28.14 + 7.43% respectively). We do find that some IRS4^{PVH} neurons express Trh (40.54 + 1.10%), and more than half of the TRH^{PVH} neuronal population expresses Irs4 mRNA (60.43 + 3.14%). Taken together, these data suggest that Irs4 expression marks a circumscribed population of PVH neurons defined by the relative absence of OXT, AVP, and NOS1, but some overlap with CRH, PDYN, and TRH.

IRS4^{PVH} neurons are capable of regulating both feeding and energy expenditure

Given the published role of IRS4 in energy homeostasis and its expression in the PVH, we sought to determine the ability of these neurons to regulate distinct aspects of energy balance. To achieve this, we employed Cre-dependent DREADD (Designer Receptors Exclusively Activated by Designer Drugs) viruses to acutely modulate neuronal activity in response to peripheral injection of an otherwise inert compound, clozapine N-oxide (CNO).[15] To achieve remote activation of IRS4^{PVH} neurons, we performed bilateral PVH injections of AAV-Flex-hM3Dq in IRS4-iCre mice (Figure 2.3 A,B). Following recovery, PVH-directed AAV-Flex-hM3Dq injected IRS4-iCre mice were fasted during the day and injected with either vehicle or CNO at the onset of the dark cycle, a time when feeding normally occurs. Activation of IRS4^{PVH} neurons results in robust suppression of feeding (Figure 2.3 C, $p = 0.0005$, paired t-test, $t = 5.680$). Feeding effects are not attributable to CNO or its metabolites as a separate cohort of wildtype mice injected with AAV-Flex-hM3Dq failed to suppress feeding with no change in nuclear Fos expression following injection of CNO (Figure 2.4 A,B). As pan-activation of PVH neurons suppresses feeding and increases energy expenditure, we placed

IRS4^{PVH} mice injected with AAV-Flex-hM3Dq in metabolic chambers to measure energy expenditure and locomotor activity following CNO-mediated activation.[10] In the absence of food, activation of IRS4^{PVH} neurons increases energy expenditure, VO2 and total activity without a significant change in RER (Figure 2.3 D–H; VO2: $p = 0.0027$, $t = 4.897$; VO2 lean body mass (LBM): $p = 0.0025$, $t = 5.001$; Energy Expenditure $p = 0.0026$, $t = 4.946$; total X activity: $p = 0.0007$, $t = 6.297$; all paired t-test). To examine the effect of IRS4^{PVH} activation on resting energy expenditure (REE), we measured VO2 at timepoints before and after CNO injection in which physical activity was similar (Figure 2.3 I–K), as performed previously.[10] This demonstrates that IRS4^{PVH} activation results in increased VO2 (normalized to bodyweight or LBM) that is independent of increased physical activity (VO2 REE $p = 0.0022$, $t = 5.113$; VO2/LBM $p = 0.0019$, $t = 5.254$). Thus, activation of IRS4^{PVH} neurons suppresses dark-cycle feeding and promotes energy expenditure in the absence of food.

IRS4^{PVH} neurons project to hindbrain and spinal cord regions

To identify the neural circuits engaged by IRS4^{PVH} neurons, we used injection of a Cre-dependent adenovirus, synaptophysin-mCherry (syn-mCherry) in the PVH area to label the IRS4^{PVH} synaptic terminals. Unilateral injection of syn-mCherry (Figure 2.5 A) in the PVH area of IRS4-iCre mice identifies robust IRS4^{PVH} projections to hindbrain projection targets including the parabrachial nucleus (PBN, Figure 2.5 B), nucleus of the solitary tract (NTS), and the dorsal motor nucleus of the vagus (DMV) (Figure 2.5 C). IRS4^{PVH} neurons also send projections to the median eminence, a site important for endocrine control of pituitary function (Figure 2.5 D). In addition to hindbrain regions, syn-mCherry

projections were identified in the intermediolateral column (IML) of the thoracic spinal cord in close proximity to choline acetyltransferase (ChAT)-producing neurons, suggesting a circuit mechanism for the regulation of sympathetic activity by IRS4^{PVH} neurons (Figure 2.5 E). Of note, these results are strikingly similar to projections originating from NOS1^{PVH} neurons, despite the fact that these populations do not appear to overlap in the PVH.[10]

Projection-specific modified rabies tracing identifies unique inputs to IRS4^{PVH} subpopulations

As IRS4^{PVH} neurons project to various brain regions implicated in feeding and energy expenditure, we hypothesized that the afferent input to distinct IRS4^{PVH} circuits might differ based on IRS4^{PVH} neuronal projection site. To test this hypothesis, we labeled monosynaptic inputs to either NTS-projecting or PBN-projecting IRS4^{PVH} neurons in the same animal using a modified rabies virus approach that requires Cre-dependent helper virus (AAV-Flex-TVA-B19G) expression. Due to the limited efficacy and applicability of available helper virus reagents for our desired approach, we generated a Cre-dependent helper virus that co-expresses both the TVA receptor and B19 glycoprotein (B19G) via a self-cleaving 2A peptide linker (Figure 2.6 A). Modified rabies virus (EnvA-ΔG-mCherry (rabies-mCherry, Figure 2.6 B) or EnvA-ΔG-GFP (rabies-GFP, Figure 2.6C)) cannot enter cells without the TVA receptor and is modified to express a fluorescent protein (mCherry or GFP) instead of B19G.[16,17] Therefore, infection of the modified rabies virus requires viral expression of the TVA receptor and retrograde transport of rabies-mCherry or rabies-GFP requires viral expression of the B19G (Figure

2.6 D). The fidelity of this system is demonstrated by a lack of rabies-mCherry expression in the brain of Sim1-Cre mice in which the helper virus injection missed the PVH (determined by a lack of 2A staining in the PVH), despite rabies-mCherry injection into the NTS (Figure 2.7 A,B). In this approach, neurons upstream of primary infected neurons theoretically do not express Cre recombinase, and therefore do not produce B19G; this limits rabies-mCherry or rabies-GFP expression to monosynaptic inputs to $IRS4^{PVH}$ neurons.

Cre-dependent expression of the TVA receptor throughout the cell body and synaptic terminals of transduced neurons allows terminal-specific rabies infection.[18] To determine if subpopulations of $IRS4^{PVH}$ neurons might be engaged by discrete afferent inputs, we performed dual rabies virus injections at anatomically separable projection targets in the same mouse (Figure 2.6 D). Three weeks following helper virus injection, rabies-mCherry was injected in the NTS whereas rabies-GFP was injected in the PBN. Following 5 days of incubation, we found that $IRS4^{PVH}$ neurons that project to the NTS or PBN are largely distinct as evidenced by the lack of significant fluorescence colocalization in the PVH (colocalized cells: $n = 27 \pm 5.7$ cells, $n = 2$ mice). The fact that some co-localization between GFP and mCherry occurs in the PVH suggests the existence of PVH neurons capable of regulating both the NTS and PBN presumably either through collateralization or intra-PVH microcircuitry (Figure 2.6 E–G).

Consistent with published literature examining PVH circuitry, our rabies monosynaptic labeling demonstrates that the arcuate nucleus (ARC) is an upstream site of NTS-projecting $IRS4^{PVH}$ neurons (Figure 2.6 H,H^{II}).[19] Additional hypothalamic sites engaging NTS-projecting $IRS4^{PVH}$ neurons include the lateral hypothalamic area (LHA, Figure 2.6

H^{I}) and the dorsomedial hypothalamus (DMH, Figure 2.6 H), whereas sites upstream of PBN-projecting IRS4^{PVH} neurons largely include the ventromedial hypothalamus (VMH) and LHA (Figure 2.6 H). Although monosynaptic rabies tracing is not a quantitative methodology, a small number of LHA neurons co-express GFP and mCherry, suggesting LHA modulation of both IRS4^{PVH}-PBN and IRS4^{PVH}-NTS circuits (Figure 2.6 H^{I}, n = 8 ± 11.3 cells, n = 2 mice). In contrast, very few afferent neurons in the ARC co-express GFP and mCherry (n = 2 ± 2.1 cells, n = 2 mice). Forebrain sites including the preoptic area (POA, Figure 2.6 L^{II}) and bed nucleus of the stria terminalis (BNST, Figure 2.6 L^{I}) include largely non-overlapping populations upstream of both IRS4^{PVH} circuits, suggesting distinct forebrain circuits may modulate IRS4^{PVH} neuronal function.

IRS4^{PVH} neurons are necessary for normal feeding and energy balance

To test the necessity of IRS4^{PVH} neuron activity in physiologic body weight regulation, we permanently silenced IRS4^{PVH} neurons using a Cre-dependent tetanus toxin virus (AAV-Flex-TetTox) that cleaves the SNARE protein, synaptobrevin, and inhibits synaptic vesicle release.[20] This construct has been modified to express the A subunit and does not travel retrogradely, therefore limiting neuronal silencing to IRS4 Cre-expressing neurons.[21] We performed bilateral PVH injections of AAV-Flex-TetTox in IRS4-iCre mice (Figure 2.8 A,B). In comparison to control Cre-dependent viral injections into the PVH of IRS4-iCre mice (PVH^{Flex}) or AAV-Flex-TetTox injections in the PVH of wildtype mice (WT^{TetTox}), mice with IRS4^{PVH} neuronal silencing show modest obesity within one week of injection (Figure 2.8 C: PVH^{TetTox} v. WT^{TetTox} p = 0.0162; Figure 2.8 D: PVH^{TetTox} v. WT^{TetTox} p = 0.0008, PVH^{TetTox} v. PVH^{Flex} p = 0.0003; mixed effects

analysis followed by Tukey's post-hoc). Obesity following elimination of IRS4^{PVH} signaling is likely driven primarily by early hyperphagia, demonstrated by increased food intake in the second week of the study (Figure 2.8 E, PVH^{TetTox} v. WT^{TetTox} $p = 0.0303$; one-way ANOVA followed by Tukey's post-hoc). Mice with silenced IRS4^{PVH} neurons demonstrate a non-significant trend towards decreased energy expenditure during the second and third weeks of the study (Figure 2.8 G,I,J, energy expenditure $p = 0.074$; RER $p = 0.075$; one-way ANOVA), without changes in total X activity (Figure 2.8H). Body composition analysis indicates that IRS4^{PVH} neuronal silencing leads to an increased fat percentage at both early (Figure 2.8 F, left; PVH^{TetTox} v. PVH^{Flex} $p = 0.0259$, one-way ANOVA followed by Tukey's post-hoc) and late (Figure 2.8 F, right; PVH^{TetTox} v. WT^{TetTox} $p = 0.0377$; one-way ANOVA followed by Tukey's post-hoc) time points after injection. Unilateral IRS4^{PVH} neuronal silencing was also associated with increased bodyweight throughout the course of the experiment, with trends toward similar effects on feeding and energy expenditure (Table 2.1, one-way ANOVA followed by Tukey's post-hoc if applicable)

IRS4^{PVH} neurons are dispensable for melanocortin-induced feeding suppression

Given the important role of the PVH in mediating melanocortin-induced satiety, and the identification of numerous ARC inputs to IRS4^{PVH} neurons, we hypothesized that IRS4^{PVH} neurons might contain melanocortin 4 receptors (MC4R) and participate in melanocortin agonist-induced anorexia. To test this, we performed in situ hybridization for Mc4r and Irs4 in wildtype mice (Figure 2.9 A). Although most IRS4^{PVH} neurons do not contain Mc4r mRNA (9.67% + 1.11% of IRS4^{PVH} with Mc4R, $n = 3$ mice), a

significant fraction of MC4RPVH neurons do express Irs4 mRNA (53.66% + 1.13%). To test the physiologic importance of melanocortin action in IRS4 neurons, we attempted to delete MC4R expression from IRS4 neurons by crossing IRS4-iCre and the Cre-dependent lox-Mc4R mouse line.[7] Unfortunately, developmental expression of Cre recombinase from the IRS4-iCre allele resulted in germline deletion of Mc4R (data not shown). We then tested the ability of the melanocortin agonist melanotan-II (MTII) to suppress dark cycle feeding in mice with AAV-Flex-TetTox or control injections in the PVH at 4–5 weeks post-injection. Despite the inability to transmit information from $IRS4^{PVH}$ neurons (and therefore a significant portion of $MC4R^{PVH}$ neurons), MTII injection (150 ug/mouse) still suppressed both two and four hour feeding in all cohorts of mice, suggesting that $IRS4^{PVH}$ neuron activity is not required for the melanocortin feeding response (Figure 2.9 B,C; two-way repeated measures ANOVA vehicle vs. MT2; two hour PVH^{TetTox} $p = 0.0312$, $t = 2.714$, WT^{TetTox} $p = 0.0001$, $t = 4.763$, PVH^{Flex} $p < 0.0001$, $t = 6.113$; four-hour PVH^{TetTox} $p = 0.0535$, $t = 2.486$, WT^{TetTox} $p = 0.0025$, $t = 3.681$, PVH^{Flex} $p = -0.0004$, $t = 4.355$).

Discussion

The combination of genetic mouse models with site-specific delivery of chemogenetic and optogenetic tools has greatly advanced our understanding of the role of the PVH in modulating energy balance through feeding and/or energy expenditure. Nonetheless, few studies have genetically identified specific PVH populations crucial for these functions. Our previous work suggests the importance of a non-OXT $Nos1^{PVH}$ population in feeding regulation.[10] Here, we identify a different (non-OXT and non-

NOS1^{PVH}) population expressing insulin receptor substrate-4 (Irs4) that is necessary for normal bodyweight maintenance.

Genetic deletion of Irs4 results in modest obesity and altered glucose homeostasis; whether this phenotype reflects simply a loss of Irs4 function or developmental compensation in response to Irs4 loss is unknown.[12,22] In our approach, we used site and temporal specific manipulations in adult organisms to circumvent developmental issues and directly examine the function of IRS4-expressing cells predominantly within the PVH. Whereas chemogenetic activation reveals the potential function of IRS4^{PVH} neuronal function in adult mice, neuronal silencing with tetanus toxin addresses the physiologic necessity of this population in various energy balance parameters. Indeed, permanent inhibition of IRS4^{PVH}-specific synaptic release results in obesity due to altered feeding and a trend toward lower energy expenditure.

An important caveat to this study flows from its methodologic approach. Stereotaxic injections to defined brain regions are not always exclusively limited to cells within a classically defined neuroanatomical region. In our study we have excluded data for physiologic analyses from animals with significant extra-PVH viral transduction. All analyses were performed using data from animals with limited extra-PVH viral expression. However, post-hoc immunocytochemistry of brain sections from analyzed animals revealed transduction of IRS4 Cre-expressing cells adjacent to the PVH. The contribution of these subparaventricular and periventricular IRS4 cells to the outputs measured cannot be determined from the current study. In our study there were no cases of PVH-targeted injections that were limited to just the subparaventricular or periventricular IRS4-expressing cells that would allow physiologic comparisons with the

PVH and peri-PVH-transduced cohort. Highly refined injections limited to cells solely in the PVH or solely in adjacent areas would be needed to completely define the contributions of these peri-PVH IRS4-expressing cells to energy balance control.

Cre-dependent efferent tract tracing suggests that the circuitries engaged by IRS4^{PVH} neurons used to regulate feeding and energy expenditure are similar to those identified for both NOS1^{PVH} and MC4R^{PVH} neurons and include the PBN and NTS and sparse projections to the spinal cord.[7,10,11] While our current studies cannot discriminate which projection site is relevant for controlling feeding and energy expenditure, it is possible that IRS4^{PVH} neurons projecting to the PBN contribute to feeding modulation since the PBN is the relevant output in MC4R-mediated feeding suppression.[11] However, our data indicate that IRS4^{PVH} neurons and MC4R^{PVH} neurons overlap only in part, and that MC4R-mediated feeding suppression is unaffected by IRS4^{PVH} neuronal silencing. Therefore, it remains possible that other projection output sites may drive the IRS4^{PVH}-mediated satiety response.

Given their minimal overlap in the PVH, the functional redundancy of the IRS4^{PVH} and NOS1^{PVH} neuronal populations in energy expenditure and feeding control is intriguing. A recent report suggests that nonoverlapping MC4R^{PVH} and PDYN^{PVH} neuron populations function together to coordinate a full PVH satiety response.[23] The contribution of other non-MC4R PVH neurons in energy expenditure control is less clear. Here, we demonstrate that despite neuronal silencing of IRS4^{PVH} neurons, which includes half of the MC4R^{PVH} population, the satiety response to the melanocortin agonist MT-II remains intact. Thus, the anorectic response to melanocortin agonist is not dependent on IRS4^{PVH} neurons, even though they compromise ~50% of the

MC4R^{PVH} population. Although most IRS4^{PVH} neurons do not express Pdyn, chemogenetic activation of IRS4^{PVH} will activate a subset of PDYN^{PVH} neurons. Whether this subset is responsible for the feeding effects seen following IRS4^{PVH} activation remains to be determined. IRS4 and TRH overlap significantly in the PVH. However, feeding suppression following IRS4^{PVH} activation is unlikely mediated by TRH^{PVH} neurons since activation of this population has been shown to promote feeding by targeting orexigenic AgRP neurons in the ARC.[24] Future studies will be needed to determine whether the IRS4/TRH^{PVH} subset modulates energy expenditure through direct effects on autonomic output or alterations in the pituitary-thyroid axis. In addition, whether distinct PVH populations control feeding and energy expenditure via disparate projection sites (e.g. PBN vs. NTS vs. spinal cord) requires additional investigation.

The PVH is a hypothalamic relay station for energy balance control. It receives dense innervation from sites critical for feeding and energy expenditure regulation, integrates this incoming energy balance information and then transmits an output signal to hindbrain sites to achieve appropriate physiologic and behavioral responses.[19,25-27] Whether PVH inputs can be mapped on to distinct PVH outputs (either anatomical or physiological) is not known. Here, we used monosynaptic rabies tracing to identify the possibility of unique afferent inputs to NTS-projecting versus PBN-projecting IRS4^{PVH} neurons. We demonstrate that NTS-projecting IRS4^{PVH} neurons receive dense innervation from the ARC, confirming this approach in a historically defined circuit. Additionally, PBN-projecting IRS4^{PVH} neurons receive innervation from the VMH. Given the role for direct PVH connections to the PBN in mediating MC4R-induced satiety, it is possible that the VMH-IRS4^{PVH}-PBN circuit is relevant in feeding control, though future

studies will be necessary to test the function of this circuit and better characterize its genetic signature.[11] It is of interest that a few LHA neurons appear to be upstream of both PBN and NTS-projecting IRS4^{PVH} neurons. Given the role for the LHA in controlling both energy expenditure and feeding behavior, this raises the possibility that the PVH input neurons originating in the LHA might be coordinating distinct energy balance parameters via divergent IRS4^{PVH} circuits.[28-30]

PVH neurons are predominantly glutamatergic and highly interconnected through PVH interneurons that may coordinate neural activity between PVH subsets.[31-33] Our modified rabies tracing findings suggest that projection-defined IRS4^{PVH} neurons are likely innervated by other local PVH populations based on the dense expression of rabies virus throughout the PVH (Figure 2.6 E–G). Since some PVH populations suppress feeding without affecting energy expenditure (i.e. MC4R^{PVH}), whereas others increase energy expenditure absent of feeding regulation (i.e. OXT^{PVH}), it seems likely that separate circuitries exist to coordinate these nodes. By extension, this suggests that some PVH populations (such as OXT^{PVH}) are differentially connected and/or insulated from other PVH circuits in terms of feeding regulation. One potential model for PVH action could include a final common output from the PVH that is responsible for coordinating feeding regulation. In such a scenario, NOS1^{PVH} and/or IRS4^{PVH} neurons might lie upstream of or parallel to MC4R^{PVH} neurons and coordinate feeding suppression via projections to the PBN. Certainly, connections between separate PVH populations are well documented.[34-36] Moreover, the dense PVH interconnectivity highlighted by projection-specific monosynaptic retrograde tracing suggests the possibility that anatomically and functionally separable IRS4^{PVH} neuronal circuits can be

coordinately regulated in order to promote an orchestrated physiologic output through simultaneous transmission to multiple brain sites.

Taken together, our results clearly demonstrate that IRS4^{PVH} neurons are a genetically defined PVH population capable of controlling feeding behavior and overall energy balance, presumably through projections to hindbrain and spinal cord regions. Moreover, tetanus toxin sensitive vesicle fusion in IRS4^{PVH} cells is essential in preventing hyperphagia and obesity. Furthermore, our studies support the concept of a complex, intra-PVH network that regulates hindbrain structures previously shown to control energy balance parameters. While the significance of this local communication between PVH subpopulations in the control of distinct aspects of energy balance remains to be elucidated, further characterization of the composition and connectivity of individual PVH populations is necessary to fully understand the control of feeding and energy expenditure by an essential hypothalamic output center.

Materials and Methods:

Experimental animals

IRS4-ires-Cre (IRS4-iCre) mice were generated using methods previously described.[37] Briefly, genomic DNA including the 3' UTR of the murine Irs4 gene was PCR amplified from R1 ES cells and cloned into a plasmid for insertion of an Frt-flanked neomycin selection cassette followed by an internal ribosomal entry sequence fused to a Cre recombinase transgene (iCre) between the STOP codon and the polyadenylation site. Constructs were linearized and electroporated into R1 ES cells by the University of

Michigan Transgenic Animal Model Core. Correctly targeted ES cells were identified by quantitative real-time PCR and Southern blots and then injected into C57Bl/6J blastocysts to generate chimeric animals. Chimeras were then bred to C57Bl/6J females to confirm germline transmission and generate the IRS4-neo-iCre mice. To remove the Frt-flanked neo cassette, IRS4-neo-iCre mice were then bred to Flp deleter mice (Jax 012930).

Adult male mice (8–16 weeks old) were used for all studies. Irs4 is located on the X-chromosome which confounds experiments using IRS4-iCre in females given the random lyonization of the X chromosome. All animals were bred and housed within our colony according to guidelines approved by the University of Michigan Committee on the Care and Use of Animals. Unless otherwise noted, mice were provided ad libitum access to food and water. All mice were acclimatized to intraperitoneal (i.p.) injections three days prior to any experimental i.p. injection.

Generation of modified rabies virus

Replication deficient modified rabies virus containing fluorescent reporters in place of the B19 glycoprotein (EnvA-ΔG-mCherry and EnvA-ΔG-GFP) were generated in the University of Michigan viral vector core using conditions previously described.[16,17]

Stereotaxic injections

Stereotaxic injections were performed in IRS4-iCre and non-transgenic (WT) mice as previously described.[10] Briefly, mice were placed in a digital stereotaxic frame (Model 1900, Kopf Instruments) under isofluorane and provided with pre-surgical analgesia. Viral injections were performed using a pressurized picospritzer system coupled to a pulled glass micropipette (coordinates from bregma: PVH: A/P = −0.500, M/L = +/− 0.220, D/V = −4.800). For tract tracing experiments, 50 nl of the adenoviral synatophysin-mCherry terminal tracer (Ad-iN/syn-mCherry[38]) was unilaterally injected in IRS4-iCre mice. For functional analysis of IRS4^{PVH} neurons, bilateral PVH injections of AAV-Flex-hM3Dq-mCherry (AAV-Flex-hM3Dq, purchased from UNC Vector Core), AAV-Flex-TetTox (purchased from the Stanford Viral Vector core) or control injections of AAV-Flex-GFP were performed in IRS4-iCre or WT mice (50 nl/side). For analysis of monosynaptic upstream inputs to IRS4^{PVH} neurons, IRS4-iCre mice were unilaterally injected with AAV-Flex-TVA-B19G in the PVH and allowed to recover for at least 21 days to ensure adequate helper virus expression throughout both cell bodies and terminals.[39] Mice then underwent a second surgery with dual stereotaxic injections into ipsilateral PVH projection targets with rabies-GFP in the PBN (A/P = −4.770, M/L = +/− 1.35, D/V = −2.8) and rabies-mCherry injected into the NTS. NTS injections were performed as previously described, whereby the fourth ventricle was identified and used as a geographic landmark to determine the site of injection.[10] A glass micropipette was lowered into the site (D/V: −0.550) and ~25 nl of virus was injected. Mice injected with the Ad-iN/syn-mCherry tracer were individually housed for five days following injection to allow for viral transduction and protein transport before perfusion, whereas

mice injected with modified rabies virus were perfused seven days following rabies virus injections. Mice injected with AAV-Flex-hM3Dq were allowed to recover for fourteen days following surgery before further experiments were performed.

Effect of PVH^{IRS4} neuronal activation on feeding and energy expenditure

Following recovery, IRS4-iCre + AAV-Flex-hM3Dq mice underwent feeding and energy expenditure assays as previously described.[10] Briefly, to measure changes in energy expenditure, IRS4-iCre + AAV-Flex-hM3Dq mice were acclimatized for two consecutive days to the Comprehensive Laboratory Monitoring System (CLAMS, Columbus Instruments) in the University of Michigan's Small Animal Phenotyping Core to obtain multi-parameter analysis including open circuit calorimetry and activity via optical beam breaks. Following acclimatization, food was removed from metabolic cages during the light cycle on experimental days beginning two hours prior to experiments. Mice received an i.p. injection of vehicle (10% β-cyclodextrin, Sigma) and CLAMS measurements were analyzed for the following four hours. Mice remained in the chambers with food access at the onset of the dark cycle and the experiment repeated at the same time the following day instead with i.p. injection of CNO (0.3 mg/kg in 10% B-cyclodextrin). While measurements were performed throughout the duration of the experiment, data shown are averaged over the 4 hours following injection of vehicle or CNO. Resting energy expenditure data shown was determined by analyzing data oxygen consumption values at data points in which activity levels were approximately matched during the four hours before and after CNO administration. In experiments aimed to identify feeding changes induced by IRS4^{PVH} neuronal activation, mice were

fasted during the day and received an i.p. injection of vehicle at the onset of the dark cycle with the presentation of food. Food intake was measured at two and four hours after injection and the experiment repeated the following day upon injection of CNO at the onset of the dark cycle. In a separate cohort of mice, the effects of CNO were tested on wildtype mice injected with AAV-Flex-hM3Dq and compared to IRS4-iCre mice injected with AAV-Flex-hM3Dq. In these experiments, CNO or vehicle (0.9% sodium chloride) injections were counterbalanced and performed 4 days apart.

Longitudinal bodyweight, food intake, and calorimetry measurements

Mice injected with AAV-Flex-TetTox or control viruses were allowed to recover for 7 days before weekly body weight and food intake measurements began. Energy expenditure was determined using the Comprehensive Laboratory Monitoring System (CLAMS, Columbus Instruments) in the University of Michigan's Small Animal Phenotyping Core to obtain multi-parameter analysis including open circuit calorimetry and activity via optical beam breaks between 11–24 days post-injection. Mice were allowed to acclimatize to the chambers for two days, followed by VO2 and locomotor activity data collection for three consecutive days. Analysis of CLAMS data was averaged across all three days of recording. Body composition analysis (Minispec LF90 II, Bruker Optics) was performed at both two weeks and 7 weeks following injection.

MT-II-induced feeding suppression

Five weeks following viral injection, IRS4-iCre mice injected with AAV-Flex-TetTox and appropriate controls were fasted during the light cycle (10:00–18:00). At the onset of the dark cycle, mice received an i.p. injection of 0.9% sodium chloride (APP Pharmaceuticals, 63323-186-10) or melanotan-II (MT-II, 150 ug/mouse, Bachem) and ad libitum access to food. Food intake was measured two and four hours post injection. The following week, injections were counter balanced and corresponding food intake measured.

Perfusion and Immunohistochemistry (IHC)

At the end of all experiments, mice were perfused to verify viral injection sites. Briefly, mice were deeply anesthetized with an overdose of pentobarbital (150 mg/kg, IP) and transcardially perfused with sterile PBS followed by 10% neutral buffered formalin or 4% paraformaldehyde (for perfusions with spinal cord removal. Brains and spinal cords (syn-mCherry injections only) were removed, post-fixed, and dehydrated in 30% sucrose before sectioning into 30 µm slices on a freezing microtome (Leica). Coronal brain sections were collected in four representative sections whereas longitudinal thoracic spinal cord sections were collected in three representative sections and stored at −20 °C. For 2A peptide and cFos immunohistochemistry (IHC), free floating brain and spinal cord sections were pretreated with 30% H2O2 to remove endogenous peroxidase activity and then blocked with normal goat or donkey serum and incubated in primary antibody overnight (rabbit anti-2A 1:1,000, Millipore ABE457; rabbit anti-cFos).

Detection of primary antibody was performed by avidin-biotin/diaminobenzidine (DAB) method (Biotin-SP-conjugated Donkey Anti-Rabbit, Jackson Immunoresearch, 1:200; ABC kit, Vector Labs; DAB reagents, Sigma). mCherry and choline acetyltransferase (ChAT) were detected using with primary antibodies for dsRed (rabbit 1:1000, Clontech, 632496) or TdTomato (rat, 1:1000, Kerafast 16D7) and ChAT (spinal cords only; goat, 1:500, Millipore AB144P) respectively followed by secondary immunofluorescence detection with donkey anti-rabbit-Alexa 568 or donkey anti-goat-Alexa 488 (1:200, Invitrogen). For PVH colocalization, rabies experiments, cFos (non-DAB method) and TetTox-GFP expression, IHC immunostaining was performed using primary antibodies for cFos (rabbit, 1:1000, Cell Signaling 9F6), GFP (rabbit 1:20,000, Invitrogen A6455), nNos1 (sheep 1:1500, (24), kindly provided by Dr. Vincent Prevot), neurophysin (goat, 1:1000, Santa Cruz Biotechnology, sc-7810) and copeptin (goat 1:1000, Santa Cruz Biotechnology, sc-7812). For all AAV-TetTox and AAV-hM3Dq injections, bilateral or unilateral PVH hit sites were verified and misses eliminated from data analysis, with viral injections that modestly leaked into the peri-PVH included in the PVH groups. Viral leak into any other area outside of this region were excluded. Imaging was performed using an Olympus BX-53 upright microscope with G6000 camera.

In situ hybridization

Mice were deeply anesthetized with an overdose of inhaled isofluorane and brains removed and flash frozen in 2-methylbutane. Brains were sectioned into 16 µm sections onto glass slides using a cryostat (Leica CM 1950) and stored at −80 °C. The probes were purchased from Advanced Cell Diagnostics, and the assays were performed

according to the manufacturer's protocol. The sections were fixed in cold 10% formalin for 1 hour, followed by dehydration in 50% and 75% ethanol for 5 minutes each, and 100% ethanol twice. Sections were dried at 40 °C for 30 minutes. For fluorescent staining, sections were pretreated in protease IV for 30 minutes, washed in PBS twice, and then incubated with the desired probes for 2 hours and then washed twice in 1x wash buffer (ACD, 310091) for 2 minutes each. Amplification and detection steps were performed using the RNAscope® Fluorescent Multiplex Reagent Kit (320850). Sections were incubated with Amp1 for 30 min, Amp2 for 15 min, Amp3 for 30 min, and Amp 4 Alt C for 15 min. There were 2 washes between each amplification, and all amplifications were performed at 40 °C in the EZ Hybridization oven. To demonstrate overlapping expression of IRS4 and Cre mRNA, IRS4 and Cre probes were used. To quantify overlapping expression of IRS4 and CRH, PDYN and TRH, fluorescent probes were used. For the tissues exposed to the IRS4, CRH, PDYN, TRH and Cre probes, the slides were stained with DAPI for 30 seconds before coverslipping using Prolong Gold antifade reagent (Invitrogen). To investigate MC4R and IRS4 expression in the PVH, chromogen staining was conducted using the RNAscope® 2.5 HD Duplex Reagent Kit (ACD 320701). The sections were treated with H2O2 for 10 min and then incubated with the protease K IV for 30 min. After hybridization with probes against MC4R and IRS4 mRNA, the sections were washed 2 times, followed with amplification from Amp1 to Amp6 with 2 washes in between. To detect the red signal component, Red-B was diluted 1:60 in component Red-A and incubated on the tissue for 10 minutes at room temperature. Slides were then rinsed two times in wash buffer to stop the chromogen reaction. Amplification continued with Amp7 through Amp10, followed by detection of

the green signal, which was achieved by diluting component Green-B 1:50 in component Green-A and incubating for 10 minutes at room temperature. Counterstaining was performed by immersing the slides in 50% hematoxylin for 30 seconds. The slides were then dried and mounted in VectaMount mounting medium (Vector Laboratories, INC). Imaging for fluorescent staining was performed using an Olympus BX-53 microscope with a G6000 camera. Imaging for the chromogen staining used an Olympus BX-51 microscope with a DP80 camera (Olympus). For the purposes of quantification, images from the coronal sections were processed uniformly using Photoshop (Adobe) to remove background and to mark cells that expressed a given probe. Cells (indicated by DAPI/hematoxylin stain) determined to be positive for each probe were quantified using ImageJ and summed for each mouse, with the percentages of overlapping expression averaged between the mice.

Statistical analysis

Paired t-tests, one-way ANOVAs followed by Tukey post-hoc tests (if applicable), two-way ANOVAs followed by Sidak's multiple comparisons (if applicable), or mixed model analyses were calculated using GraphPad Prism 8 as appropriate. Significance was determined for $p < 0.05$.

References:

1. Locke AE, Kahali B, Berndt SI, et al. Genetic studies of body mass index yield new insights for obesity biology. *Nature.* 2015;518(7538):197-206.
2. Sawchenko PE, Swanson LW. Immunohistochemical identification of neurons in the paraventricular nucleus of the hypothalamus that project to the medulla or to the spinal cord in the rat. *J Comp Neurol.* 1982;205(3):260-272.
3. Schwartz MW, Woods SC, Porte D, Jr., Seeley RJ, Baskin DG. Central nervous system control of food intake. *Nature.* 2000;404(6778):661-671.
4. Caverson MM, Ciriello J, Calaresu FR. Paraventricular nucleus of the hypothalamus: an electrophysiological investigation of neurons projecting directly to intermediolateral nucleus in the cat. *Brain Res.* 1984;305(2):380-383.
5. Gold RM. Hypothalamic obesity: the myth of the ventromedial nucleus. *Science.* 1973;182(4111):488-490.
6. Sims JS, Lorden JF. Effect of paraventricular nucleus lesions on body weight, food intake and insulin levels. *Behav Brain Res.* 1986;22(3):265-281.
7. Shah BP, Vong L, Olson DP, et al. MC4R-expressing glutamatergic neurons in the paraventricular hypothalamus regulate feeding and are synaptically connected to the parabrachial nucleus. *Proc Natl Acad Sci U S A.* 2014;111(36):13193-13198.
8. Balthasar N, Dalgaard LT, Lee CE, et al. Divergence of melanocortin pathways in the control of food intake and energy expenditure. *Cell.* 2005;123(3):493-505.
9. Xi D, Gandhi N, Lai M, Kublaoui BM. Ablation of Sim1 neurons causes obesity through hyperphagia and reduced energy expenditure. *PLoS One.* 2012;7(4):e36453.
10. Sutton AK, Pei H, Burnett KH, Myers MG, Jr., Rhodes CJ, Olson DP. Control of food intake and energy expenditure by Nos1 neurons of the paraventricular hypothalamus. *J Neurosci.* 2014;34(46):15306-15318.
11. Garfield AS, Li C, Madara JC, et al. A neural basis for melanocortin-4 receptor-regulated appetite. *Nat Neurosci.* 2015;18(6):863-871.
12. Sadagurski M, Dong XC, Myers MG, Jr., White MF. Irs2 and Irs4 synergize in non-LepRb neurons to control energy balance and glucose homeostasis. *Mol Metab.* 2014;3(1):55-63.
13. Lein ES, Hawrylycz MJ, Ao N, et al. Genome-wide atlas of gene expression in the adult mouse brain. *Nature.* 2007;445(7124):168-176.
14. Pei H, Sutton AK, Burnett KH, Fuller PM, Olson DP. AVP neurons in the paraventricular nucleus of the hypothalamus regulate feeding. *Mol Metab.* 2014;3(2):209-215.
15. Alexander GM, Rogan SC, Abbas AI, et al. Remote control of neuronal activity in transgenic mice expressing evolved G protein-coupled receptors. *Neuron.* 2009;63(1):27-39.
16. Wickersham IR, Lyon DC, Barnard RJ, et al. Monosynaptic restriction of transsynaptic tracing from single, genetically targeted neurons. *Neuron.* 2007;53(5):639-647.

17. Wall NR, Wickersham IR, Cetin A, De La Parra M, Callaway EM. Monosynaptic circuit tracing in vivo through Cre-dependent targeting and complementation of modified rabies virus. *Proc Natl Acad Sci U S A.* 2010;107(50):21848-21853.
18. Betley JN, Cao ZF, Ritola KD, Sternson SM. Parallel, redundant circuit organization for homeostatic control of feeding behavior. *Cell.* 2013;155(6):1337-1350.
19. Cowley MA, Pronchuk N, Fan W, Dinulescu DM, Colmers WF, Cone RD. Integration of NPY, AGRP, and melanocortin signals in the hypothalamic paraventricular nucleus: evidence of a cellular basis for the adipostat. *Neuron.* 1999;24(1):155-163.
20. Verderio C, Coco S, Bacci A, et al. Tetanus toxin blocks the exocytosis of synaptic vesicles clustered at synapses but not of synaptic vesicles in isolated axons. *J Neurosci.* 1999;19(16):6723-6732.
21. McMahon HT, Foran P, Dolly JO, Verhage M, Wiegant VM, Nicholls DG. Tetanus toxin and botulinum toxins type A and B inhibit glutamate, gamma-aminobutyric acid, aspartate, and met-enkephalin release from synaptosomes. Clues to the locus of action. *J Biol Chem.* 1992;267(30):21338-21343.
22. Fantin VR, Wang Q, Lienhard GE, Keller SR. Mice lacking insulin receptor substrate 4 exhibit mild defects in growth, reproduction, and glucose homeostasis. *Am J Physiol Endocrinol Metab.* 2000;278(1):E127-133.
23. Li MM, Madara JC, Steger JS, et al. The Paraventricular Hypothalamus Regulates Satiety and Prevents Obesity via Two Genetically Distinct Circuits. *Neuron.* 2019;102(3):653-667 e656.
24. Krashes MJ, Shah BP, Madara JC, et al. An excitatory paraventricular nucleus to AgRP neuron circuit that drives hunger. *Nature.* 2014;507(7491):238-242.
25. Marsh DJ, Hollopeter G, Huszar D, et al. Response of melanocortin-4 receptor-deficient mice to anorectic and orexigenic peptides. *Nat Genet.* 1999;21(1):119-122.
26. Kishi T, Aschkenasi CJ, Lee CE, Mountjoy KG, Saper CB, Elmquist JK. Expression of melanocortin 4 receptor mRNA in the central nervous system of the rat. *J Comp Neurol.* 2003;457(3):213-235.
27. Swanson LW, Kuypers HG. The paraventricular nucleus of the hypothalamus: cytoarchitectonic subdivisions and organization of projections to the pituitary, dorsal vagal complex, and spinal cord as demonstrated by retrograde fluorescence double-labeling methods. *J Comp Neurol.* 1980;194(3):555-570.
28. Brown JA, Woodworth HL, Leinninger GM. To ingest or rest? Specialized roles of lateral hypothalamic area neurons in coordinating energy balance. *Front Syst Neurosci.* 2015;9:9.
29. Woodworth HL, Beekly BG, Batchelor HM, et al. Lateral Hypothalamic Neurotensin Neurons Orchestrate Dual Weight Loss Behaviors via Distinct Mechanisms. *Cell Rep.* 2017;21(11):3116-3128.
30. Pei H, Patterson CM, Sutton AK, Burnett KH, Myers MG, Jr., Olson DP. Lateral Hypothalamic Mc3R-Expressing Neurons Modulate Locomotor Activity, Energy Expenditure, and Adiposity in Male Mice. *Endocrinology.* 2019;160(2):343-358.

31. Daftary SS, Boudaba C, Szabo K, Tasker JG. Noradrenergic excitation of magnocellular neurons in the rat hypothalamic paraventricular nucleus via intranuclear glutamatergic circuits. *J Neurosci.* 1998;18(24):10619-10628.
32. Csaki A, Kocsis K, Halasz B, Kiss J. Localization of glutamatergic/aspartatergic neurons projecting to the hypothalamic paraventricular nucleus studied by retrograde transport of [3H]D-aspartate autoradiography. *Neuroscience.* 2000;101(3):637-655.
33. Latchford KJ, Ferguson AV. ANG II-induced excitation of paraventricular nucleus magnocellular neurons: a role for glutamate interneurons. *Am J Physiol Regul Integr Comp Physiol.* 2004;286(5):R894-902.
34. van den Pol AN. The magnocellular and parvocellular paraventricular nucleus of rat: intrinsic organization. *J Comp Neurol.* 1982;206(4):317-345.
35. Herman JP, Cullinan WE, Ziegler DR, Tasker JG. Role of the paraventricular nucleus microenvironment in stress integration. *Eur J Neurosci.* 2002;16(3):381-385.
36. Liposits Z, Paull WK, Setalo G, Vigh S. Evidence for local corticotropin releasing factor (CRF)-immunoreactive neuronal circuits in the paraventricular nucleus of the rat hypothalamus. An electron microscopic immunohistochemical analysis. *Histochemistry.* 1985;83(1):5-16.
37. Greenwald-Yarnell ML, Marsh C, Allison MB, et al. ERalpha in Tac2 Neurons Regulates Puberty Onset in Female Mice. *Endocrinology.* 2016;157(4):1555-1565.
38. Opland D, Sutton A, Woodworth H, et al. Loss of neurotensin receptor-1 disrupts the control of the mesolimbic dopamine system by leptin and promotes hedonic feeding and obesity. *Mol Metab.* 2013;2(4):423-434.
39. Meek TH, Nelson JT, Matsen ME, et al. Functional identification of a neurocircuit regulating blood glucose. *Proc Natl Acad Sci U S A.* 2016;113(14):E2073-2082.

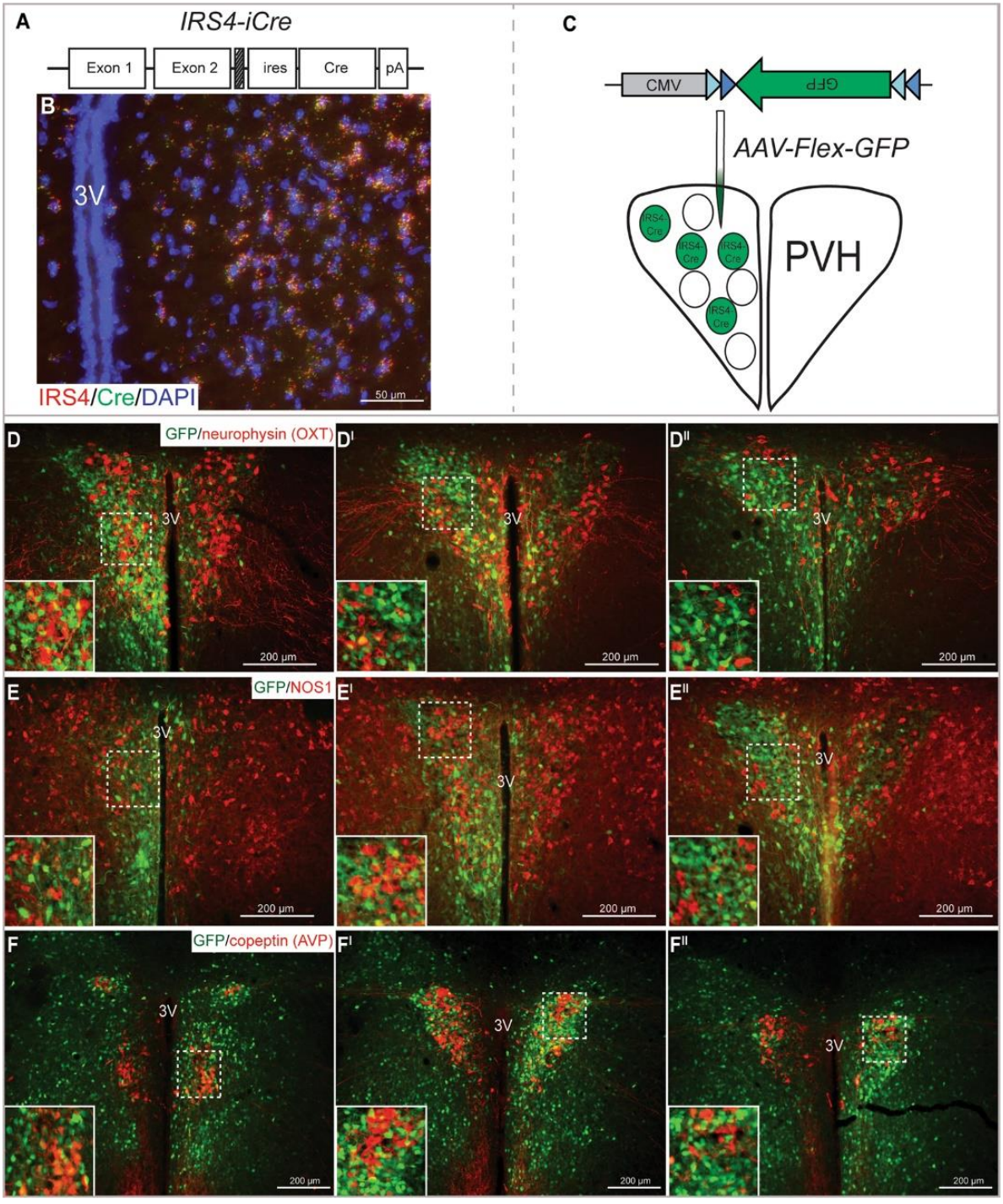

Figure 2.1: Irs4 expression defines a PVH subpopulation. In situ hybridization was performed on coronal slices from adult IRS4-iCre mice (A) for Irs4 (red) and Cre

(green), showing substantial overlap between Cre and Irs4 mRNA in the PVH (B). To identify overlap between IRS4^{PVH} neurons and other PVH populations, mice were stereotaxically injected in the PVH with a Cre-dependent GFP reporter virus (AAV-Flex-GFP, C) to visualize Cre-expressing neurons in the adult mouse. Immunohistochemistry (IHC) in the PVH demonstrates limited co-localization between GFP-labeled IRS4^{PVH} neurons (green) and OXT (D), NOS1 (E), or AVP (F) neurons in the PVH. Dashed boxes indicate regions that are digitally enlarged and shown as insets. 3 V = third ventricle.

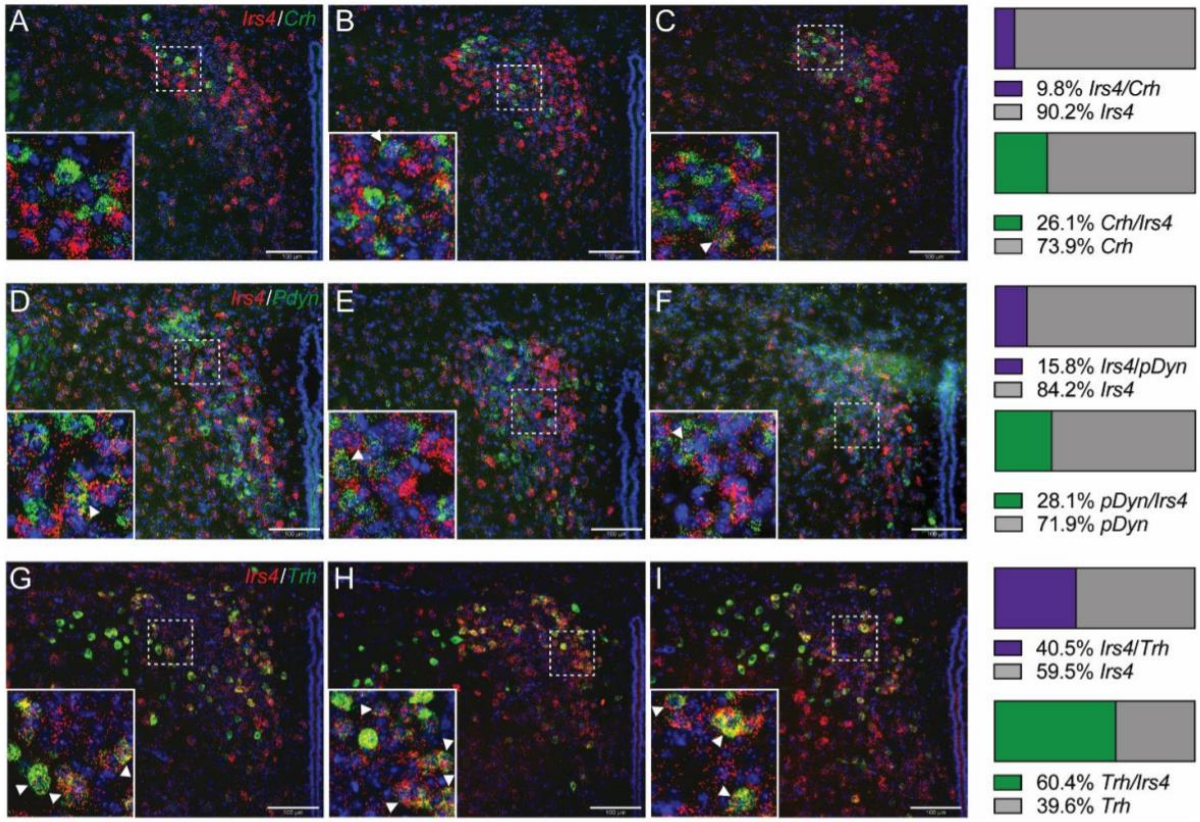

Figure 2.2: Overlap of IRS4 with CRH, pDYN, and TRH in the PVH. Fluorescent in situ hybridization images demonstrate Irs4 expression (red) overlaid with Crh (AC, green), Pdyn (D-E, green), or Trh (G-I, green) and DAPI throughout. Co-expression of Irs4 (purple) with Crh (A-C, right), Pdyn (D-F, right), or Trh (G-I, right), whereas the mean percentage of cells expressing Crh, Pdyn, or Trh that were Irs4+ are represented in green (n=3). Dashed boxes represent insets that were digitally enlarged in bottom left of images. White arrowheads point to colocalized cells within insets. Scale bars represent 100 µm.

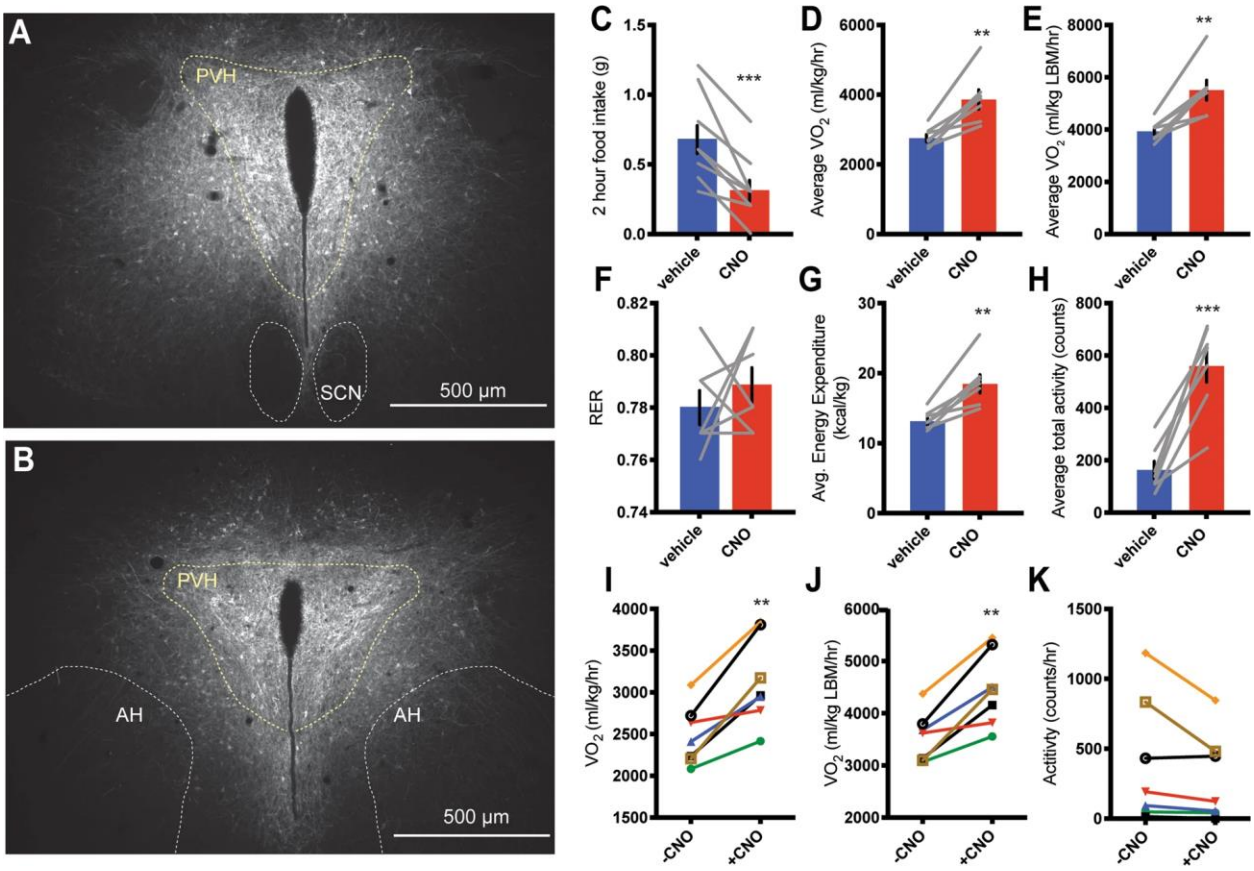

Figure 2.3: Acute activation of IRS4^{PVH} neurons decreases feeding and increases energy expenditure. IHC for mCherry identifies AAV-hM3Dq expression in IRS4^{PVH} neurons throughout the PVH (A,B: yellow dotted line). (C) Two-hour food intake at the onset of dark following activation of IRS4^{PVH} neurons with an i.p. injection of CNO (0.3 mg/kg) in comparison to vehicle. Activation of IRS4^{PVH} neurons increases total oxygen consumption (D,E), energy expenditure (G), and activity (H) over a four-hour time period in the absence of food, whereas respiratory exchange ratio (RER) is not significantly different (F). (I–K) IRS4^{PVH} neuronal activation increases activity-independent changes in oxygen consumption (I,J), measured at time points four hours before (−CNO) or after (+CNO) activation when activity levels were relatively matched (K). Average values ± SEM are shown, significance was determined using a paired-t-

test in comparison to vehicle values. **p < 0.01, ***p < 0.001; feeding n = 9, CLAMS n = 7; AH = anterior hypothalamus, SCN = suprachiasmatic nucleus, PVH = paraventricular nucleus of the hypothalamus.

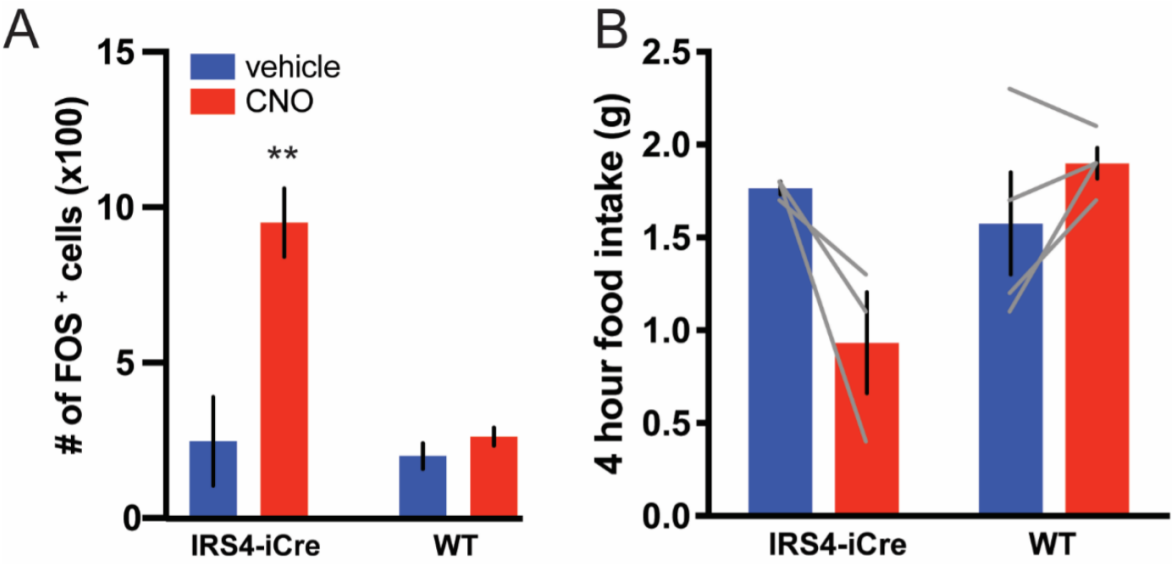

Figure 2.4: Activation of IRS4^{PVH} neurons requires hM3Dq expression and CNO administration. Quantification of unilateral FOS induction demonstrates increased FOS in CNO-injected IRS4-iCre mice with Flex-hM3Dq expression compared to those injected with vehicle (p=0.006), whereas WT controls had no significant change in nuclear FOS with CNO administration. (A). Differences in four-hour (B) feeding is not observed between WT mice injected with vehicle or CNO at the onset of the dark cycle (p=0.2255, t=1.522), whereas a trend exists for decreased food intake in IRS4-iCre mice with Flex-hM3Dq expression in the PVH (p=0.1066, t=2.813). Average values ± SEM are shown for food intake values, average values ± SD are shown for FOS quantification. Significance was determined using a paired-t-test in comparison to vehicle values for food intake (WT n=4, IRS4-iCre n=3), and a one-way ANOVA followed by Tukey's post-hoc for FOS quantification (n=2/group).

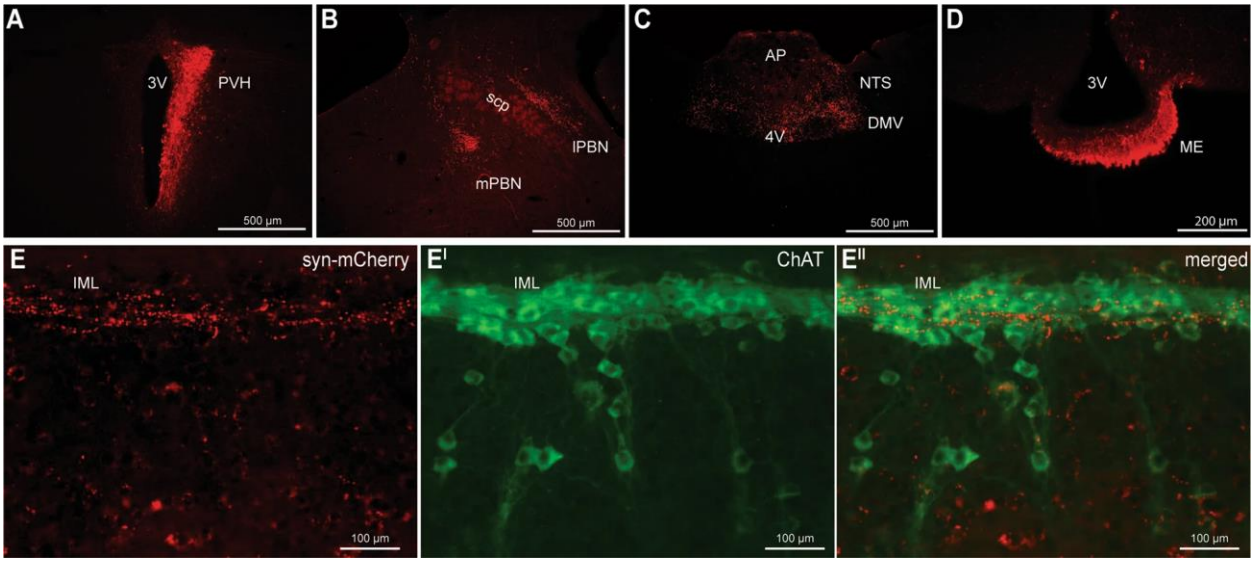

Figure 2.5: IRS4^{PVH} neurons project to hindbrain and spinal cord regions. (A) A Cre-dependent synaptophysin-mCherry adenovirus (syn-mCherry) was unilaterally injected in the PVH area of IRS4-iCre mice to trace synaptic terminals throughout the brain. (B,C) Syn-mCherry positive terminals are observed in hindbrain regions including the medial and lateral parabrachial nucleus (mPBN, lPBN, respectively, (B), as well as the dorsal motor nucleus of the vagus (DMV) and nucleus of the solitary tract (NTS, C). (D) IRS4^{PVH} neurons also project to the median eminence (ME). (E) Syn-mCherry (red) identifies synaptic terminals in the intermediolateral column of the spinal cord (IML) in close proximity to neurons expressing choline acetyltransferase (ChAT, green). scp = superior cerebellar peduncle, 4 V = fourth ventricle, 3 V = third ventricle, AP = area postrema.

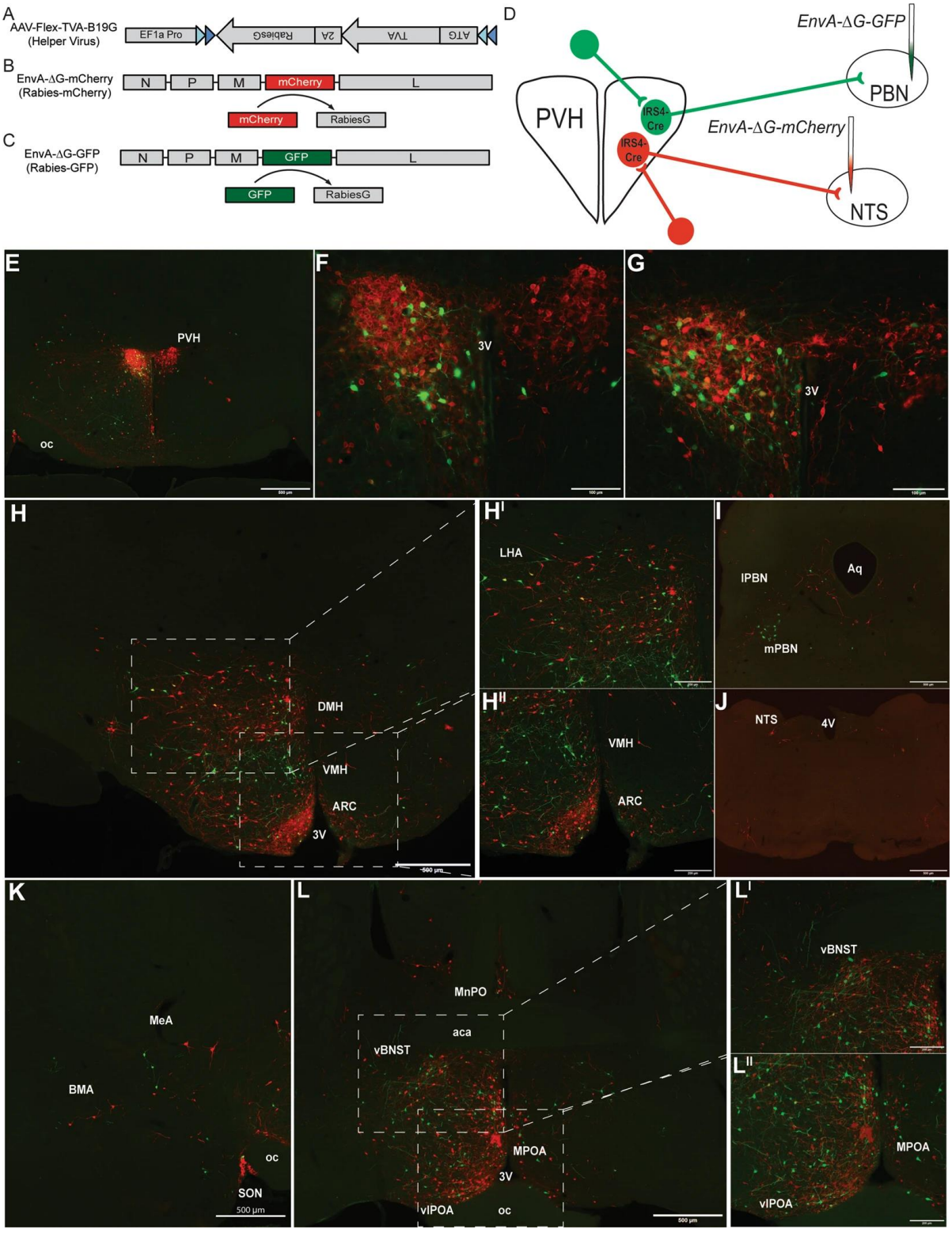

Figure 2.6: Identification of monosynaptic inputs to NTS-projecting or PBN-projecting IRS4^{PVH} neurons using modified rabies virus. A Cre-dependent helper

virus construct (AAV-Flex-TVA-B19G) is used to insert rabies B19 glycoprotein (B19G) and the TVA receptor in IRS4^{PVH} cell bodies and terminals. Modified rabies virus expresses a fluorescent tag (mCherry, B; GFP, C) instead of B19G. After initial infection with helper virus, rabies-mCherry is injected at one projection site (NTS), whereas rabies-GFP is injected at another (PBN) in the same mouse (D). IHC for mCherry and GFP identify largely non-overlapping NTS-projecting and PBN-projecting IRS4^{PVH} neurons, respectively (E–G). Sites upstream of both NTS and PBN-projecting IRS4^{PVH} neurons include the lateral hypothalamic area (LHA, H), supraoptic nucleus (SON, K), amygdala (K), bed nucleus of the stria terminalis (BNST, L), and the preoptic area (POA, L). The ventromedial hypothalamus (VMH) is upstream of PBN-projecting IRS4^{PVH} neurons (H^{II}, green), whereas both the arcuate nucleus (ARC, H^{II}, red) and PBN (I, red) are upstream of IRS4^{PVH} neurons projecting to the NTS. Glial damage represents injection site in the PBN (I, green) and NTS (J, red). 3 V = third ventricle, oc = optic chiasm, MeA = medial amygdala, BMA = basomedial amygdala, vBNST = ventral BNST, vlPOA = ventral lateral POA, MPOA = medial POA, MnPO = median preoptic nucleus, aca = anterior part of anterior commissure, DMH = dorsomedial hypothalamus, aq = aqueduct, 4 V = fourth ventricle.

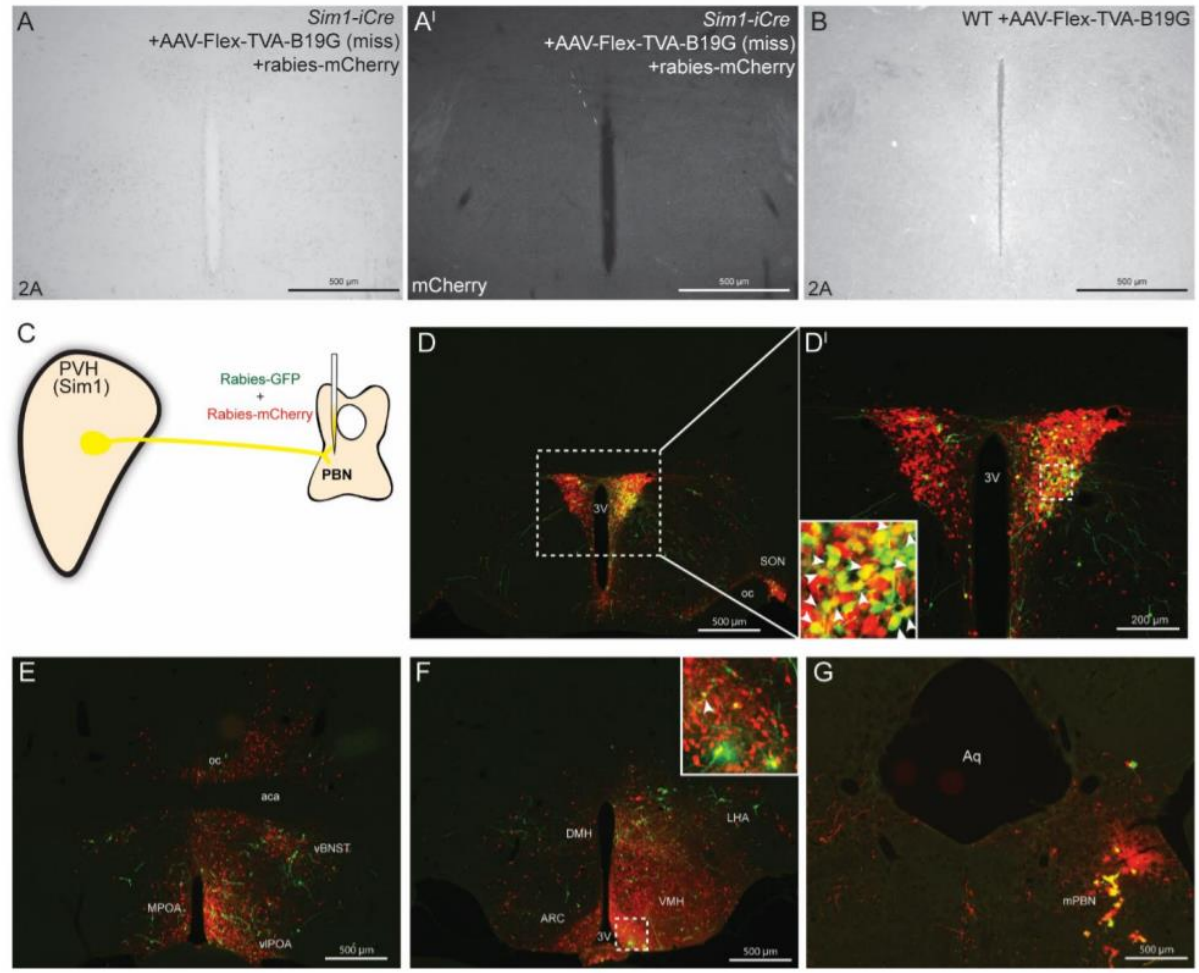

Figure 2.7: Monosynaptic rabies virus tracing is Cre-dependent, dependent on helper virus expression, and capable of dual rabies infection. IHC in the PVH of Sim1-Cre +AAV-Flex-TVA-B19G mice validates a “miss” since 2A staining (reflective of AAV-Flex-TVA-B19G expression) is not detected (A). Still, NTS-directed rabies-mCherry injection in the same mouse displays limited mCherry expression in the PVH, therefore confirming the requirement of AAV-Flex-TVA-B19G expression for modified rabies virus expression (AI). B) 2A expression in wildtype mice injected with AAV-Flex-TVA-B19G demonstrates that Cre recombinase is required for helper virus expression. C) Injection of both rabies-mCherry and rabies-GFP in the same PBN projection target

in Sim1-Cre +AAV-FlexTVA B19G mice illustrates that both rabies viruses can be expressed in PBN-projecting PVH neurons (D). Sites upstream including the bed nucleus of the stria terminalis (BNST, E), preoptic area (POA), arcuate nucleus (ARC, F) and VMH (F) show limited co-labeling. G) Gliosis in the PBN due to rabies-mCherry/rabies-GFP injection demonstrates that both rabiesGFP and rabies mCherry were mixed and injected at the same site. Dashed boxes indicate regions that are digitally enlarged and shown as insets. White arrowheads indicate colocalization in neurons with both rabies-GFP and rabies-mCherry. 3V=third ventricle, aca= anterior part of anterior commissure, DMH=dorsomedial hypothalamus, oc=optic chiasm, LHA=lateral hypothalamic area.

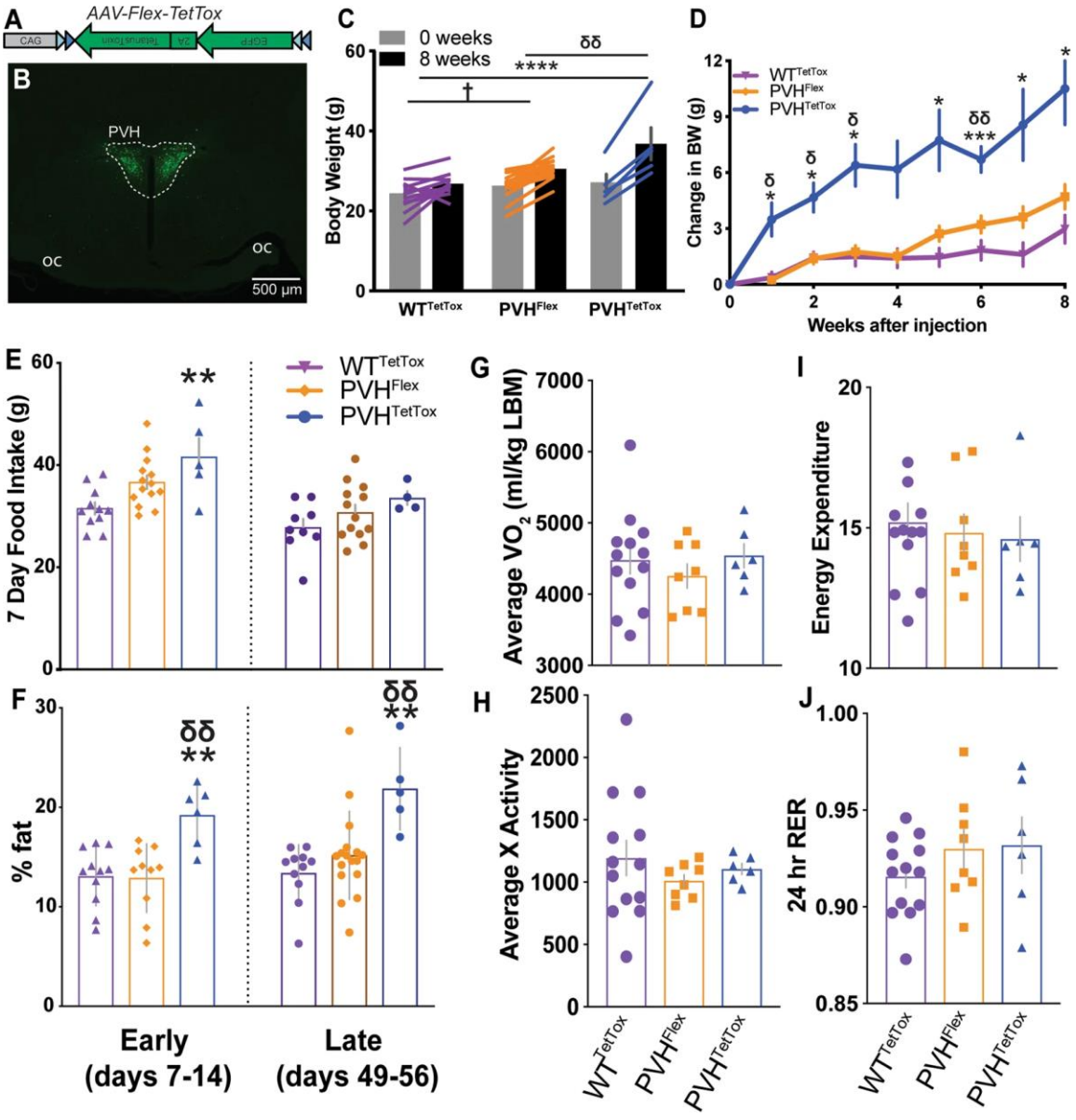

Figure 2.8: IRS4^{PVH} neurons are necessary for normal feeding and bodyweight. A Cre-dependent adeno-associated virus expresses tetanus toxin A and GFP exclusively in Cre-expressing neurons to inhibit synaptic vesicle exocytosis and GFP visualization of the transduced cells (A). (B) Example hit site of IRS4-iCre mice injected with AAV-Flex-TetTox (PVH^{TetTox}). Bilateral IRS4^{PVH} neuronal silencing in IRS4-iCre mice (PVH^{TetTox}) results in both increased bodyweight (C) and increased bodyweight gain (D) in comparison to IRS4-iCre mice injected with a control AAV (PVH^{Flex}) or wildtype mice

injected with AAV-Flex-TetTox (WT^{TetTox}, mixed-model analysis followed by Tukey's post-hoc). (E) PVH^{TetTox} mice (blue) show increased 7-day food intake at early stages of the study (left) in comparison to WT^{TetTox} mice (orange; one-way ANOVA followed by Tukey's post-hoc) whereas later stage food intake shows a trend towards increased feeding (dark blue, one-way ANOVA). (F) PVH^{TetTox} mice show have increased fat mass percentages (F) at early and late stages of obesity development (one-way ANOVA followed by Tukey's post-hoc). (G–J) 3-day averages of CLAMS measurements were measured during weeks 2–4 of experiments and compared across groups. While PVH^{TetTox} mice show a trend towards decreased energy expenditure (I), none of these groups are significantly different from one another (one-way ANOVA. Average values ± SEM are shown, *$p < 0.05$, **$p < 0.01$, ***$p < 0.001$, ****$p < 0.0001$ compared to WT^{TetTox}; ƩƩ$p < 0.05$, ƩƩ Ʃ$p < 0.01$, ƩƩ Ʃ Ʃ$p < 0.001$ compared to PVH^{Flex}; BW/feeding: PVH^{TetTox} n = 6, PVH^{Flex} n = 17, WT^{TetTox} n = 13; body composition: PVH^{TetTox} early n = 6, PVH^{TetTox} late n = 5, PVH^{Flex} early n = 10, PVH^{Flex} late n = 17, WT^{TetTox} n = 11; CLAMS: PVH^{TetTox} n = 6, PVH^{Flex} n = 8, WT^{TetTox} n = 13.

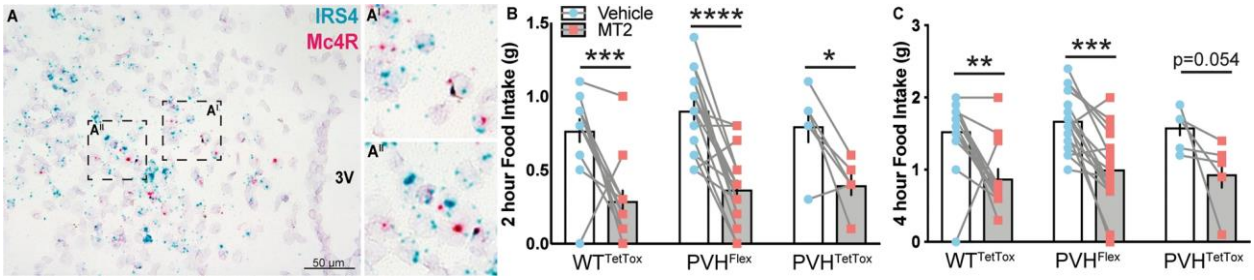

Figure 2.9: IRS4^{PVH} neuron activity is dispensable for melanocortin agonist-mediated satiety. In situ hybridization for Irs4 (A, blue) and Mc4r (A, red) mRNA in the PVH of adult wildtype mice. Melanocortin agonist-induced satiety was tested in mice with IRS4^{PVH} neuronal silencing (B,C). Two-hour (B) and four-hour (C) feeding was significantly decreased following i.p. injection of the MC4R agonist MT-II (150 ug/mouse) in all cohorts of mice, despite the silencing of IRS4^{PVH} neurons in the PVH^{TetTox} group. Average values ± SEM are shown, **p < 0.01, ***p < 0.001, ****p < 0.0001; PVH^{TetTox} n = 6, PVH^{Flex} n = 17, WT^{TetTox} n = 13. Significance was determined using a paired t-test between vehicle and MTII injected mice within the same cohort. Dashed boxes (AI, AII) indicate regions cropped and digitally enlarged.

	PVH^{TetTox}	Unil. PVH^{TetTox}	PVH^{Flex}	WT^{TetTox}
BW (g, t=0)	27.17 ±2.02	24.78 ±0.60	25.97 ±0.69	23.78 ±1.01
BW (g, t=8wk)	36.80 ±4.02***†	31.64 ±1.73	30.58 ±0.72	26.54 ±0.71
Change in BW (g, t=8wk)	10.50 ±1.92***††	7.14 ±1.46	4.71 ±0.66	2.96 ±0.75
Early weekly food intake (g)	39.27 ±3.78*	36.42 ±2.36	35.90 ±1.24	30.03 ±1.46
Late weekly food intake (g)	33.55 ±1.35	30.30 ±4.11	32.30 ±2.36	27.81 ±1.67
VO_2 (ml/kg LBM)	4540 ±167.0	4294 ±194.0	4255 ±170.2	4477 ±191.8
Average total X activity (counts/hr)	1106 ±44.98	1392 ±37.84	1011 ±49.13	1194 ±140.3
body fat (%, early)	19.21 ±1.24**††	12.89 ±0.98§	12.90 ±1.09	13.05 ±0.89
body fat (%, late)	21.86 ±1.85**†	12.66 ±1.83§§	15.17 ±1.08	13.38 ±0.861

Table 2.1: Unilateral IRS4^{PVH} silencing alters bodyweight physiology. Comparison of bodyweight and CLAMS results from IRS4^{PVH} TetTox cohorts with viral injections that only targeted one side of the PVH (Unil. PVH^{TetTox}) still demonstrate trends toward changes in physiology. Data represented includes results illustrated in Fig. 5. Data was analyzed using a one-way ANOVA followed by Tukey's multiple comparisons if appropriate, or an unpaired t-test (number of cells infected with AAV-Flex-TetTox between PVH^{TetTox} and Unil. PVH^{TetTox} cohorts). Average values ± SEM are shown. *p<0.05, ***p<0.001 for PVH^{TetTox} compared to WT^{TetTox}; † p<0.05 for PVH^{TetTox} compared to PVH^{Flex}; § p<0.05 for PVH^{TetTox} compared to Unil. PVH^{TetTox}; &p<0.05 for PVH^{Flex} compared to WT^{TetTox}; $ p<0.05 for Unil. PVH^{TetTox} compared to WT^{TetTox}. PVH^{TetTox} n=6 (BW, t=0; early food intake, CLAMS, early body composition), n=5 (BW, t=8wk, change in BW, late body composition), n=4 (late food intake); Unil. PVH^{TetTox} n=6 (BW t=0wk, early food intake), n=5 (BW t=8wk, change in BW, late food intake), n=4 (CLAMS, body composition); WT^{TetTox} n=13 (BW t=0wk, early food intake, CLAMS), n=11 (BW t=8wk, change in BW, body composition), n=9 (late food intake); PVH^{Flex} n=17 (BW t=0, early food intake, late body composition), n=16 (BW t=8wk, change in BW), n=8 (late food intake, CLAMS), n=10 (early body composition).

Chapter 3

CalcR-Expressing Neurons of the PVH Modulate Energy Balance

The following chapter discusses two related but separate projects concerning the calcitonin receptor (CalcR) expressing neurons in the PVH and is subdivided into two sections. The first section investigates the necessity of CalcR expression in the PVH in the anorectic response to a CalcR agonist and the impact on energy balance following deletion of CalcR from Sim1 neurons. The second section focuses on the physiologic function of $CalcR^{PVH}$ neurons by manipulating the neural activity of this PVH neuronal population. For this project, we used viral techniques to acutely active and chronically silence these neurons, as well as characterize them through their downstream projection targets and through their overlap with other known subpopulations of the PVH that are responsible for energy homeostasis. It is important to state that this second approach varies from the first in that it studies $CalcR^{PVH}$ neurons as a whole rather than through the expression and signaling activity of CalcR. This is a critical distinction, as manipulating $CalcR^{PVH}$ neurons activity will alter other yet unidentified mechanisms of this neuronal population aside from those mediated by CalcR. It is for this reason that identifying the overlap of $CalcR^{PVH}$ neurons with other studied neuronal populations of the PVH is crucial to understanding how $CalcR^{PVH}$ neurons may operate.

Investigating energy homeostatic role of CalcR^{PVH} neurons through CalcR deletion from Sim1 neurons[2]

Introduction:

Calcitonin (CT) and amylin are peptides that are functionally and structurally related.[1] In addition to reducing blood calcium levels and reducing glucose incorporation into the glycogen of soleus muscle, these peptides also play a role in regulating food intake.[1-6] CT is a 32-amino acid peptide that is a product of CALC gene that is generated in and secreted from parafollicular cells of the thyroid gland in humans and mice.[6] It was first associated with satiety when it was observed that following a meal, plasma CT concentrations increased.[7,8] It was later found that the subcutaneous application of CT in mice, rats, monkeys and humans resulted in a reduction in feeding behavior.[9] More so, intracerebroventricular (ICV) application of salmon calcitonin (sCT) (which has a higher potency than mammalian CT) as well as amylin was found to be more potent in reducing feeding than when applied peripherally, suggesting these peptides exert their anorectic activities through a centrally expressed receptor.[10,11] The area postrema (AP) and solitary nucleus (NTS) are considered to be the most likely site through which peripherally applied sCT and amylin exert their anorectic effects.[12,13] Hypothalamic regions are also thought to be important for mediating the anorectic effects of centrally applied sCT and amylin. This was supported by the finding that sCT delivered via cannula to various regions of the hypothalamus, such as the

[2] This section contains material previously published in Cell Metabolism: Cheng W, **Gonzalez I**, Pan W, et al. Calcitonin Receptor Neurons in the Mouse Nucleus Tractus Solitarius Control Energy Balance via the Non-aversive Suppression of Feeding. Cell Metab. 2020;31(2):301-312 e305.

paraventricular nucleus of the hypothalamus (PVH), the suprachiasmatic part of the preoptic area (POA) and the perifornical area resulted in a significant decrease in food intake.[14] It should be noted that aminoprocalcitonin (N-PCT), which is derived from procalcitonin, is expressed in brain regions of rats known to influence energy balance including the PVH. Intracerebroventricular application of N-PCT suppresses food intake behavior and weight gain in rats and induces CRH expression and production in the hypothalamus.[15]

Amylin is a 37-residue peptide hormone that is co-released with insulin from the B-cells of the pancreas in response to feeding behavior.[16-19] Amylin serves to promote gastric acid secretion, limit gastric emptying and reduces glucagon secretion from the pancreas.[20] Further, amylin reduces feeding behavior through regulating meal size in a non-aversive manner.[21,22] Due to its release from peripheral systems and through lesioning studies, it is supported that amylin interacts with the AP of the hindbrain and by extension the NTS due to lack of blood-brain barrier protection.[12,22,23] Further, amylin maybe a necessary modulator of the anorectic action of Cholecystokinin (CCK).[24,25] In obese humans, the application of the synthetic amylin analogue pramlintide inhibits feeding and reduces body weight.[26-28] Leptin, which is a neurohormone secreted by adipocytes and act on the hypothalamus, is crucial for maintaining long-term energy homeostasis.[29] Humans that are leptin-deficient experience hyperphagic obesity and treatment with metreleptin can reverse this obesity.[30-32] In cases of obesity that is not due to leptin-deficiency, metreleptin alone is ineffective at producing weight loss.[33] Amylin is capable of restoring leptin sensitivity in obese patients and co-administration of amylin and leptin in rodents and pramlintide and metreleptin (recombinant methyl-

human leptin) in humans synergistically generate reductions in food intake and weight loss as a treatment.[34-38] This is not so in more extreme cases, as rats that have undergone extreme diet-induced obesity experience lesser effects from amylin/leptin treatment when compared to less obese rats.[39] This is also found to be true in human patients, as pramlintide/metreleptin treatment was only notable effective in humans with a body mass index lower than 35 kg/m^2.[39]

CT, sCT and amylin are ligands to the calcitonin receptor (CalcR), a G protein-coupled receptor.[40] It has been found to be expressed in many regions of the hypothalamus and hindbrain such as the PVH, arcuate nucleus (ARC), substantia nigra, bed nucleus of the stria terminalis, locus coeruleus and the NTS through in situ hybridization and immunohistochemistry.[41,42] It heterodimerizes with receptor activity modifying proteins (RAMPs) which allows it have distinct binding efficiencies with different ligands.[43,44] There are three flavors of RAMPs, which are RAMP1, RAMP2 and RAMP3.[45] CalcR alone interacts with the CT peptide, while CalcR with RAMP1, RAMP2 or RAMP 3 (termed AMY1, AMY2 and AMY3 respectively) interact with amylin as a ligand.[46,47]

As the direct application of sCT to the PVH suppresses feeding in rodents, we examined the role of calcitonin receptor (CalcR) expression in the PVH in food intake regulation.[14] To investigate the role of PVH CalcR expression in feeding, we used Cre/Lox technology to delete CalcR expression from single-minded homolog 1 (Sim1) expressing neurons, which represent most if not all PVH neurons.[48,49] Deletion of CalcR expression from Sim1 neurons does not perturb body weight, body composition or food intake. Further, deletion of CalcR from Sim1 neurons does not disrupt the anorexia or

weight loss induced by peripheral injection of sCT. Our study shows that CalcR expression in Sim1 neurons and thus the PVH is not essential to maintain energy homeostasis, nor is it necessary to produce the anorectic effects produced by sCT. Therefore, CalcR expression in another region of the brain must be necessary for sCT mediated anorexia.

Materials and Methods:

Animals

Mice were bred in our colony at the University of Michigan Unit for Laboratory Animal Medicine. The University of Michigan Committee on the Use and Care of Animals have approved the procedures performed on these mice and our studies are in accordance with the Associate for the Assessment and Approval of Laboratory Animal Care and National Institutes of Health guidelines. Mice were provided with food and water ad libitum in rooms that were temperature controlled and maintained at 25^{o}C with 12 hour light-dark cycles with daily health status checks.

CalcR^{flox} mice were crossed two times onto Sim1^{cre} to produce Sim1$^{cre/+}$;CalcR$^{flox/flox}$ mice, which were bred to CalcR$^{flox/flox}$ mice to produce Sim1$^{cre/+}$;CalcR$^{flox/flox}$ (Calcr^{Sim1}KO) and CalcR$^{flox/flox}$ control mice.[50,51] Sibling controls were used in these studies and all mouse models were on a C57BL/6 genetic background. Male and female mice were used in experiments that do not specify a single sex as used and no sex differences were detected in the observed phenotypes.

Phenotypic Studies

From the time of weaning, Calcr^{Sim1KO} mice and their controls were singly housed and body weight and food intake was monitored weekly. For stimulation studies, these mice were at least two months old when treated with saline or sCT (4033011, Bachem) at the start of the dark cycle, with food intake monitored over the course of four hours. When measuring chronic feeding and changes in body weight, mice received saline injections for two days prior to injecting saline or sCT twice per day (5:30PM and 8:00 AM) for 3 days, followed by saline injections for an additional two days to assess recovery from the treatment.

Perfusion and Immunohistochemistry

Mice (at least 8 weeks of age) were anesthetized using a lethal dose of pentobarbital and were transcardially perfused with phosphate-buffered saline (PBS) followed by 10% buffered formalin. Following removal, the brains were placed in 10% buffered formalin overnight and then dehydrated using 30% sucrose for 24 hours. A freezing microtome (Leica, Buffalo Grove, IL) was used to cut brains into 30um sections. For immunohistochemistry, brain sections were treated with 1% hydrogen peroxide/0.5% sodium hydroxide, 0.3% glycine, 0.03% sodium dodecyl sulfate, and blocking solution (PBS with 0.1% triton, 3% normal donkey serum). The sections were then incubated overnight in rabbit anti-FOS (Santa Cruz, sc-52; 1:1,000) and the following day were exposed to biotinylated secondary antibody (1:200 followed by avidinbiotin complex (ABC) amplification and 3,3-diaminobenzidine (DAB) reaction). Images were collected

using a BX-51 microscope with a DP80 camera (Olympus). Images were pseudocolored with Photoshop software (Adobe) and were quantified using ImageJ (NIH).

RNA Extraction, Reverse Transcription and RT-qPCR

At 8 weeks of age or older, Calcr^{Sim1}KO and control mice were euthanized using inhalation anesthetic isoflurane (McKesson, Piramal Critical Care #6679401725) in a drop jar. For RNA preparation, PVH tissue was microdissected and stored in a -80C freezer. An RNeasy Mini kit (QIAGEN) was used for RNA extraction and quantified using a NanoDrop 1000 (ThermoScientific). The RNA was treated with DNase (TURBO DNA-free Kit, ThermoFisher Scientific, Cat #AM1907) and was then quantified with a NanoDrop 1000. Approximately 500 ng of total RNA per sample was used for reverse transcription (iScript cDNA Synthesis Kit, Bio-Rad, Cat #1708891) with a thermocycler (Mastercycler pro S, Eppendorf). A StepOnePlus Real Time PCR System (Applied Biosystems) was used for quantitative PCR (qPCR) with SYBR Green PCR Master Mix (Applied Biosystems, Cat #4309155) and CalcR primers (Forward: 50 -GCTGCTGGATGCTCAGTACA-30, Reverse: 50-AGTGTCGTCCCAGCACATC-30). As a reference gene, hypoxanthine guanine phosphoribosyl transferase (Hprt) gene was used (amplified using primers; Forward: 50-GATTAGCGATGATGAACCAGGTT-30, Reverse: 50-CCTCCCATCTCCTTCATGACA-30). cDNA was pooled from each sample and made into 5 serial dilutions to make a standard curve ladder which was used to determine the relative RNA concentration of each sample. The samples were run in duplicate and the values underwent a Grubbs' test to discard outliers before running a statistical analysis.

Statistics

Mean ± standard error of the mean was used to report our data. Statistical analysis of the data was conducted using Prism software (version 7), as well as to ensure the data fit a normal distribution. Paired or unpaired t tests and two way ANOVA were used as described in the text and figure legends. $P<0.05$ indicates statistical significance.

Results:

$CalcR^{flox}$ mice were crossed with $Sim1^{cre}$ mice to produce $Calcr^{Sim1}KO$ knockouts (Figure 3.1 A).[50,51] We found that FOS signal in the PVH increased due to sCT stimulation in $CalcR^{Sim1}KO$ mice despite the decreased expression of Calcr in the PVH of $CalcR^{Sim1}KO$ mice (Figure 3.1 B-G). This indicates that activation of neurons in the PVH due to sCT stimulation is facilitated indirectly by other neurons expressing CalcR and that CalcR in the PVH may suppress sCT dependent activation of PVH neurons through a different population of neurons that express CalcR. We found that $Calcr^{Sim1}KO$ mice did not have altered body weight, food intake or body composition (Figure 3.2 A-C). We can therefore conclude that CalcR expression in PVH neurons does not under normal conditions influence long-term energy balance. We studied food intake following sCT administration in $Calcr^{Sim1}KO$ mice to determine the anorectic response of these animals to CalcR agonists. For overnight feeding studies, we found that administering sCT at the start of the dark cycle decreased feeding by over 40% after 4 hours following the injection (Figure 3.2 D). Further, 3 days of twice-daily

administration of sCT reduced food intake and decreased body weight in Calcr^{Sim1}KO mice and their controls (Figure 3. 2E-F). We have therefore determined that Calcr expression in Sim1^{PVH} neurons are not needed for the anorectic effects of sCT.

Discussion:

Peripheral application of sCT and related peptides such as amylin have been found to suppress feeding behavior in rodents.[11] More compelling was finding that direct injection of sCT to the PVH dramatically suppressed feeding behavior and therefore marked the PVH as a potential region in which CalcR expression was responsible for sCT induced anorexia.[14] Our knockout studies, however, indicate that CalcR expression in the PVH is dispensable in the anorectic behavior induced by peripherally applied sCT. Further, CalcR expression in the PVH is not necessary to maintain energy balance. Because the PVH FOS responses to sCT in Calcr^{Sim1}KO mice were not reduced, this suggests that hypothalamic FOS induced by sCT could be facilitated indirectly through CalcR neurons that send projections to the hypothalamus, such as the CalcR^{NTS} neurons. It is important to note, that Sim1 is not exclusively expressed in the PVH and that deletion of CalcR expression from Sim1 expressing neurons may delete CalcR from overlapping regions beyond the PVH, such as the amygdala.[52]

While we have determined that CalcR expression in Sim1 neurons is not needed for sCT induced anorexia, CalcR expression in NTS neurons is necessary for this response and do so in a non-aversive manner.[53] Further, activating CalcR^{NTS} neurons through DREADDs technology suppresses food intake and body weight gain and does

so without promoting aversion much like the CCK^{NTS} neurons that project to the PVH, which is in contrast to the CCK^{NTS} neurons that project to the PBN, which have been found to be aversive when activated.[54] These $CalcR^{NTS}$ neurons project to the PBN and activate non-calcitonin gene-related peptide cells in this region. Finally, silencing $CalcR^{NTS}$ neurons produces hyperphagic obesity and blunts the anorectic behavior produced by sCT. It has therefore been demonstrated that CalcR expression in the NTS is necessary for the regulation of energy balance, while this is not so in the PVH.[53]

Although we have determined that CalcR expression in the PVH is dispensable to the regulation of energy balance and the anorectic response to sCT, there is still value in investigating the CalcR expressing neurons of the PVH. Our in situ hybridization studies indicate that the PVH contains a large population of $CalcR^{PVH}$ neurons and could therefore potentially engage in aspects of energy balance associated with neurons of the PVH. Because of their abundance, $CalcR^{PVH}$ neurons may overlap with or could be distinct from other known populations of the PVH that have been identified to regulate energy homeostasis. In either case, through investigating the $CalcR^{PVH}$ neurons, we would further our goal to characterize the neurons of the PVH involved in energy balance circuitry. With this goal in mind, we generated a mouse line that allowed us to use viral tools to investigate these $CalcR^{PVH}$ neurons.

Paraventricular Calcitonin Receptor-Expressing Neurons Modulate Energy Homeostasis in Male Mice[3]

Abstract

The paraventricular nucleus of the hypothalamus (PVH) is a heterogeneous collection of neurons that play important roles in modulating feeding and energy expenditure. Abnormal development or ablation of the PVH results in hyperphagic obesity and defects in energy expenditure whereas selective activation of defined PVH neuronal populations can suppress feeding and may promote energy expenditure. Here, we characterize the contribution of calcitonin receptor-expressing PVH neurons ($CalcR^{PVH}$) to energy balance control. We used Cre-dependent viral tools delivered stereotaxically to the PVH of $CalcR^{2Acre}$ mice to activate, silence and trace $CalcR^{PVH}$ neurons and determine their contribution to body weight regulation. Immunohistochemistry of fluorescently-labelled $CalcR^{PVH}$ neurons demonstrates that $CalcR^{PVH}$ neurons are largely distinct from several PVH neuronal populations involved in energy homeostasis; these neurons project to regions of the hindbrain that are implicated in energy balance control, including the nucleus of the solitary tract and the parabrachial nucleus. Acute activation of $CalcR^{PVH}$ neurons suppresses feeding without appreciably augmenting energy expenditure, whereas their silencing leads to obesity that may be due in part due to loss of PVH melanocortin-4 receptor (MC4R) signaling. These data show that $CalcR^{PVH}$ neurons are an essential component of energy balance neurocircuitry and

[3] This section was previously published in Endocrinology: **Gonzalez IE**, Ramirez-Matias J, Lu C, et al. Paraventricular Calcitonin Receptor-Expressing Neurons Modulate Energy Homeostasis in Male Mice. Endocrinology. 2021;162(6).

their function is important for body weight maintenance. A thorough understanding of the mechanisms by which CalcR^{PVH} neurons modulate energy balance might identify novel therapeutic targets for the treatment and prevention of obesity.

Introduction

The paraventricular nucleus of the hypothalamus (PVH) is a brain region that is critical for normal feeding and energy expenditure. The PVH serves as a hypothalamic node that receives ascending neuronal and humoral energy balance inputs, integrates this information and then relays output signals to regions such as the hindbrain and spinal cord to drive physiologic responses to maintain energy homeostasis [55-57]. The essential role of the PVH is revealed by mechanical lesions of this region that produce hyperphagic obesity and glucose dysregulation in both rodent models and humans [58,59]. Whereas complete inactivation of SIM1, a transcription factor required for PVH development, is incompatible with life, *Sim1* haploinsufficiency disrupts PVH formation and results in profound hyperphagic obesity [49,60-62]. Post-natal ablation of SIM1-expressing neurons leads to obesity with hyperphagia and a reduction in energy expenditure revealing a critical role for PVH cell function in the regulation of both feeding and energy expenditure [48]. Indeed, chemogenetic activation of SIM1^{PVH} neurons acutely suppresses feeding and increases oxygen consumption and locomotor activity [63], while their inhibition leads to a robust increase in food intake [64]. Given the importance of SIM1^{PVH} neurons in energy balance and metabolic control, defining the energy balance contributions of subpopulations of SIM1^{PVH} neurons may yield novel approaches to modulating discrete aspects of energy homeostasis.

The unique roles of several PVH neuronal subsets in energy balance have been identified using cell-specific manipulations with Cre-LoxP technology [63,65-67]. We have shown that activation of PVH neurons expressing nitric oxide synthase-1 ($NOS1^{PVH}$) suppresses feeding and increases oxygen consumption [63]. Importantly, activation of oxytocin (OXT)-expressing PVH neurons, which are a subpopulation of the $NOS1^{PVH}$ neurons, has no effect on feeding but does promote energy expenditure albeit to a lesser degree than NOS1 neurons [63]. In contrast to the $NOS1^{PVH}$ neurons, acute activation of melanocortin-4 receptor (MC4R)-expressing PVH neurons suppresses feeding but has no effect on energy expenditure [67]. These experiments underscore the anatomical and functional differences between diverse PVH neuronal populations and suggest that the modulation of feeding and energy expenditure may be compartmentalized to subsets of PVH neurons. Therefore, manipulation of genetically-defined PVH cells uncovers the physiological roles of these neuronal subpopulations and delineates the neural circuitries responsible for discrete aspects of energy balance control.

Peripheral application of the polypeptide calcitonin suppresses feeding in several species [9,11,68,69]. Calcitonin receptors (CalcR) are expressed in the PVH and direct application of salmon calcitonin (sCT) to the PVH dramatically suppresses feeding in rats suggesting that the activity of $CalcR^{PVH}$ neurons may contribute to energy balance control [14,42]. To determine the role of CalcRs in PVH neurons in the anorectic actions of peripherally applied sCT, we deleted CalcRs selectively from the PVH using Cre-loxP technology. We found that loss of CalcRs from the PVH did not alter energy balance at baseline or attenuate the anorectic response to peripherally applied sCT [53]. Although

CalcR expression in the PVH is not necessary for the sCT-induced anorexia, the dramatic suppression of feeding following direct PVH application of calcitonin suggests that the PVH neurons that express CalcR likely play an important in energy homeostasis [14]. To understand the contribution of $CalcR^{PVH}$ neurons to energy balance control, we used our $CalcR^{2ACre}$ transgenic mouse line and viral vectors to selectively target and manipulate $CalcR^{PVH}$ cells in male mice. This approach uses CalcR expression as a means to genetically access $CalcR^{PVH}$ neurons and is not a surrogate for calcitonin signaling in the PVH. Acute activation of $CalcR^{PVH}$ neurons suppresses feeding and promotes locomotor activity. To test the necessity of $CalcR^{PVH}$ neurons in the regulation of energy balance, we chronically silenced $CalcR^{PVH}$ neurons using Cre-dependent expression of tetanus toxin. Silencing $CalcR^{PVH}$ neurons leads to obesity due to increased food intake and a possible alteration in energy expenditure. We find that CalcR and MC4R expression overlap in the PVH, suggesting that the obesity seen with $CalcR^{PVH}$ silencing may be in part due to loss of melanocortin action in the PVH. Overall, this study demonstrates that $CalcR^{PVH}$ neurons lie within energy balance neurocircuitry and their activity is important for body weight maintenance. Moreover, selectively modulating $CalcR^{PVH}$ neuronal activity may represent a potential novel therapeutic approach to treating and preventing obesity and its comorbidities.

Material and Methods:

Experimental Animals

CalcR-2a-Cre (or CalcR^{2ACre}) mice were previously generated and validated as described [70]. Adult male CalcRcre^{2ACre} mice (7-16 weeks old) were used for activation and silencing studies. Adult male mice (8-17 weeks old) expressing Cre recombinase in MC4R neurons (MC4R^{Cre}, JAX stock 030759; kindly provided by Dr. Brad Lowell) [71,72] were used for the silencing studies. As preliminary data revealed similar responses to CalcR^{PVH} neuron manipulation in both sexes, we conducted our studies in male mice to avoid potential confounding issues of hormonal cyclicity and to align our approach with previously published data[66]. Immunohistochemical analysis of CalcR^{PVH} neurons was performed using brains from CalcR^{2ACre} mice crossed to a Cre-dependent GFP reporter (CalcR$^{2ACre+GFP}$ mice) [63,73] . In accordance with the Association for the Assessment and Approval of Laboratory Animal Care and National Institutes of Health guidelines, the procedures performed were approved by the University of Michigan Committee on the Care and Use of Animals. Animals were bred and housed within our colony, with ad libitum access to food and water provided (unless specified otherwise) in temperature-controlled rooms that followed a 12-hour light/dark cycle.

Stereotaxic injections

Stereotaxic injections were conducted on CalcR^{2Acre}, MC4R^{Cre} and non-transgenic wildtype (WT) mice as described previously [70,71] . Following induction of isoflurane anesthesia and application of pre-surgical analgesia (carprofen), mice were placed in a

digital stereotaxic frame (Model 1900, Kopf Instruments). A pressurized picospritzer was used to perform viral injections into the PVH (coordinates relative to bregma: A/P= -.500, M/L= +/- .200, D/V= -4.77) through a pulled glass micropipette. For the anterograde tracing experiments, 50 nL of the adeno-associated virus with a Cre-dependent synaptophysin-GFP (rAAV8-flex Syn-EGFP, titer: $5.69x10^{14}$ vg/mL, produced by the Viral Vector Core at the University of Michigan) terminal tracer was injected unilaterally into the PVH of $CalcR^{2ACre}$ mice. The synaptophysin-GFP anterograde tracer traffics preferentially to the synaptic terminals of the neurons which aids in the identification of downstream targets. To allow temporal and spatial control of $CalcR^{PVH}$ neural activity, we used Cre-dependent expression of the stimulatory Designer Receptors Exclusively Activated by Designer Drugs (DREADDs; hM3Dq). hM3Dq is a modified human muscarinic receptor coupled to the stimulatory Gq-protein which activates neurons upon binding the synthetic ligand clozapine N-oxide (CNO)[74,75]. Cre-dependent AAV-Flex-hM3Dq-mCherry (AAV-Flex-hM3Dq, titer: $4x10^{12}$ virus molecules/mL, purchased from UNC Vector Core) was bilaterally injected (50 nL/side) into the PVH of $CalcR^{2ACre}$ mice to specifically manipulate these cells. Mice for the tracing and acute activation studies were given at least 21 days to recover and ensure sufficient viral expression in the cell bodies and their terminals. For $CalcR^{PVH}$ neuron silencing studies, Cre dependent tetanus toxin was used. Tetanus toxin cleaves synaptobrevin, a component of the SNARE core and prevents release of synaptic vesicles from targeted neurons [76,77]. 50nL of AAV-Flex-TetTox (titer: $1.2x10^{12}$ virus molecules/mL, generated at the UNC vector viral core based on a plasmid kindly provided by Dr. Wei Xu, UTSW) or control viruses were injected bilaterally in $CalcR^{2ACre}$

mice. For the MC4R^{PVH} studies, MC4R^{Cre} and WT mice were bilaterally injected in the PVH with AAV-Flex-TetTox or a Cre-dependent GFP reporter virus (AAV-Flex-GFP).

Effects of CalcR^{PVH} neuronal activation on feeding behavior and energy expenditure

Feeding and energy expenditure studies were performed at least 3 weeks after surgery to allow for surgical recovery and viral expression in CalcR^{2ACre} and control mice (wildtype mice and CalcR^{2ACre} mice injected with a control virus). For the acute feeding studies, mice received daily i.p. injections of vehicle 3 days prior to the experiment. On the day of the feeding studies, the mice were fasted from 10AM to 6PM and received i.p. injection of CNO or vehicle at the onset of the dark cycle with the presentation of food. Food intake was then measured one, two and four hours after the injection and the experiment was repeated at least 4 days later with the treatments switched (CalcR^{2ACre} +AAV-Flex-hM3Dq mice N=12, Controls N=7). To measure energy expenditure, CalcR^{2ACre} +AAV-Flex-hM3Dq mice were acclimated to daily saline injections for 3 days prior to entering a Comprehensive Laboratory Animal Monitoring System (CLAMS, Columbus Instruments) in the University of Michigan's Small Animal Phenotyping Core for multi-parameter assessments. Mice were given 24 hours to acclimate to the CLAMS unit. On the second day of CLAMS, food was removed between 9AM and 5PM and the mice received i.p. injection of either vehicle (0.9% sodium chloride) or CNO (0.3 mg/kg in saline) at 12:00PM. On the fourth day of CLAMS, the mice received the alternate treatment (saline or CNO). Measurements were taken continuously during the experiment; energy expenditure measurements were then averaged over the course of 4 hours following the injection of either CNO or

vehicle (CalcR^{2ACre} +AAV-Flex-hM3Dq N=10). To demonstrate that the activation of the CalcR^{PVH} neurons required both DREADDs expression and CNO injection, we quantified nuclear FOS expression in the PVH of CalcR^{2ACre} Flex-hM3Dq and control mice injected with either CNO or saline. Counts were conducted by summing the FOS positive cells in the PVH across 6 sections between Bregma -0.47mm and -1.07mm (CalcR^{2ACre} +AAV-Flex-hM3Dq + Saline N=4, CalcR^{2ACre} +AAV-Flex-hM3Dq + CNO N=8, Control + Saline N=4, Control + CNO N=3).

Long-term body weight, food intake and energy expenditure measurements

Mice injected with AAV-Flex-TetTox or control viruses were weighed just prior to surgery and were given 7 days to recover before weekly food intake and body weight measurements were taken for the CalcR^{2ACre} (CalcR^{2ACre}+AAV-Flex-TetTox N=13, controls N=25) and MC4R^{Cre} (MC4R^{Cre}+AAV-Flex-TetTox N=11, MC4R^{Cre}+GFP N=6, WT+AAV-Flex-TetTox N=10) experiments. CLAMS was used to measure oxygen consumption, carbon dioxide production and locomotor activity via optical beam breaks between 8 and 10 weeks post-injection for CalcR^{2Acre} mice (CalcR^{2ACre}+AAV-Flex-TetTox N=9, controls N=20). MC4R^{Cre} mice had CLAMS conducted between 3 to 4 weeks post-injection (MC4R^{Cre}+AAV-Flex-TetTox N=8, MC4R^{Cre}+GFP N=5, WT+AAV-Flex-TetTox N=7). Mice were placed in CLAMS for four days; data collected from the second and third days was used for analysis to allow acclimatization to occur during the first day. Body composition analysis was conducted just prior to CLAMS for the CalcR^{2Acre} mice (CalcR^{2ACre}+AAV-Flex-TetTox N=9, controls N=20) and between 7 and 8 weeks post-injection for the MC4R^{Cre} mice (Minispec LF90 II, Bruker Optics)(

MC4R^{Cre}+AAV-Flex-TetTox N=11, MC4R^{Cre}+GFP N=6, WT+AAV-Flex-TetTox N=10). Nine weeks following viral injection, CalcR^{2ACre} mice that received AAV-Flex-TetTox injections and the controls were acclimated to daily saline injections for 3 days prior to the day of the feeding experiment. They were then fasted during the light cycle between 10AM and 6PM and at the beginning of the dark cycle (6PM), mice were given ad libitum access to food and either an i.p. injection of salmon calcitonin at 100 ug/kg (sCT, Bachem, 4033011) or 0.9% sodium chloride. Food intake was then measured two and four hours following the injection. At least 4 days later, the injection treatments were switched, and food intake was measured (CalcR^{2ACre}+AAV-Flex-TetTox N=9, controls N=20).

In situ hybridization

Mice were overdosed with the inhaled anesthetic isoflurane, then the brains were removed and flash frozen in 2-methylbutane. The brains were cut using a cryostat (Leica CM 1950) into 16 µm sections onto glass slides and were immediately stored at -80^{o}C. The assays were conducted according to the protocol provided by the RNAscope manufacturer (Advanced Cell Diagnostics). Sections were fixed for 1 hour in cold 10% formalin and then dehydrated in 50% and 75% ethanol, each for 5 minutes followed by two times in 100% ethanol. The sections were then dried for 30 minutes at 40^{o}C. To determine the PVH expression of *Mc4r* and *Calcr* mRNAs in the PVH, chromogen staining was performed with an RNAscope® 2.5 HD Duplex Reagent Kit (ACD 322430). Sections were treated for 10 minutes with H_2O_2 and then incubated for 30 minutes with protease K IV. Following hybridization of *Mc4r* and *Calcr* mRNA probes, the sections

were washed twice and then underwent amplification with Amp1 to Amp2 with 2 washes in between. The red signal component was detected through diluting Red-B 1:60 in component Red-A, which was then incubated on the tissue at room temperature for 10 minutes. The slides were rinsed two times in wash buffer to conclude the chromogen reaction. Amplification proceeded with Amp7 through Amp10, after which the green signal was detected by diluting Green-B 1:50 in component Green-A and incubating at room temperature for 10 minutes. The tissue was then counter stained by immersing the slides into 50% hematoxylin for 30 seconds, after which they were dried and mounted in VectaMount mounting medium (Vector Laboratories, INC). Imaging for the chromogen stained tissue was conducted with an Olympus BX-51 microscope with a DP80 camera (Olympus). To quantify cells expressing probe signal, images from coronal sections were processed in a uniform manner with Photoshop (Adobe) in order to remove the background and better visualize the individual probes. Hematoxylin stained cells that were determined to be positive for each probe were quantified using ImageJ and overlapping expression was compared to the expression of a singular probe within each of the mouse groups (N=3).

Perfusion and Immunohistochemistry (IHC)

To confirm the accuracy of each viral injection, at the conclusion of all surgical experiments, mice were deeply anesthetized with inhaled isoflurane and then transcardially perfused with sterile PBS and then 10% buffered formalin. Brains were removed, post-fixed in 10% buffered formalin and dehydrated in 30% sucrose. Brains were then sectioned into four representative series of 30um coronal slices using a

freezing microtome (Leica) and stored at -20ºC. For immunohistochemistry (IHC), we blocked brain tissue using 3% normal donkey serum, followed by incubation in primary and then secondary antibodies. For the AAV-Flex-hM3Dq-mCherry experiments, mCherry expression was detected using a primary antibody for dsRed (rabbit 1:1000, Clontech, 632496) [78], followed by secondary immunofluorescence detection with donkey anti-rabbit-Alexa 568 (1:200, Invitrogen) [79] . For cFos imaging of CalcR^{2ACre} +AAV-Flex-hM3Dq mouse brains, primary antibodies for cFos (rabbit 1:1000, Cell Signaling, 2250S) [80] and tdTomato (rat 1:1000, Kerafast, Inc. EST203, which also recognizes mCherry) [81] were used, followed by donkey anti-rabbit-Alexa 488 (1:200, Invitrogen) [82] and goat anti-rat-Alexa 568 (1:200, Invitrogen) [83] secondary antibodies. For the anterograde tracing and TetTox-GFP experiments, a primary antibody for GFP (chicken 1:1000, Aves GFP–1020) [84] was used followed by a goat anti-chicken-Alexa 488 (1:200, Invitrogen) [85] secondary antibody. For the colocalization experiments (quantification took place in the PVH across 6 sections between Bregma -0.47mm and -1.07mm, N=3 CalcR$^{2ACre+GFP}$ mice were used per peptide investigated), we used primary antibodies for GFP (chicken 1:1000, Aves GFP–1020 or rabbit 1:1000, Invitrogen A6455) [84,86] , nNos1 (sheep 1:1000, kindly provided by Dr. Vincent Prevot), OXT (rabbit 1:4000, Peninsula Laboratories, LLC T-4084) [87] and AVP (rabbit 1:4000, Millipore AB1565) [88]. To trap TRH and CRH in PVH cell bodies for IHC visualization, we utilized intracerebral (ICV) injections of colchicine (coordinates relative to bregma: 3rd ventricle A/P= -.340, M/L= -1.000, D/V= -2.400) into CalcR$^{2ACre+GFP}$ mice [89]. We delivered 250 nL of colchicine solution (0.040mg/mL colchicine in water) to the 3rd ventricle of the mice and perfused two days later. For these mice, primary antibodies for Pro-TRH (rabbit

1:1000, Millipore ABN1658) [90] and CRH (rabbit 1:1000, Peninsula Laboratories, LLC T-4037) [91] were used. Secondary immunofluorescence for the colocalization experiments was conducted using goat anti-chicken-Alexa 488 [85] , donkey anti-goat-Alexa 488 [92] , donkey anti-rabbit-Alexa 488 [82] , donkey anti-sheep-Alexa 594 and donkey anti-rabbit-Alexa 568 (1:200, Invitrogen) [93] .

Data and Statistical Analysis

For experiments utilizing mice with the stereotaxic viral injections data analysis was only performed using mice in which the viral expression was constrained to the PVH (as determined by post-hoc immunohistochemistry) in order to avoid confounding effects from viral transduction of cells outside the PVH. Unpaired t-tests, paired t-tests, one-way and 2-way ANOVAs with Sidak's or Tukey's multiple comparisons test post-hoc tests (when appropriate), mixed model analyses and simple linear regression and correlation analysis were conducted using GraphPad Prism 8, as noted in the figure legends. $P<0.05$ indicates significance.

Results

Activation of CalcR^{PVH} neurons regulates feeding but not energy expenditure

The anorectic effect of sCT delivered directly to the PVH suggests that activation of CalcR^{PVH} cells may suppress feeding. To determine the contribution of CalcR^{PVH} neurons to energy balance control, we used chemogenetics to acutely activate

CalcR^{PVH} neurons and examine the effects on food intake and energy expenditure [74,75]. We bilaterally injected a Cre-dependent activating DREADD (designer receptors exclusively activated by designer drugs) virus (AAV-Flex-hM3Dq) into the PVH of CalcR^{2ACre} mice (Figure 3.3 A). After at least three weeks to allow for surgical recovery and viral expression, CalcR^{2ACre} Flex-hM3Dq mice were fasted during the day and were then injected with either vehicle or CNO at the beginning of the dark cycle, the time at which mice typically start to feed. CalcR^{PVH} neuron activation significantly decreased food intake over the first 2 hours of feeding (Figure 3.3 B). By 16 hours following the administration of CNO to the CalcR^{2ACre} Flex-hM3Dq mice, cumulative food intake was comparable to controls, indicating that compensatory food intake occurred after the activating effects of the CNO dissipated (data not shown). Wildtype mice and CalcR^{2ACre} mice injected with a control virus had no response to CNO (data were pooled as a single control group) demonstrating that neither CNO nor its metabolites alter food intake in this paradigm. CalcR^{2ACre} Flex-hM3Dq mice injected with CNO expressed significantly more nuclear FOS in the PVH (Figure 3.3 D,E) than CalcR^{2ACre} Flex-hM3Dq mice injected with saline (Figure 3.3 C,E) and control mice injected with CNO or saline (Figure 3.3 E) indicating a CNO+DREADD-dependent effect on neuron activity. Thus activation of CalcR^{PVH} neurons is sufficient to suppress feeding behavior and demonstrates that CalcR^{PVH} neurons lie within the neurocircuitry that modulates feeding.

As activation of some subsets of PVH neurons promotes oxygen consumption and locomotor activity [63,94] , we next assessed whether CalcR^{PVH} neuron activation could alter energy expenditure. CalcR^{2ACre} Flex-hM3Dq mice were placed into CLAMS to

measure oxygen consumption and locomotor activity following CNO activation. In the absence of food, activation of CalcR^{PVH} neurons did not significantly change energy expenditure or respiratory exchange ratio (Figure 3.3 F-G). Although acute activation of CalcR^{PVH} neurons increases locomotor activity slightly (Figure 3.3 H), this behavioral change is not sufficient to alter overall energy expenditure at least as measured by changes in oxygen consumed or carbon dioxide produced in the CLAMS. Taken together, these findings indicate that activation of CalcR^{PVH} neurons suppresses feeding without an appreciable effect on energy expenditure.

CalcR^{PVH} neurons project to regions of the hindbrain and display unique neuropeptide expression

Having established a potential role for CalcR^{PVH} neurons in energy balance control, we sought to characterize the neural circuitry in which CalcR^{PVH} neurons reside. A Cre-dependent viral anterograde tracer, AAV-Flex-synaptophysin-GFP was unilaterally injected into the PVH of CalcR^{2ACre} mice (Figure 3.4 A). Dense projection terminals from CalcR^{PVH} neurons were found in hindbrain regions such as the parabrachial nucleus (PBN) and the nucleus of the solitary tract (NTS) (Figure 3.4 B,C) brain regions known to be involved in feeding and energy expenditure regulation. Projections to the PBN range between -5.07mm and -5.63mm relative to Bregma, with prominent signal in the medial PBN (MPBN) as well as the lateral PBN (LPBN) and its sub-nuclei including the central, external, lateral crescent, dorsal, internal lateral, and ventral lateral regions of the LPBN (Figure 3.4 B). NTS projections were found between Bregma -7.19mm and -7.67mm, with signal in the gelatinous subnucleus, dorsolateral subnucleus, central

subnucleus, central subnucleus, intermediate tract nucleus, medial subnucleus, dorsomedial subnucleus, commissural subnucleus, interstitial subnucleus and limited signal in the parasolitary nucleus. Signal was also found in the area postrema (AP) and the dorsal motor nucleus of vagus nerve (10N) (Figure 3.4 C). CalcR^{PVH} neurons also project to the external zone of the median eminence indicating engagement with the hypophyseal portal system and a potential role in pituitary regulation (Figure 3.4 D) [95]. These tracing data demonstrate that CalcR^{PVH} neurons are anatomically positioned to alter energy balance through projections to critical brain regions.

DREADD-mediated control of CalcR^{PVH} neuron activity is not a simple surrogate for calcitonin signaling but enforces activation of CalcR^{PVH} neurons and presumably their neurotransmitter contents. To determine if CalcR^{PVH} neuron manipulations may impact other previously described PVH cell systems, we employed immunohistochemistry (IHC) to examine co-expression of several neuropeptides in CalcR^{PVH} neurons. To identify CalcR^{PVH} cells, we used the CalcR^{2ACre} mouse to drive Cre dependent GFP expression in all CalcR-expressing cells (CalcR$^{2ACre\ +eGFP}$) and then co-stained for GFP in conjunction with primary antibodies that specifically bind to NOS1, OXT, AVP, CRH and TRH. As CRH and TRH are quickly trafficked to the synaptic terminals of their neurons, we treated CalcR$^{2ACre+GFP}$ mice with colchicine (intracerebroventricularly) to trap these peptides in the cell bodies. Co-expression of GFP with each antigen was performed using brain sections from three mice for quantification. We found that CalcR^{PVH} neurons are largely distinct from NOS1 (8.3 $\pm$ 1.1% of CalcR neurons express NOS1 and 5.9 $\pm$ 0.8% of NOS1 neurons express CalcR), OXT (1.6 $\pm$ 0.5% of CalcR neurons express OXT and 2.4 $\pm$ 1.2% of OXT neurons express CalcR) and AVP (2.0 $\pm$

0.6% of CalcR neurons express AVP and 3.9 ± 1.8% of AVP neurons express CalcR) neurons in the PVH (Figure 3.5 B-D). A small amount of overlap is observed with the TRH^{PVH} neuronal population (4.7 ± 0.7% of CalcR neurons express TRH and 22.1 ± 0.5% of TRH neurons express CalcR) and there is a greater degree of overlap with the CRH^{PVH} population (11.1 ± 0.7% of CalcR neurons express CRH and 38.8 ± 0.7% of CRH neurons express CalcR) (Figure 3.5 E,F).

$CalcR^{PVH}$ neurons are required for normal feeding and body weight maintenance

Although chemogenetic manipulation of neurons reveals their capacity to alter energy balance, this approach is not informative regarding the contribution of a neuronal subset to basal physiology. To determine the importance of $CalcR^{PVH}$ neurons in maintaining energy homeostasis, we chronically silenced $CalcR^{PVH}$ neurons using Cre-dependent viral-expression of tetanus toxin (AAV-Flex-TetTox). AAV-Flex-TetTox or a Cre-dependent AAV control virus was bilaterally injected into the PVH of $CalcR^{2ACre}$ mice (Figure 3.6A). Following the surgery, $CalcR^{2ACre}$ -Flex-TetTox mice gained more weight compared to the $CalcR^{2Acre}$ mice injected with the AAV control virus (Figure 3.6 B,C). Weight gain in the $CalcR^{2ACre}$ -Flex-TetTox was associated with increased fat mass and a trend towards increased lean mass relative to controls (Figure 3.6 D). The obesity in $CalcR^{2ACre}$ -Flex-TetTox mice was potentially driven by increased caloric intake, as food intake was significantly higher in $CalcR^{2ACre}$ -Flex-TetTox mice compared to controls when measured three weeks following the injection (Figure 3.6 E). This difference in food intake between the two groups is no longer discernable by week 7 (Figure 3.6 F), suggesting that compensatory responses to blunt persistent hyperphagia may have

occurred as obesity developed. As was expected from our previous PVH-specific CalcR deletion studies [53], the anorectic effects of sCT was preserved in CalcR^{2ACre}-Flex-TetTox mice (Figure 3.6 G) demonstrating that the anorectic effect of peripheral sCT is not dependent on PVH CalcR expression or CalcR^{PVH} neuronal function.

Energy expenditure was also examined in CalcR^{2ACre} -Flex-TetTox mice 8-10 weeks following injection of virus. To avoid the confounds of energy expenditure assessments of animals with different body weights, we plotted 24hr energy expenditure as a function of body weight. While the change in energy expenditure as a function of body weight in this cohort of CalcR^{2ACre} -Flex-TetTox mice was slightly less than the controls, this observed trend is strongly influenced by the two heaviest animals in the dataset (Figure 3.6 H). RER and locomotor activity levels (measuring X-total activity) over a 24 hour period were not significantly different between the CalcR^{2ACre} -Flex-TetTox mice and controls (Figure 3.6 I-J). Taken together, CalcR^{PVH} silencing studies suggest that CalcR^{PVH} neurons likely modulate feeding with at most a small contribution to energy expenditure control.

MC4R signaling may be an essential component of CalcR^{PVH} neuron mediated energy balance

MC4R expression in PVH neurons is critical for normal feeding and body weight regulation with loss of MC4R signaling in the PVH characterized by hyperphagia and significant obesity [50,67,73] . Given the increased food intake and obesity seen with silencing of CalcR^{PVH} neurons, we examined the overlap of *Mc4r* and *Calcr* transcripts

in the PVH. In situ hybridization revealed that almost half of $MC4R^{PVH}$ neurons express *Calcr* mRNA (43.6 ± 6.9%, n=3 mice) whereas less than a quarter of $CalcR^{PVH}$ neurons express *Mc4r* mRNA (16.7 ± 1.3%, n=3 mice) (Figure 3.7 A). Therefore, $CalcR^{PVH}$ neuron silencing might significantly impact $MC4R^{PVH}$ neuron function. In an effort to estimate the contribution of abrogated MC4R-signaling to the obesity phenotype provoked by $CalcR^{PVH}$ silencing, we selectively silenced $MC4R^{PVH}$ neurons and examined the effect on feeding and bodyweight regulation. We bilaterally injected 50nL of the AAV-Flex-TetTox into the PVH of MC4R-Cre mice ($MC4R^{Cre}$ -Flex-TetTox) (Figure 3.7 B). For controls, WT mice were injected with the AAV-Flex-TetTox and $MC4R^{Cre}$ mice were injected with an AAV-Flex-GFP virus. In line with a prior study [71], silencing of $MC4R^{PVH}$ neurons resulted in rapid development of obesity (Figure 3.7 C,D). Fat mass and lean mass increased significantly in the $MC4R^{Cre}$ -Flex-TetTox mice compared to the controls. Fat and lean mass also increased slightly in the $MC4R^{Cre}$ -Flex-GFP mice control group relative to WT controls which may be inherent to the genetic targeting of the *Mc4r* locus for Cre expression [71,96] (Figure 3.7 E). $MC4R^{Cre}$ -Flex-TetTox mice consumed more food than WT controls on week 3 and week 7 post injection (Figure 3.7 F-G). It is important to note that $MC4R^{Cre}$ -Flex-GFP mice also exhibited increased food intake relative to WT controls; the effect on feeding was similar to that seen for $MC4R^{Cre}$ -Flex-TetTox mice, at least at 3 weeks following virus injection. Thus the significant weight gain seen with $MC4R^{Cre}$ -Flex-TetTox relative to $MC4R^{Cre}$ -Flex-GFP mice control group (Figure 3.7 C,D) cannot be attributed solely to hyperphagia. Given the overlap of *Calcr* and *Mc4r* expression in the PVH, the silencing of $CalcR^{PVH}$ neurons would be expected to silence a significant fraction of $MC4R^{PVH}$

neurons which likely contributes to the CalcR^{2ACre}-Flex-TetTox obesity phenotype. These findings indicate that the CalcR^{+}/MC4R^{+} subpopulation of the PVH is potentially responsible for some of the obesity observed when all CalcR^{PVH} neurons are silenced.

Discussion

Body weight maintenance is largely determined by actions of the central nervous system (CNS). Successfully targeting the CNS for obesity treatment or prevention will require a deeper understanding of the mechanisms and neurocircuitry that modulate feeding and energy expenditure [55]. CalcR agonists, such as calcitonin and amylin, promote anorexia and weight loss in both humans and rodents [9,11,97,98]. CalcR is expressed in many regions of the CNS known to regulate energy balance suggesting that the site(s) of action for CalcR agonists may be distributed. Recently, we used Cre-loxP technology to delete CalcR from different regions of the brain in order to identify the neurocircuitry mediating the anorexic effects of peripherally administered CalcR agonists [53]. Despite the significant expression of CalcR in the PVH, a brain region known to play critical roles in the energy balance control, deletion of CalcR from the PVH does not perturb physiologic feeding or body weight, and mice lacking CalcRs in the PVH have a normal anorectic response to peripherally applied sCT. These findings indicate that CalcR expression in the PVH is not required for body weight maintenance or sCT-induced anorexia. Nevertheless, the anorexia induced by the direct application of sCT to the PVH suggests that the CalcR-expressing PVH neurons lie within feeding neural circuits and that CalcR^{PVH} neuron activity may regulate feeding behavior [14]. It is for this reason that we used site-directed, temporal manipulations to specifically

investigate the contribution of the CalcR-expressing neurons of the PVH to energy homeostasis.

Acute activation of CalcR^{PVH} neurons using chemogenetic tools was sufficient to suppress feeding thereby demonstrating that CalcR^{PVH} neurons engage neural circuits that modulate feeding behavior. We and others have found that chemogenetic activation of a variety of genetically tagged PVH neurons is sufficient to alter feeding [63], [71]. It is important to note, however, that this is not a ubiquitous property of PVH cells, as direct activation of oxytocin expressing PVH neurons does not alter feeding, thus highlighting the compartmentalization of PVH cell function [63]. Chemogenetic activation can reveal the functional potential of a group of neurons but does not elucidate its role in normal physiological states. To probe the contribution of CalcR^{PVH} neurons to bodyweight regulation, we chronically silenced these neurons in adult animals and found that their activity was necessary for restraining feeding and bodyweight gain. In line with our previous findings that demonstrated that mice lacking CalcRs in the PVH respond normally to peripheral application of sCT, the anorectic properties of sCT are still present even when CalcR^{PVH} neurons are silenced. The contribution of CalcR^{PVH} neurons on feeding and body weight regulation are revealed by both activating and silencing manipulations, and demonstrate that these neurons lie within and modulate neural circuitry that is crucial to the regulation of energy homeostasis.

While we have demonstrated that CalcR^{PVH} neurons modulate feeding and locomotor activity and are necessary for bodyweight maintenance, we have yet to determine the neurocircuitry through which these neurons alter feeding and energy balance. PVH neurons, such as the NOS1^{PVH} neurons, project to hindbrain regions

known to contribute to energy balance [54,63,73,99]. Similarly, CalcR^{PVH} neurons send projection terminals to the PBN, a hindbrain region strongly associated with both appetitive and aversive feeding circuitry [54,67]. CalcR^{PVH} neurons also send projections to the NTS, a region that integrates neuronal and hormone satiety signals that originate from the periphery [99]. The NTS also influences sympathetic outflow through neurons with polysynaptic contact with brown adipose tissue (BAT) and can both activate and inhibit BAT thermogenesis [100-103]. Our current studies do not distinguish the physiological responses driven by CalcR^{PVH} neuronal projections to either the PBN or NTS specifically; terminal specific manipulations (e.g., via optogenetics) will be necessary to discriminate these effects. As the PVH is largely glutamatergic and intra-PVH connections are known to exist, it remains possible that activation of a defined cell population could be cascaded through neighboring cells to effect physiological outputs [55-57,104]. In this regard, CalcR^{PVH} neurons when activated may serve to transmit a signal within the PVH rather than directly to a downstream target. Technologies that manipulate discrete CalcR^{PVH} outputs will be needed to better characterize the brain regions targeted by CalcR^{PVH} neurons to modulate defined energy balance parameters.

The PVH is composed of a variety of neuronal subpopulations that have been implicated in energy balance regulation [56,57,105]. Discriminating these subsets of neurons by receptor or neuropeptide expression is important for understanding PVH function. Neurochemical characterization of genetically-tagged PVH neurons is a critical step in interpreting the mechanisms and potential novelty of functional manipulations and helps formulate hypotheses regarding the molecular mechanisms engaged to drive physiologic responses to changes in PVH activity. In the case of CalcR^{PVH} neurons, we

found them to be distinct from the NOS1^{PVH}, OXT^{PVH} and AVP^{PVH} neuronal subpopulations, each of which alter energy balance when acutely activated [63,65,106]. This raises the intriguing possibility of the additive benefits of selectively activating combinations of these populations. Such studies would also reveal whether there is a threshold for the beneficial effects of PVH stimulation on feeding and energy expenditure.

Subsets of CalcR^{PVH} neurons express corticotropin releasing hormone (CRH) or thyrotropin releasing hormone (TRH), neuropeptides implicated in feeding and energy expenditure [107,108]. ICV injection of CRH in genetically obese and lean mice decreases feeding, decreases oxygen consumption and decreases activity level [107]. Mice lacking CRH, however, display a normal body weight [109] ; whether developmental loss of CRH provokes compensation in bodyweight neural circuitry to prevent obesity is not known. CRH^{PVH} neuron activity is rapidly reduced following refeeding after a fast indicating that CRH^{PVH} neuron activity may be more responsive to alterations in stress than feeding directly [71]. In addition, chronic silencing of CRH^{PVH} neurons is not associated with hyperphagia in contrast to what we find with CalcR^{PVH} neuron silencing [71]. There is a small amount of overlap between the CalcR and TRH neuronal populations of the PVH. TRH^{PVH} neurons regulate the thyroid axis which directly contributes to resting energy expenditure [53,108]. Chemogenetic activation of TRH^{PVH} neurons stimulates feeding through projections to AGRP neurons, which is opposite to the anorectic effect of activating CalcR^{PVH} neurons [110]. Taken together, it seems unlikely that CRH^{PVH} or TRH^{PVH} neurons contained within the CalcR^{PVH} field are responsible for the physiologic effects on body weight and feeding following CalcR^{PVH} neuron manipulations.

The central melanocortin system is a critical component of energy balance control and direct manipulations of MC4Rs in the PVH have profound effects on feeding and body weight [50,67,73] . Since manipulation of CalcR^{PVH} neurons altered feeding, we examined the overlap of MC4R and CalcRs in the PVH and found that nearly half of the MC4R^{PVH} neurons co-express CalcR. Selective silencing of CalcR^{PVH} neurons therefore effectively disables signaling from about half of the MC4R^{PVH} neurons. Given the gene dosage effect associated with MC4R-mediated obesity, loss of ~1/2 of MC4R^{PVH} through inactivation of CalcR^{PVH} neurons would be predicted to produce a fraction of the overall obesity seen upon complete MC4R^{PVH} inactivation. Consistent with this prediction, we find that the change in body weight in the MC4R^{PVH} silenced mice is nearly twice as much as compared to the CalcR^{PVH} silenced mice. This comparative approach is an indirect method of determining the necessity of MC4R expression in CalcR^{PVH} neurons to mediate energy homeostasis. To definitively assess the contribution of melanocortin signaling CalcR^{PVH} neurons to body weight control, specific deletion of MC4Rs from CalcR^{PVH} neurons is required. Simply crossing the CalcR^{2ACre} line to a loxP-flanked MC4R transgenic line would delete MC4R expression from all CalcR neurons, including those expressed outside the PVH, and confound the data interpretation (this will be further explored in Chapter 4).

There are important caveats associated with our experimental approach. Tethering Cre recombinase activity to CalcR gene expression allows us to target CalcR-expressing neurons specifically, but subsequent activation or silencing of these neurons with chemogenetics or tetanus toxin expression impacts a variety of signaling systems within these cells. Indeed, manipulations of CalcR^{PVH} neuron activity with viral vectors

should not be viewed as a surrogate for calcitonin agonist signaling in these neurons. The interpretation of any physiologic effect attributed to CalcR^{PVH} neuron activation or silencing must take into account that a range of signaling pathways and neurotransmitter release are being affected. This highlights the importance of identifying other neuropeptides (e.g., CRH or TRH) and signaling systems (NOS1) that function within CalcR^{PVH} neurons, as these systems likely contribute to the modulation of energy balance parameters revealed by our viral manipulations.

Through Cre-dependent viral tools and Cre-LoxP technology, we find that CalcR^{PVH} neuron activity is required for maintaining normal body weight in mice which highlights an important role for CalcR^{PVH} neurons in energy homeostasis. CalcR^{PVH} neurons are largely distinct from other known PVH neurons and project to brain regions known to be involved in energy balance control. A thorough understanding of CalcR^{PVH} neurons and their neurocircuitry will deepen our understanding of central energy balance control and may uncover novel approaches to targeting disordered eating and obesity.

References:

1. Wimalawansa SJ. Amylin, calcitonin gene-related peptide, calcitonin, and adrenomedullin: a peptide superfamily. *Crit Rev Neurobiol.* 1997;11(2-3):167-239.
2. Freed WJ, Perlow MJ, Wyatt RJ. Calcitonin: inhibitory effect on eating in rats. *Science.* 1979;206(4420):850-852.
3. Lutz TA, Althaus J, Rossi R, Scharrer E. Anorectic effect of amylin is not transmitted by capsaicin-sensitive nerve fibers. *Am J Physiol.* 1998;274(6):R1777-1782.
4. Lutz TA, Del Prete E, Scharrer E. Reduction of food intake in rats by intraperitoneal injection of low doses of amylin. *Physiol Behav.* 1994;55(5):891-895.
5. Morley JE, Flood JF, Horowitz M, Morley PM, Walter MJ. Modulation of food intake by peripherally administered amylin. *Am J Physiol.* 1994;267(1 Pt 2):R178-184.
6. Masi L, Brandi ML. Calcitonin and calcitonin receptors. *Clin Cases Miner Bone Metab.* 2007;4(2):117-122.
7. Phillippo M, Bruce JB, Lawrence CB. The effect of adrenaline on calcitonin secretion in conscious sheep. *J Endocrinol.* 1970;46(2):12-13.
8. Talmage RV, Doppelt SH, Cooper CW. Relationship of blood concentrations of calcium, phosphate, gastrin and calcitonin to the onset of feeding in the rat. *Proc Soc Exp Biol Med.* 1975;149(4):855-859.
9. Perlow MJ, Freed WJ, Carman JS, Wyatt RJ. Calcitonin reduces feeding in man, monkey and rat. *Pharmacol Biochem Behav.* 1980;12(4):609-612.
10. Twery MJ, Obie JF, Cooper CW. Ability of calcitonins to alter food and water consumption in the rat. *Peptides.* 1982;3(5):749-755.
11. Lutz TA, Tschudy S, Rushing PA, Scharrer E. Amylin receptors mediate the anorectic action of salmon calcitonin (sCT). *Peptides.* 2000;21(2):233-238.
12. Lutz TA, Senn M, Althaus J, Del Prete E, Ehrensperger F, Scharrer E. Lesion of the area postrema/nucleus of the solitary tract (AP/NTS) attenuates the anorectic effects of amylin and calcitonin gene-related peptide (CGRP) in rats. *Peptides.* 1998;19(2):309-317.
13. Rowland NE, Richmond RM. Area postrema and the anorectic actions of dexfenfluramine and amylin. *Brain Res.* 1999;820(1-2):86-91.
14. Chait A, Suaudeau C, De Beaurepaire R. Extensive brain mapping of calcitonin-induced anorexia. *Brain Res Bull.* 1995;36(5):467-472.
15. Tavares E, Maldonado R, Garcia-Martinez A, Minano FJ. Central administration of aminoprocalcitonin inhibits food intake and stimulates the hypothalamic-pituitary-adrenal axis in rats via the corticotrophin-releasing factor system. *J Neuroendocrinol.* 2012;24(7):1040-1054.
16. Lutz TA. Control of food intake and energy expenditure by amylin-therapeutic implications. *Int J Obes (Lond).* 2009;33 Suppl 1:S24-27.
17. Westermark P, Wernstedt C, Wilander E, Sletten K. A novel peptide in the calcitonin gene related peptide family as an amyloid fibril protein in the endocrine pancreas. *Biochem Biophys Res Commun.* 1986;140(3):827-831.

18. Badman MK, Flier JS. The gut and energy balance: visceral allies in the obesity wars. *Science.* 2005;307(5717):1909-1914.
19. Lutz TA. Pancreatic amylin as a centrally acting satiating hormone. *Curr Drug Targets.* 2005;6(2):181-189.
20. Young A, Denaro M. Roles of amylin in diabetes and in regulation of nutrient load. *Nutrition.* 1998;14(6):524-527.
21. Reidelberger RD, Haver AC, Arnelo U, Smith DD, Schaffert CS, Permert J. Amylin receptor blockade stimulates food intake in rats. *Am J Physiol Regul Integr Comp Physiol.* 2004;287(3):R568-574.
22. Mollet A, Gilg S, Riediger T, Lutz TA. Infusion of the amylin antagonist AC 187 into the area postrema increases food intake in rats. *Physiol Behav.* 2004;81(1):149-155.
23. Lutz TA, Mollet A, Rushing PA, Riediger T, Scharrer E. The anorectic effect of a chronic peripheral infusion of amylin is abolished in area postrema/nucleus of the solitary tract (AP/NTS) lesioned rats. *Int J Obes Relat Metab Disord.* 2001;25(7):1005-1011.
24. Bhavsar S, Watkins J, Young A. Synergy between amylin and cholecystokinin for inhibition of food intake in mice. *Physiol Behav.* 1998;64(4):557-561.
25. Mollet A, Meier S, Grabler V, Gilg S, Scharrer E, Lutz TA. Endogenous amylin contributes to the anorectic effects of cholecystokinin and bombesin. *Peptides.* 2003;24(1):91-98.
26. Aronne L, Fujioka K, Aroda V, et al. Progressive reduction in body weight after treatment with the amylin analog pramlintide in obese subjects: a phase 2, randomized, placebo-controlled, dose-escalation study. *J Clin Endocrinol Metab.* 2007;92(8):2977-2983.
27. Smith SR, Aronne LJ, Burns CM, Kesty NC, Halseth AE, Weyer C. Sustained weight loss following 12-month pramlintide treatment as an adjunct to lifestyle intervention in obesity. *Diabetes Care.* 2008;31(9):1816-1823.
28. Smith SR, Blundell JE, Burns C, et al. Pramlintide treatment reduces 24-h caloric intake and meal sizes and improves control of eating in obese subjects: a 6-wk translational research study. *Am J Physiol Endocrinol Metab.* 2007;293(2):E620-627.
29. Zhang Y, Proenca R, Maffei M, Barone M, Leopold L, Friedman JM. Positional cloning of the mouse obese gene and its human homologue. *Nature.* 1994;372(6505):425-432.
30. Farooqi IS, Jebb SA, Langmack G, et al. Effects of recombinant leptin therapy in a child with congenital leptin deficiency. *N Engl J Med.* 1999;341(12):879-884.
31. Farooqi IS, Matarese G, Lord GM, et al. Beneficial effects of leptin on obesity, T cell hyporesponsiveness, and neuroendocrine/metabolic dysfunction of human congenital leptin deficiency. *J Clin Invest.* 2002;110(8):1093-1103.
32. Montague CT, Farooqi IS, Whitehead JP, et al. Congenital leptin deficiency is associated with severe early-onset obesity in humans. *Nature.* 1997;387(6636):903-908.
33. Heymsfield SB, Greenberg AS, Fujioka K, et al. Recombinant leptin for weight loss in obese and lean adults: a randomized, controlled, dose-escalation trial. *JAMA.* 1999;282(16):1568-1575.

34. Roth JD, Roland BL, Cole RL, et al. Leptin responsiveness restored by amylin agonism in diet-induced obesity: evidence from nonclinical and clinical studies. *Proc Natl Acad Sci U S A.* 2008;105(20):7257-7262.
35. Trevaskis JL, Coffey T, Cole R, et al. Amylin-mediated restoration of leptin responsiveness in diet-induced obesity: magnitude and mechanisms. *Endocrinology.* 2008;149(11):5679-5687.
36. Turek VF, Trevaskis JL, Levin BE, et al. Mechanisms of amylin/leptin synergy in rodent models. *Endocrinology.* 2010;151(1):143-152.
37. Osto M, Wielinga PY, Alder B, Walser N, Lutz TA. Modulation of the satiating effect of amylin by central ghrelin, leptin and insulin. *Physiol Behav.* 2007;91(5):566-572.
38. Ravussin E, Smith SR, Mitchell JA, et al. Enhanced weight loss with pramlintide/metreleptin: an integrated neurohormonal approach to obesity pharmacotherapy. *Obesity (Silver Spring).* 2009;17(9):1736-1743.
39. Trevaskis JL, Wittmer C, Athanacio J, Griffin PS, Parkes DG, Roth JD. Amylin/leptin synergy is absent in extreme obesity and not restored by calorie restriction-induced weight loss in rats. *Obes Sci Pract.* 2016;2(4):385-391.
40. Lin HY, Harris TL, Flannery MS, et al. Expression cloning and characterization of a porcine renal calcitonin receptor. *Trans Assoc Am Physicians.* 1991;104:265-272.
41. Becskei C, Riediger T, Zund D, Wookey P, Lutz TA. Immunohistochemical mapping of calcitonin receptors in the adult rat brain. *Brain Res.* 2004;1030(2):221-233.
42. Sheward WJ, Lutz EM, Harmar AJ. The expression of the calcitonin receptor gene in the brain and pituitary gland of the rat. *Neurosci Lett.* 1994;181(1-2):31-34.
43. Naot D, Cornish J. The role of peptides and receptors of the calcitonin family in the regulation of bone metabolism. *Bone.* 2008;43(5):813-818.
44. Lee SM, Hay DL, Pioszak AA. Calcitonin and amylin receptor peptide interaction mechanisms. INSIGHTS INTO PEPTIDE-BINDING MODES AND ALLOSTERIC MODULATION OF THE CALCITONIN RECEPTOR BY RECEPTOR ACTIVITY-MODIFYING PROTEINS. *J Biol Chem.* 2016;291(31):16416.
45. Oliver KR, Kane SA, Salvatore CA, et al. Cloning, characterization and central nervous system distribution of receptor activity modifying proteins in the rat. *Eur J Neurosci.* 2001;14(4):618-628.
46. Muff R, Buhlmann N, Fischer JA, Born W. An amylin receptor is revealed following co-transfection of a calcitonin receptor with receptor activity modifying proteins-1 or -3. *Endocrinology.* 1999;140(6):2924-2927.
47. Poyner DR, Sexton PM, Marshall I, et al. International Union of Pharmacology. XXXII. The mammalian calcitonin gene-related peptides, adrenomedullin, amylin, and calcitonin receptors. *Pharmacol Rev.* 2002;54(2):233-246.
48. Xi D, Gandhi N, Lai M, Kublaoui BM. Ablation of Sim1 neurons causes obesity through hyperphagia and reduced energy expenditure. *PloS one.* 2012;7(4):e36453.

49. Duplan SM, Boucher F, Alexandrov L, Michaud JL. Impact of Sim1 gene dosage on the development of the paraventricular and supraoptic nuclei of the hypothalamus. *Eur J Neurosci.* 2009;30(12):2239-2249.
50. Balthasar N, Dalgaard LT, Lee CE, et al. Divergence of melanocortin pathways in the control of food intake and energy expenditure. *Cell.* 2005;123(3):493-505.
51. Yamaguchi M, Watanabe Y, Ohtani T, et al. Calcitonin Receptor Signaling Inhibits Muscle Stem Cells from Escaping the Quiescent State and the Niche. *Cell Rep.* 2015;13(2):302-314.
52. Xi D, Roizen J, Lai M, Gandhi N, Kublaoui B. Paraventricular nucleus Sim1 neuron ablation mediated obesity is resistant to high fat diet. *PLoS One.* 2013;8(11):e81087.
53. Cheng W, Gonzalez I, Pan W, et al. Calcitonin Receptor Neurons in the Mouse Nucleus Tractus Solitarius Control Energy Balance via the Non-aversive Suppression of Feeding. *Cell Metab.* 2020;31(2):301-312 e305.
54. Roman CW, Sloat SR, Palmiter RD. A tale of two circuits: CCK(NTS) neuron stimulation controls appetite and induces opposing motivational states by projections to distinct brain regions. *Neuroscience.* 2017;358:316-324.
55. Morton GJ, Meek TH, Schwartz MW. Neurobiology of food intake in health and disease. *Nat Rev Neurosci.* 2014;15(6):367-378.
56. Sutton AK, Myers MG, Jr., Olson DP. The Role of PVH Circuits in Leptin Action and Energy Balance. *Annu Rev Physiol.* 2016;78:207-221.
57. Swanson LW, Sawchenko PE. Paraventricular nucleus: a site for the integration of neuroendocrine and autonomic mechanisms. *Neuroendocrinology.* 1980;31(6):410-417.
58. Sims JS, Lorden JF. Effect of paraventricular nucleus lesions on body weight, food intake and insulin levels. *Behav Brain Res.* 1986;22(3):265-281.
59. Leibowitz SF, Hammer NJ, Chang K. Hypothalamic paraventricular nucleus lesions produce overeating and obesity in the rat. *Physiol Behav.* 1981;27(6):1031-1040.
60. Tolson KP, Gemelli T, Gautron L, Elmquist JK, Zinn AR, Kublaoui BM. Postnatal Sim1 deficiency causes hyperphagic obesity and reduced Mc4r and oxytocin expression. *J Neurosci.* 2010;30(10):3803-3812.
61. Michaud JL, Rosenquist T, May NR, Fan CM. Development of neuroendocrine lineages requires the bHLH-PAS transcription factor SIM1. *Genes Dev.* 1998;12(20):3264-3275.
62. Holder JL, Jr., Butte NF, Zinn AR. Profound obesity associated with a balanced translocation that disrupts the SIM1 gene. *Hum Mol Genet.* 2000;9(1):101-108.
63. Sutton AK, Pei H, Burnett KH, Myers MG, Jr., Rhodes CJ, Olson DP. Control of food intake and energy expenditure by Nos1 neurons of the paraventricular hypothalamus. *J Neurosci.* 2014;34(46):15306-15318.
64. Atasoy D, Betley JN, Su HH, Sternson SM. Deconstruction of a neural circuit for hunger. *Nature.* 2012;488(7410):172-177.
65. Pei H, Sutton AK, Burnett KH, Fuller PM, Olson DP. AVP neurons in the paraventricular nucleus of the hypothalamus regulate feeding. *Mol Metab.* 2014;3(2):209-215.

66. Sutton AK, Gonzalez IE, Sadagurski M, et al. Paraventricular, subparaventricular and periventricular hypothalamic IRS4-expressing neurons are required for normal energy balance. *Sci Rep.* 2020;10(1):5546.
67. Garfield AS, Li C, Madara JC, et al. A neural basis for melanocortin-4 receptor-regulated appetite. *Nat Neurosci.* 2015;18(6):863-871.
68. Plata-Salaman CR, Oomura Y. Calcitonin as a feeding suppressant: localization of central action to the cerebral III ventricle. *Physiol Behav.* 1987;40(4):501-513.
69. Bello NT, Kemm MH, Moran TH. Salmon calcitonin reduces food intake through changes in meal sizes in male rhesus monkeys. *Am J Physiol Regul Integr Comp Physiol.* 2008;295(1):R76-81.
70. Pan W, Adams JM, Allison MB, et al. Essential Role for Hypothalamic Calcitonin ReceptorExpressing Neurons in the Control of Food Intake by Leptin. *Endocrinology.* 2018;159(4):1860-1872.
71. Li C, Navarrete J, Liang-Guallpa J, et al. Defined Paraventricular Hypothalamic Populations Exhibit Differential Responses to Food Contingent on Caloric State. *Cell Metab.* 2019;29(3):681-694 e685.
72. RRID:IMSR_JAX:030759.
73. Shah BP, Vong L, Olson DP, et al. MC4R-expressing glutamatergic neurons in the paraventricular hypothalamus regulate feeding and are synaptically connected to the parabrachial nucleus. *Proc Natl Acad Sci U S A.* 2014;111(36):13193-13198.
74. Roth BL. DREADDs for Neuroscientists. *Neuron.* 2016;89(4):683-694.
75. Armbruster BN, Li X, Pausch MH, Herlitze S, Roth BL. Evolving the lock to fit the key to create a family of G protein-coupled receptors potently activated by an inert ligand. *Proc Natl Acad Sci U S A.* 2007;104(12):5163-5168.
76. Link E, Edelmann L, Chou JH, et al. Tetanus toxin action: inhibition of neurotransmitter release linked to synaptobrevin proteolysis. *Biochem Biophys Res Commun.* 1992;189(2):1017-1023.
77. Humeau Y, Doussau F, Grant NJ, Poulain B. How botulinum and tetanus neurotoxins block neurotransmitter release. *Biochimie.* 2000;82(5):427-446.
78. RRID:AB_10013483.
79. RRID:AB_2534017.
80. RRID:AB_2247211.
81. RRID:AB_2732803.
82. RRID:AB_2535792.
83. RRID:AB_141874.
84. RRID:AB_10000240.
85. RRID:AB_142924.
86. RRID:AB_221570.
87. RRID:AB_518524.
88. RRID:AB_90782.
89. Dube D, Pelletier G. Effect of colchicine on the immunohistochemical localization of somatostatin in the rat brain: light and electron microscopic studies. *J Histochem Cytochem.* 1979;27(12):1577-1581.
90. RRID:AB_2884885.
91. RRID:AB_2314240.

92. RRID:AB_2534102.
93. RRID:AB_2534083.
94. An JJ, Liao GY, Kinney CE, Sahibzada N, Xu B. Discrete BDNF Neurons in the Paraventricular Hypothalamus Control Feeding and Energy Expenditure. *Cell Metab.* 2015;22(1):175-188.
95. Fekete C, Lechan RM. Central regulation of hypothalamic-pituitary-thyroid axis under physiological and pathophysiological conditions. *Endocr Rev.* 2014;35(2):159-194.
96. Xiao C, Liu N, Province H, Pinol RA, Gavrilova O, Reitman ML. BRS3 in both MC4R- and SIM1-expressing neurons regulates energy homeostasis in mice. *Mol Metab.* 2020;36:100969.
97. Tam CS, Lecoultre V, Ravussin E. Novel strategy for the use of leptin for obesity therapy. *Expert Opin Biol Ther.* 2011;11(12):1677-1685.
98. Lutz TA, Rossi R, Althaus J, Del Prete E, Scharrer E. Amylin reduces food intake more potently than calcitonin gene-related peptide (CGRP) when injected into the lateral brain ventricle in rats. *Peptides.* 1998;19(9):1533-1540.
99. Grill HJ, Hayes MR. Hindbrain neurons as an essential hub in the neuroanatomically distributed control of energy balance. *Cell Metab.* 2012;16(3):296-309.
100. Bamshad M, Song CK, Bartness TJ. CNS origins of the sympathetic nervous system outflow to brown adipose tissue. *Am J Physiol.* 1999;276(6):R1569-1578.
101. Cao WH, Madden CJ, Morrison SF. Inhibition of brown adipose tissue thermogenesis by neurons in the ventrolateral medulla and in the nucleus tractus solitarius. *Am J Physiol Regul Integr Comp Physiol.* 2010;299(1):R277-290.
102. Fyda DM, Cooper KE, Veale WL. Modulation of brown adipose tissue-mediated thermogenesis by lesions to the nucleus tractus solitarius in the rat. *Brain Res.* 1991;546(2):203-210.
103. Madden CJ, Morrison SF. Neurons in the paraventricular nucleus of the hypothalamus inhibit sympathetic outflow to brown adipose tissue. *Am J Physiol Regul Integr Comp Physiol.* 2009;296(3):R831-843.
104. Xu Y, Wu Z, Sun H, et al. Glutamate mediates the function of melanocortin receptor 4 on Sim1 neurons in body weight regulation. *Cell Metab.* 2013;18(6):860-870.
105. Biag J, Huang Y, Gou L, et al. Cyto- and chemoarchitecture of the hypothalamic paraventricular nucleus in the C57BL/6J male mouse: a study of immunostaining and multiple fluorescent tract tracing. *J Comp Neurol.* 2012;520(1):6-33.
106. Yoshimura M, Nishimura K, Nishimura H, et al. Activation of endogenous arginine vasopressin neurons inhibit food intake: by using a novel transgenic rat line with DREADDs system. *Sci Rep.* 2017;7(1):15728.
107. Drescher VS, Chen HL, Romsos DR. Corticotropin-releasing hormone decreases feeding, oxygen consumption and activity of genetically obese (ob/ob) and lean mice. *J Nutr.* 1994;124(4):524-530.
108. Lechan RM, Fekete C. The TRH neuron: a hypothalamic integrator of energy metabolism. *Prog Brain Res.* 2006;153:209-235.

109. Muglia L, Jacobson L, Dikkes P, Majzoub JA. Corticotropin-releasing hormone deficiency reveals major fetal but not adult glucocorticoid need. *Nature.* 1995;373(6513):427-432.
110. Krashes MJ, Shah BP, Madara JC, et al. An excitatory paraventricular nucleus to AgRP neuron circuit that drives hunger. *Nature.* 2014;507(7491):238-242.

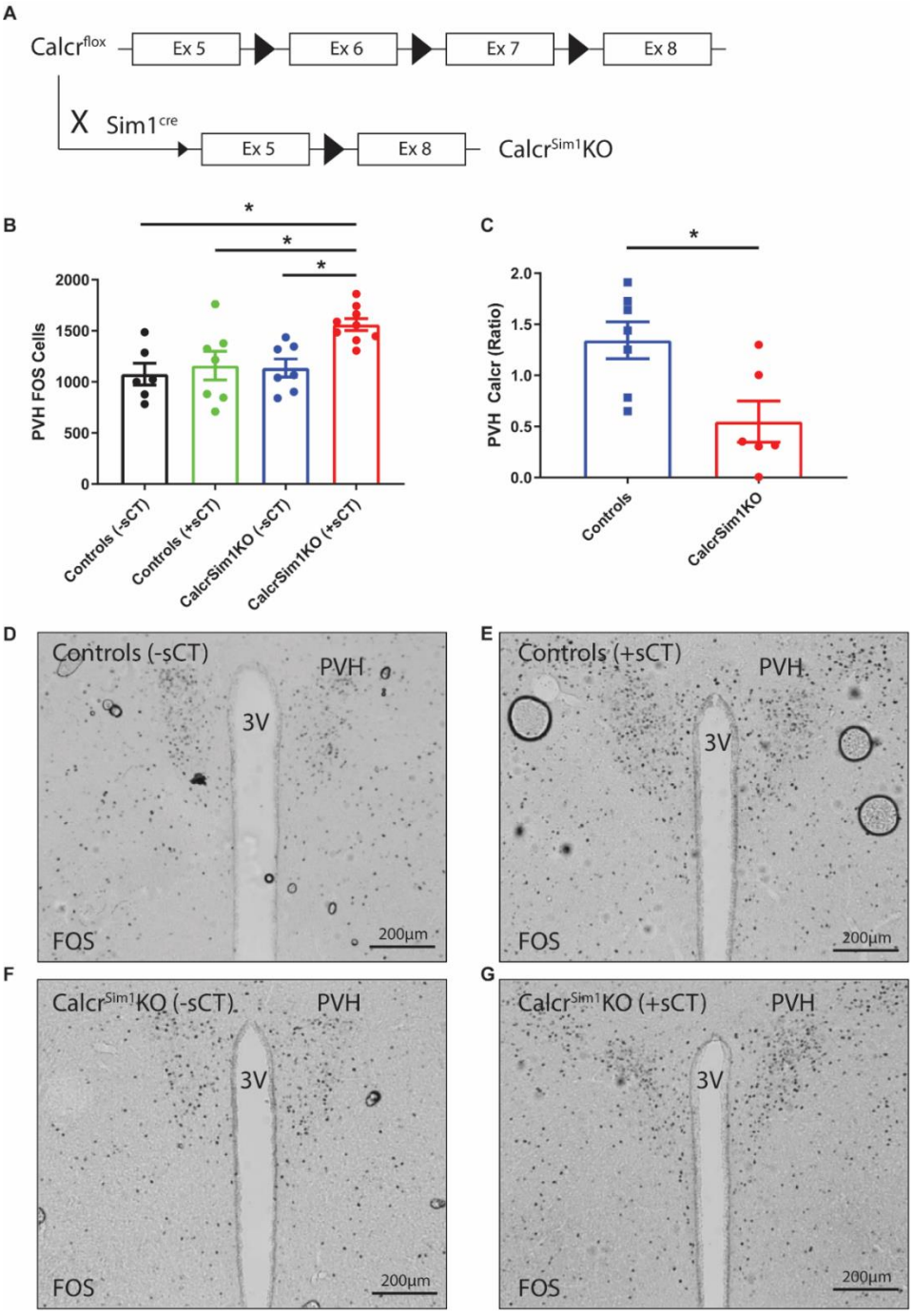

Figure 3.1: FOS response to sCT in Calcr^{Sim1}KO mice. (A) Schematic diagram of cross of CalcR^{flox} and Sim1^{cre} mice to produce Calcr^{Sim1}KO mice. (B) Quantification of PVH FOS-IR cells 2 hours after injection of sCT (100 µg/kg, IP) in control (n=7) and

Calcr^{Sim1}KO (n=9) mice. (C) Calcr mRNA quantification through qRT-PCR in PVH microdissections from Ctrl (n=6) and Calcr^{Sim1}KO (n=7) mice. IHC for FOS expression was conducted on control mice injected with saline (D) and sCT (E) and Calcr^{Sim1}KO mice injected with saline (F) and sCT (G). Average values ± SEM are shown. FOS quantification was compared using a two-way ANOVA followed by Sidak's multiple comparisons test; qRT-PCR ratios were compared using unpaired t-test. *$p<0.05$.

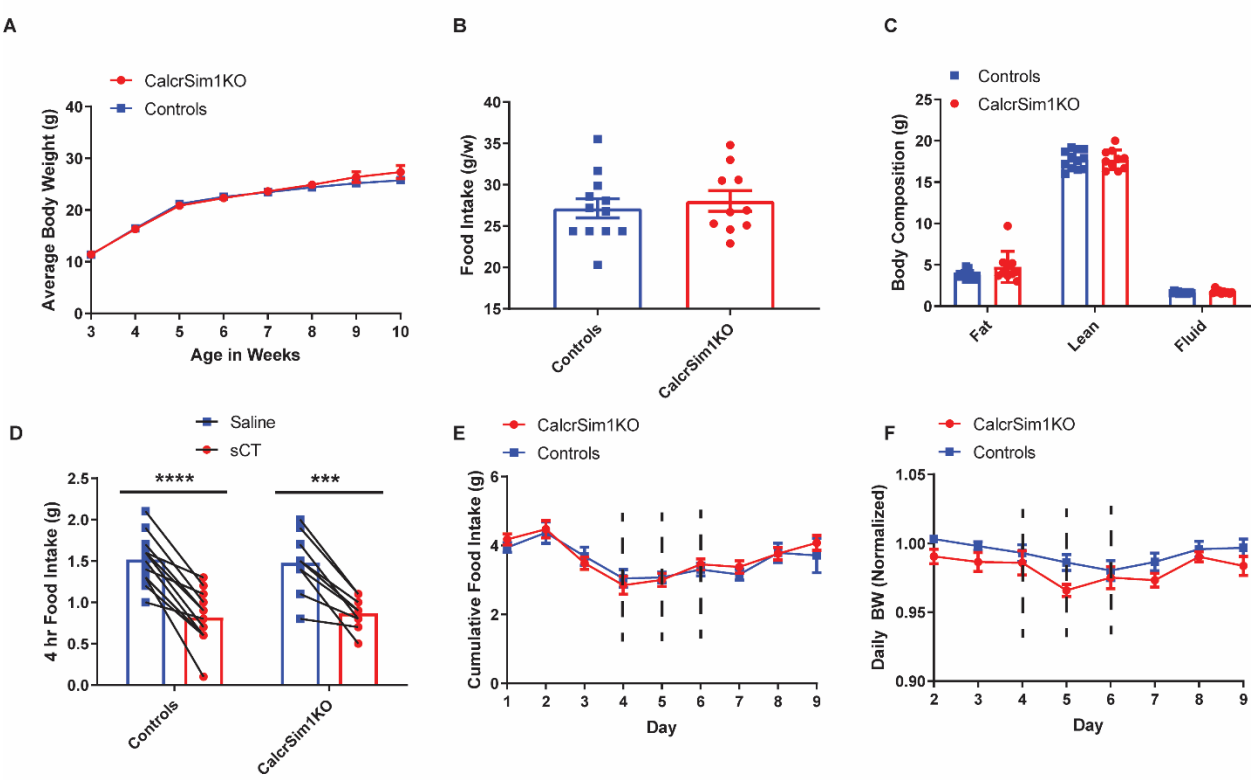

Figure 3.2: Energy balance and response to anorectic agents in Calcr^{Sim1}KO mice. (A-C) Control and Calcr^{Sim1}KO mice were studied until 10 weeks of age for body weight (A), food intake (B), and body composition (14-18 weeks of age) (C); n=4-10 per group. All comparisons were p=not significant (ns). Responses to sCT (D-F) (n=13-17 per group): Food intake for the first 4 hours of the dark cycle (D) and daily food intake (E) and body weight (change relative to baseline) (F) while chronically treated with IP vehicle (Veh) or sCT twice daily in Calcr^{Sim1}KO mice (100 ug/kg sCT). Dotted vertical lines indicate the days of sCT treatment. Average values ± SEM are shown. For 10 weeks of body weight a one-way ANOVA with Tukey's multiple comparisons test was performed; for food intake and body composition a two-way ANOVA with Sidak's multiple comparisons test was performed. For the sCT overnight food intake experiment, a one-way ANOVA with Tukey's multiple comparisons test was performed.

For the chronic treatment of sCT analyzing food intake and body weight a two-way ANOVA with Sidak's multiple comparisons test was conducted. ***$p<0.001$, ****$p<0.0001$.

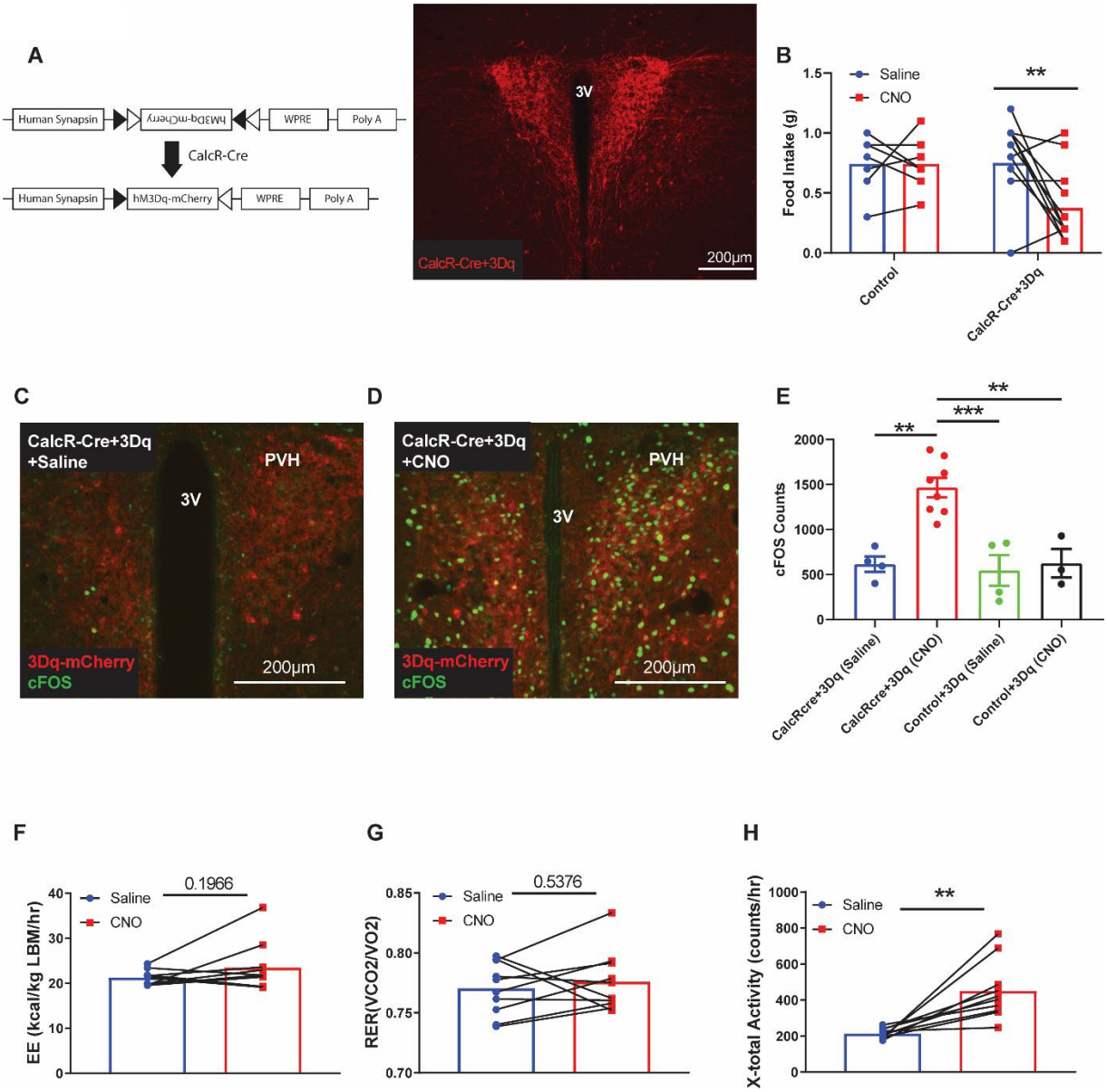

Figure 3.3: Effect of acute activation of CalcR^{PVH} neurons using DREADDs on food intake and energy expenditure. A) Diagram of Cre-dependent hM3Dq DREADDs expression vector. IHC was used to detect expression of AAV-Flex-hM3Dq bilaterally injected into the PVH of CalcR^{2ACre} mice (CalcR-Cre+3Dq). B) Two-hour food intake following i.p. injection of CNO (0.3 mg/kg) at start of the dark cycle. CalcR^{2ACre}+Flex-hM3Dq and control mice were fasted for 90 minutes prior to i.p.

injection of CNO or saline, and were perfused 2 hours following the injection. IHC for 3Dq-mCherry and FOS expression was conducted on CalcR^{2ACre}+Flex-hM3Dq mice injected with saline (C), CalcR^{2ACre}+Flex-hM3Dq mice injected with CNO (D), control mice injected with saline and control mice injected with CNO (not shown). FOS expression in the PVH was quantified and compared among the four groups (E). CLAMS measurements of energy expenditure (F), the respiratory exchange ratio (G) and total X-activity (H) following DREADD-mediated CalcR^{PVH} activation. Average values ± SEM are shown. P values for feeding behavior and FOS quantification was determined by 2-way ANOVA followed by a Sidak's multiple comparisons test; CLAMS measures, were compared using a paired-t-test. **p<0.01, ***p<0.001, PVH=paraventricular nucleus of the hypothalamus, 3V=third ventricle.

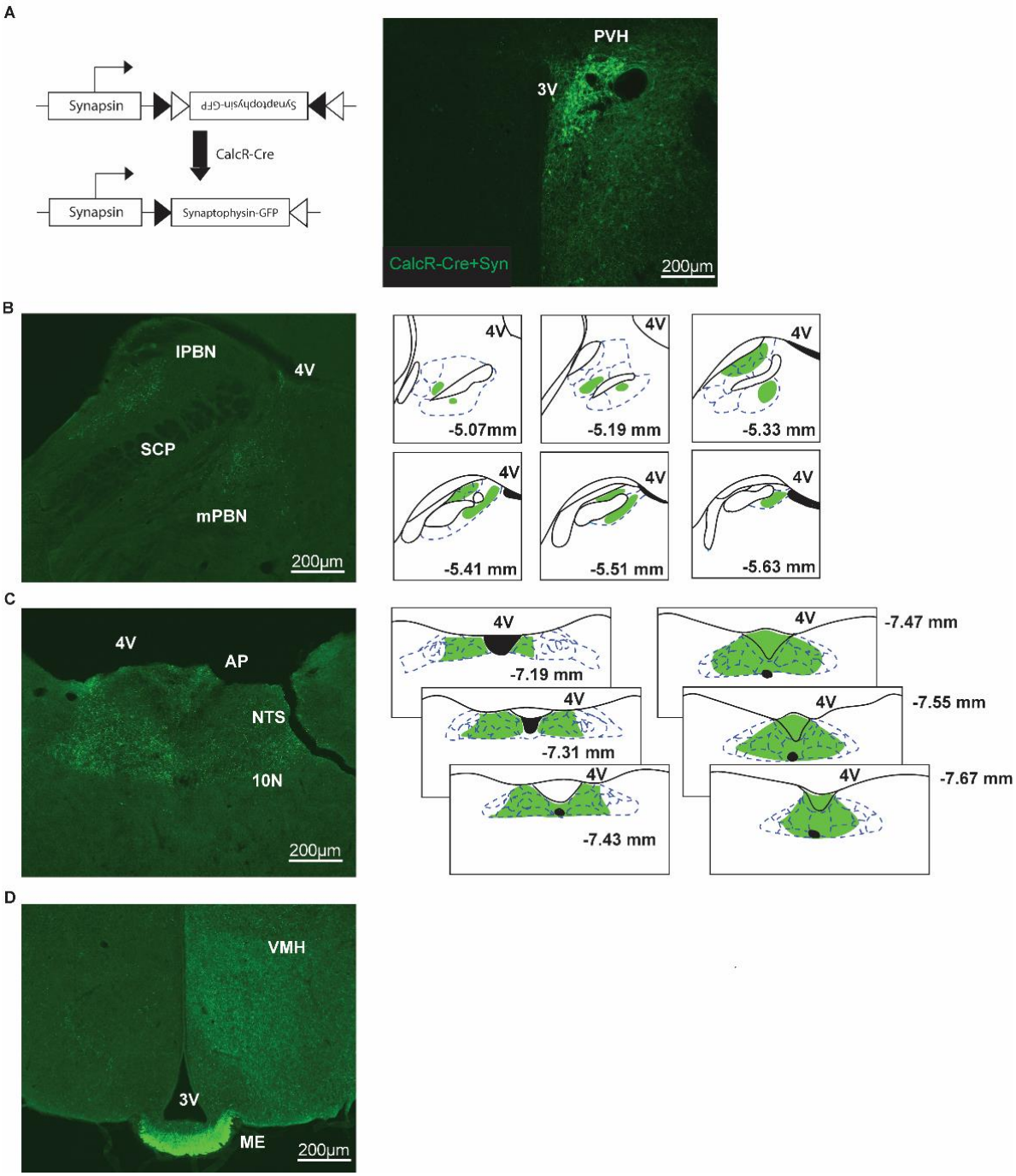

Figure 3.4: Projection targets of CalcR^{PVH} neurons using an anterograde tracer. A) Diagram of the Cre-dependent synaptophysin-GFP vector. The synaptophysin-GFP virus was unilaterally injected into the PVH of CalcR^{2ACre} mice (CalcR-Cre+Syn). CalcR^{PVH} axonal terminals were observed in the mPBN and lPBN, with an illustration

showing signal between Bregma 5.07mm and -5.63mm (B). Projections were observed in the NTS between Bregma -7.19mm and -7.67mm, with signal also shown in the AP and 10N (C). Projections were also found in the external zone of the ME (D). Illustrations are based on coronal images from the atlas Paxinos and Franklin's the Mouse Brain in Stereotaxic Coordinates 4th Edition. 3V=third ventricle, 4V=fourth ventricle, SCP=superior cerebellar peduncle, PVH=paraventricular nucleus of the hypothalamus, VMH= ventromedial nucleus of the hypothalamus, ME=median eminence, NTS=nucleus of the solitary tract, AP=area postrema, 10N=dorsal motor nucleus of vagus nerve, mPBN=medial parabrachial nucleus, lPBN=lateral parabrachial nucleus.

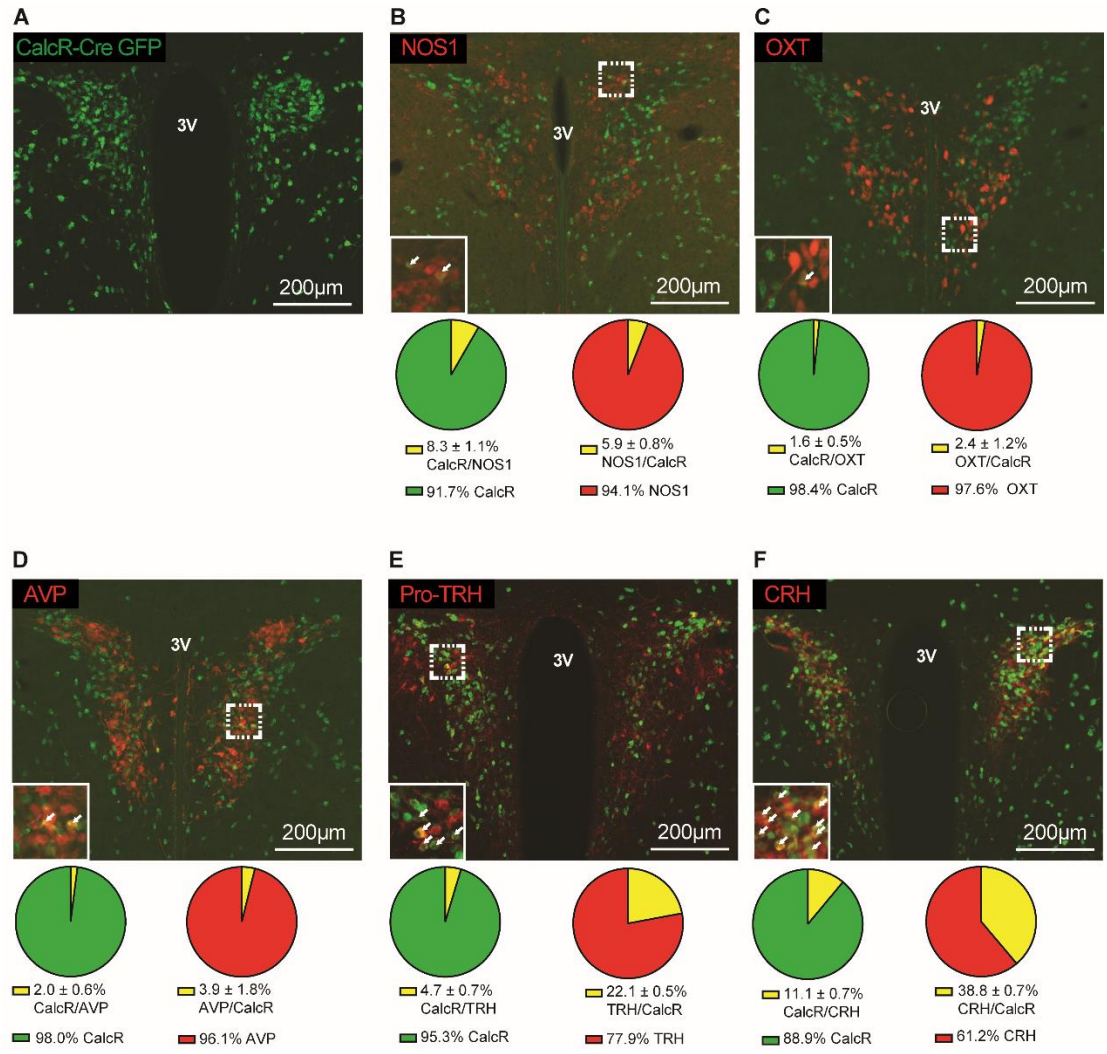

Figure 3.5: Colocalization of CalcR^{PVH} neurons with other PVH populations implicated in energy homeostasis. Representative immunofluorescent images taken of the PVH of CalcR$^{2ACre+GFP}$ mice. Mice were stained for Cre dependent GFP expression (A-F) shown in green. Sections were also stained using primary antibodies for NOS1 (B), OXT (C), AVP (D), Pro-TRH (E) and CRH (F) shown in red. Percent expression of the overlap (yellow) relative to the individual cell populations (green/red) were quantified in corresponding pie charts below their image. 3V=third ventricle.

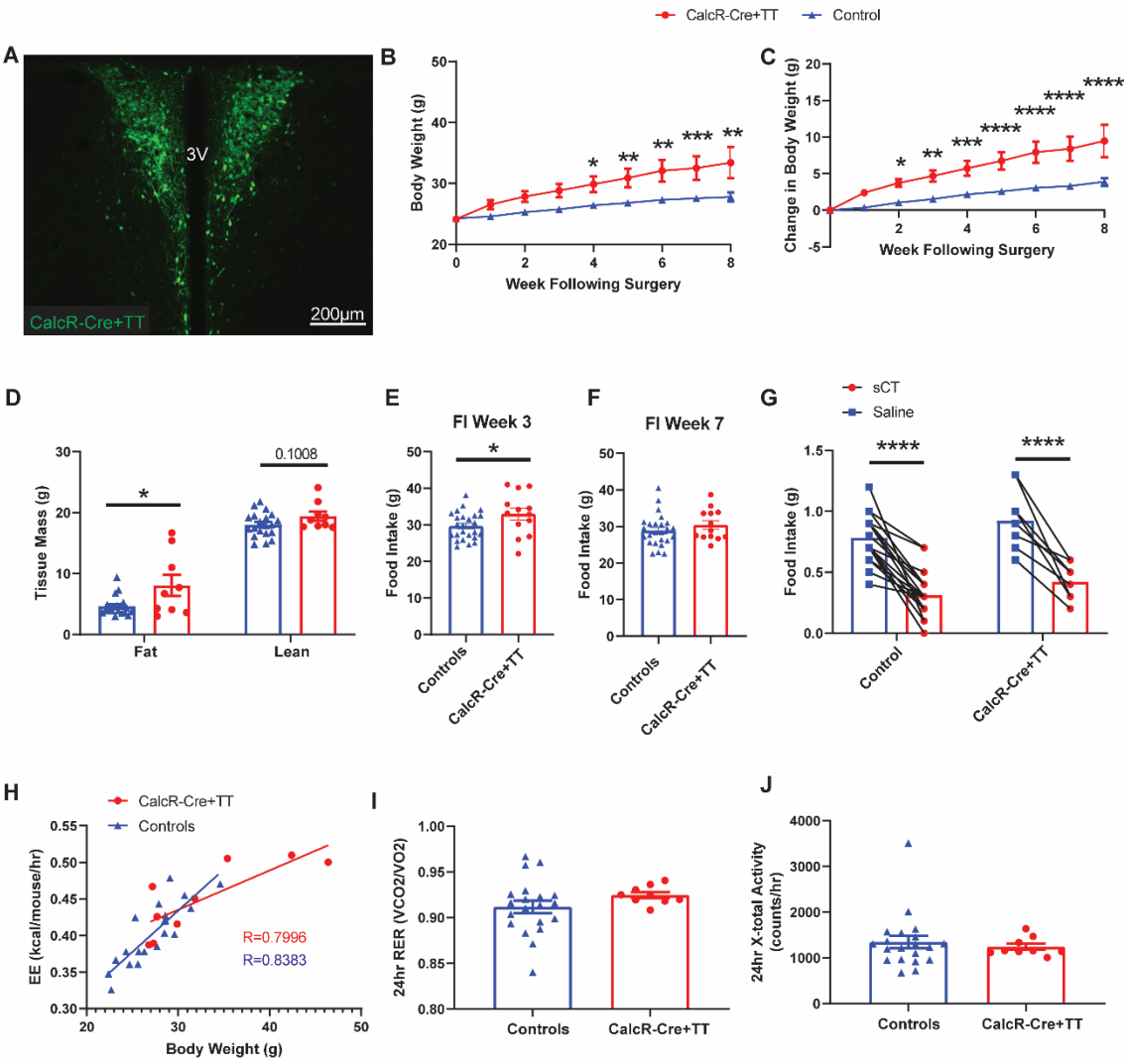

Figure 3.6: Physiological effects of silencing CalcR^{PVH} neurons. A) Bilateral expression of AAV-TetTox-GFP in the PVH of CalcR^{2ACre} mice (CalcR-Cre+TT). Effect of CalcR^{PVH} silencing on body weight (B), body weight gain (C), fat and lean mass (D) and food intake during week 3 (E) and week 7 (F). Two-hour food intake following i.p. injection of sCT (100 µg/kg) at the start of the dark cycle (G). CLAMS measurements of energy expenditure over a 24 hr period was compared to respective body weights (H). CLAMS measurements of respiratory exchange rate (I) and X-total activity (J). Average values ± SEM are shown. P values for BW, change in BW and sCT food intake were

determined using a 2-way ANOVA followed by Sidak's multiple comparisons test, and for body composition, food intake and CLAMS measurements, an unpaired t test was used. For the energy expenditure measurements over a 24 hr period comparison, a simple linear regression and correlation analysis was used to determine the Pearson correlation (R) values. * $p<0.05$, ** $p<0.01$, *** $p<0.001$, **** $p<0.0001$.

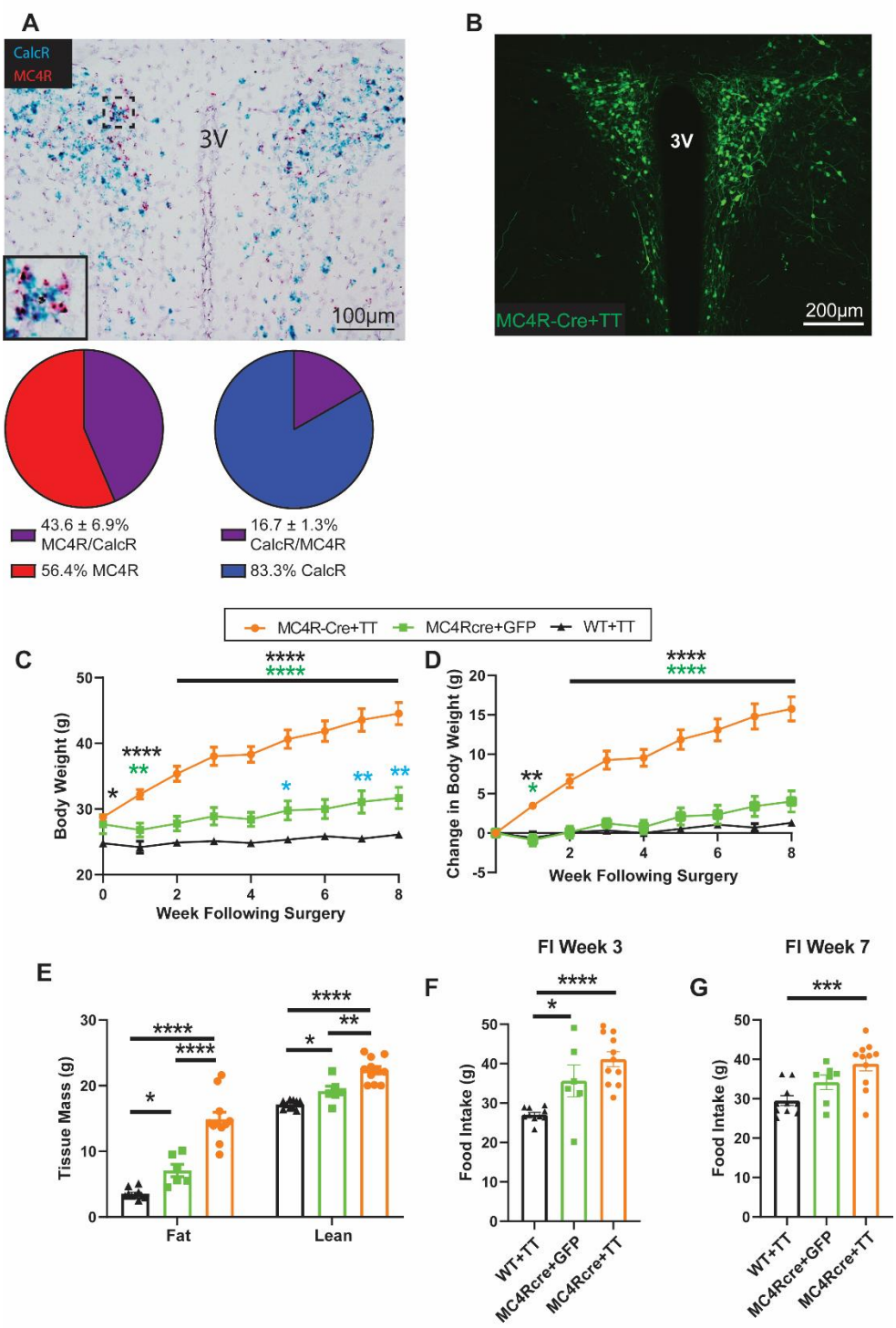

Figure 3.7: Physiological effects of silencing MC4R^{PVH} neurons. A) In situ hybridization in WT mouse for CalcR (Blue) and Mc4R RNAs (red). Percent expression of CalcR in MC4R positive cells and percent expression of MC4R in CalcR positive

cells. B) Bilateral expression of AAV-TetTox-GFP in the PVH of $MC4R^{Cre}$ mice (MC4R-Cre+TT). Effect of $MC4R^{PVH}$ silencing on body weight (C), body weight gain (D), fat and lean mass (E). Food intake in $MC4R^{PVH}$ silenced mice during week 3 (F) and during week 7 (G) following injection. Average values ± SEM are shown for BW, change in BW, body composition and food intake. P values for BW and change in BW were determined using a 2-way ANOVA followed by Tukey's multiple comparisons test, and for body composition and food intake, a one-way ANOVA followed by a Tukey's multiple comparisons test was conducted. * $p<0.05$, ** $p<0.01$, *** $p<0.001$, **** $p<0.0001$.

Chapter 4

MC4R Expression in CalcR Cells is Required for Maintaining Normal Body Weight and Feeding Behavior

Abstract

The expression of melanocortin-4-receptor (MC4R) in the paraventricular nucleus of the hypothalamus (PVH) is necessary to maintain normal body weight and food intake in mice. Further, re-expression of MC4R in the PVH of mice with a total knockout of MC4R expression normalizes feeding and reduces the obesity observed with systemic loss of MC4R. Nearly half the $MC4R^{PVH}$ neurons express calcitonin receptor (CalcR), a neuronal population of the PVH that we have demonstrated to regulate body weight and food intake. As CalcR neurons are a subpopulation of $MC4R^{PVH}$ neurons, we used the CalcR-2a-Cre transgenic mouse line and Cre/Lox technology to delete MC4R expression from CalcR neurons. Deletion of MC4R from CalcR neurons resulted in obesity in both males and females. Hyperphagia and increased body length were found in males, however no change in energy expenditure was observed. In male and female knockout mice, the anorectic response to peripheral MTII injection was still maintained. These findings indicate that MC4R expression in CalcR neurons is required for body weight and food intake regulation.

Introduction

The brain maintains energy homeostasis through the regulation of feeding and energy expenditure. It achieves this through the integration of peripheral and central signals that dictate the activity of neurons involved energy balance.[1] The melanocortin-4-receptor (MC4R) is a G protein-coupled receptor that is expressed in neurons throughout the brain and has been identified as essential to the maintenance of energy homeostasis.[2,3] Deletion of MC4R expression in mice and mutation of the receptor in humans results in obesity, indicating the essential role this receptor plays in regulating energy balance.[4-6] For MC4R null mice, obesity is due to both hyperphagia and a decrease in energy expenditure.[4,7,8]

The paraventricular nucleus of the hypothalamus (PVH) is a region of the brain that has abundant expression of MC4R.[9-11] The PVH regulates energy homeostasis through its regulation of feeding, energy expenditure and the regulation of glucose.[12] The PVH receives projections from agouti-related peptide (AgRP) and proopiomelanocortin (POMC) ARC neurons which release the MC4R antagonist and agonist, AgRP and α-MSH respectively.[13,14] Microinjections of MC4R ligands into the PVH influences feeding and energy expenditure. [14-16] The PVH contains MC4R neurons that are glutamatergic and monosynaptically engage the lateral parabrachial nucleus (LPBN) and the dorsal motor nucleus of the vagus (DMV) of the hindbrain.[17-19] $MC4R^{PVH}$ neurons are distinct from the oxytocin (OXT), corticotrophin-releasing hormone (CRH), arginine vasopressin (AVP) and prodynorphin (PDYN) neurons of the PVH.[18] Melanocortin action in the PVH is required for body weight regulation, as the deletion of MC4R from the PVH leads to hyperphagic obesity.[20] Further, the re-expression of

MC4R in the PVH of mice with a total body knockout of MC4R reduces body weight gain and reduces hyperphagia, indicating that MC4R expression in the PVH is an important component of the regulation of feeding behavior.[18] A total knock out of MC4R expression in mice results in the complete loss of the anorectic effects of the melanocortin agonist MTII when applied peripherally.[21] However, re-expression of the MC4R in the PVH and amygdala restores the anorectic response of mice to MTII.[20,22]

Our in situ studies have found that calcitonin receptor (CalcR) expressing neurons in the PVH heavily overlap with the $MC4R^{PVH}$ neuronal population. Our previous studies indicate that $CalcR^{PVH}$ neurons regulate body weight and feeding behavior through activation and silencing techniques.[23] Due to the co-localization of $CalcR^{PVH}$ and $MC4R^{PVH}$ neurons, we hypothesize that melanocortin action on $CalcR^{PVH}$ neurons is critical for homeostatic energy balance. The Olson laboratory developed a CalcR-2a-Cre transgenic mouse line, which will allow us to specifically manipulate and characterize CalcR expressing cells. We utilized Cre/Lox technology to genetically knockout MC4Rs from CalcR neurons and then examined the physiologic effects of deleting MC4Rs from CalcR neurons. We found that deletion of MC4R from all CalcR-expressing neurons produces profound hyperphagic obesity indicating that CalcR-expressing neurons play an important role in central melanocortin action. However, deletion of MC4R from CalcR neurons did not blunt the anorectic effects of MTII, suggesting the remaining $MC4R^{PVH}$ neurons still respond to the MTII to produce the anorectic phenotype. Our findings suggest that MC4R expression on CalcR neurons is essential for maintaining normal body weight and feeding behavior.

Material and Methods:

Experimental Animals

CalcR-2a-Cre (or CalcR2ACre) mice were previously generated and validated using previously described methods.[24] Mice with Cre recombinase expressed in MC4R neurons ($MC4R^{Cre}$, JAX stock 030759; kindly provided by Dr. Brad Lowell) were used for the IHC study along with the CalcR-2a-Cre mice.[25] For the MC4R deletion studies, LoxMC4R (JAX stock 023720; kindly provided by Brad Lowell) mice were crossed with our CalcR2ACre mice (JAX stock 006395).[18] Male and female mice from these breeding crosses were studied starting at 3 weeks of age. In accordance with the Association for the Assessment and Approval of Laboratory Animal Care and National Institutes of Health guidelines, the procedures performed were approved by the University of Michigan Committee on the Care and Use of Animals. Our animals were bred and housed within our colony, with ad libitum access to food and water provided (unless specified otherwise) in temperature-controlled rooms that followed a 12-hour light/dark cycle.

Long-term body weight, food intake and energy expenditure measurements

$MC4R^{Lox/+}$ mice were crossed with $CalcR^{cre/+}$ mice to generate $CalcR^{cre/+}$; $MC4R^{Lox/Lox}$ ($CalcR^{\Delta MC4R}$) as well as $CalcR^{cre/+}$, $MC4R^{Lox/Lox}$ and WT (controls) mice. Mice for these studies were monitored between 4 and 16 weeks of age for body weight in males and females. Body composition for males and females was conducted between 16-18 weeks of age (Minispec LF90 II, Bruker Optics). Weekly food intake of regular chow was

measured in singly housed males between 4 and 12 weeks of age and CLAMS was conducted at between 8 and 10 weeks of age. Body lengths of the males were measured at 22 weeks of age, after which they were deeply anesthetized using isoflurane and their brains were extracted for additional analyses.

At 17 weeks of age, CalcR$^{\Delta MC4R}$ mice and their controls were acclimatized to receiving daily saline injections 3 days prior to the day of the feeding experiment. They were then fasted during the light cycle between 10AM and 6PM and at the beginning of the dark cycle (6PM), mice were given ad libitum access to food and either an i.p. injection of melanotan-II (MTII, 150 ug/mouse, Bachem) or 0.9% sodium chloride (APP Pharmaceuticals, 63323-186-10). Food intake was then measured two and four hours following the injection. At least 4 days later, the injection treatments were switched, and food intake was measured. This same method was used to test the feeding suppression of MTII on MC4R^{Cre} and CalcR^{2ACre} mice that received AAV-Flex-TetTox injections (as described in chapter 3) and the controls nine to ten weeks following viral injection.

In situ hybridization and IHC studies

Mice were overdosed with the inhaled anesthetic isofluorane, then the brains were removed and flash frozen in 2-methylbutane. The brains were cut using a cryostat (Leica CM 1950) into 16 µm sections onto glass slides and were immediately stored at -80^{o}C. The assays were conducted according to the protocol provided by the manufacturer of RNAscope (Advanced Cell Diagnostics). Sections were fixed for 1 hour in cold 10% formalin and then dehydrated in 50% and 75% ethanol, each for 5 minutes

followed by two times in 100% ethanol. The sections were then dried for 30 minutes at 40ºC. To determine the overlapping expression of MC4R and CalcR mRNA in the PVH, chromogen staining was performed with an RNAscope® 2.5 HD Duplex Reagent Kit (ACD 320701). Sections were then treated for 10 minutes with H2O2 and were then incubated for 30 minutes with protease K IV. Following hybridization of probes for MC4R and CalcR mRNAs, the sections were washed twice and then underwent amplification with Amp1 to Amp2 with 2 washes in between. The red signal component was detected through diluting Red-B 1:60 in component Red-A, which was then incubated on the tissue at room temperature for 10 minutes. The slides were rinsed two times in wash buffer in order to conclude the chromogen reaction. Amplification proceeded with Amp7 through Amp10, after which the green signal was detected by diluting Green-B 1:50 in component Green-A and incubating at room temperature for 10 minutes. The tissue was then counter stained by immersing the slides into 50% hematoxylin for 30 seconds, after which they were dried and mounted in VectaMount mounting medium (Vector Laboratories, INC). Imaging for the chromogen stained tissue was conducted with an Olympus BX-51 microscope with a DP80 camera (Olympus). To quantify cells expressing probe signal, images from coronal sections were processed in a uniform manner with Photoshop (Adobe) in order to remove the background and better visualize the individual probes. Hematoxylin stained cells that were determined to be positive for each probe were quantified using ImageJ and overlapping expression was compared to the expression of a singular probe within each of the mouse groups. For the IHC studies in which we determined the brain regions which expressed MC4R and CalcR neurons, we used $CalcR^{Cre}$ mice that expressed a Cre-dependent GFP

reporter and MC4R^{Cre} mice that expressed a Cre-dependent TdTomato reporter. To identify the CalcR neurons that express the GFP reporter, a primary antibody for GFP (chicken 1:1000, Aves GFP–1020) was used followed by a goat anti-chicken-Alexa 488 (1:200, Invitrogen) secondary antibody. To identify the MC4R neurons that express a TdTomato reporter, we used a primary antibody for dsRed (rabbit 1:1000, Clontech, 632496), followed by secondary immunofluorescence detection with donkey anti-rabbit-Alexa 568 (1:200, Invitrogen).

Data and Statistical Analysis

Unpaired t-tests, paired t-tests, one-way and 2-way ANOVAs with Sidak's or Tukey's multiple comparisons test post-hoc tests (when appropriate), mixed model analyses and simple linear regression and correlation analysis were conducted using GraphPad Prism 8, as noted in the figure legends. $P<0.05$ indicates significance.

Results

Deletion of MC4R from CalcR cells produces hyperphagic obesity

MC4R expression in PVH neurons is critical for normal feeding and body weight regulation.[18,20] Given the hyperphagic obesity seen with silencing of CalcR^{PVH} neurons, we examined the overlap of MC4R and CalcR transcripts in the PVH. In situ hybridization revealed that almost half of MC4R^{PVH} neurons express CalcR mRNA (43.59 + 6.88%, n=3 mice) whereas less than a quarter of CalcR^{PVH} neurons express

MC4R mRNA (16.72 + 1.33%, n=3 mice) (Figure 4.1 A, the in situ image was repurposed from my published manuscript in Chapter 3).[23] Given the co-expression of CalcR and MC4R within the PVH, we examined the contribution of CalcR neurons in MC4R-mediated energy homeostasis by deleting MC4R from all CalcR-expressing cells ($CalcR^{\Delta MC4R}$). In situ hybridization of brain tissue from $CalcR^{\Delta MC4R}$ mice demonstrated a substantial reduction in MC4R expression in the PVH compared to the controls (Figure 4.1 A-C); cell counts indicate that $MC4R^{PVH}$ expression was reduced to 46.70% compared to control (MC4R Controls = 297.67 + 30.37, n=3; $CalcR^{\Delta MC4R}$ = 139 + 6.26, n=4). As expected MC4R expression was almost completely deleted from $CalcR^{PVH}$ cells (CalcR/MC4R cell counts: Controls = 132 + 28.16, n=3; $CalcR^{\Delta MC4R}$ = 11.25 + 1.97, n=4) (Figure 4.1 B,C). $CalcR^{\Delta MC4R}$ mice developed profound obesity in both males and females during the first 16 weeks of life (Figure 4.1 D,E). This obesity phenotype was driven in large part by increased food intake (Figure 4.1 F). Body composition revealed increases in fat mass and lean mass in both male and female $CalcR^{\Delta MC4R}$ mice (Figure 4.1 G,H). Body length for males was also increased with deletion of Mc4R from CalcR neurons (Figure 4.1 I). These findings demonstrate that the deletion of MC4R from CalcR-expressing cells results in hyperphagic obesity; this is in part due to loss of MC4R from the PVH, although other regions that co-express CalcR and MC4R transcripts likely contribute to energy balance control.

CalcR$^{\Delta MC4R}$ mice maintain largely normal energy expenditure and anorectic response to MTII

CLAMS assessments performed at 8-10 weeks of age revealed a slightly lower VO2 relative to body weight in the CalcR$^{\Delta MC4R}$ mice suggesting a slight perturbation in energy expenditure (Figure 4.2 A). However, we did not observe a significant difference in oxygen consumption when adjusted for body weight (Figure 4.2 B) and lean body mass (Figure 4.2 C) when compared to the controls. There was a trend towards a significant decrease in RER during a 24 hour period (Figure 4.2 D); X-total activity increased during a 24 hour period (Figure 4.2 E). At 17 weeks of age, male and female CalcR$^{\Delta MC4R}$ mice underwent MTII feeding experiments that showed that the anorectic behavior induced by MTII was still maintained with the deletion of MC4R from CalcR cells (Figure 4.3 A). Interestingly, MTII feeding experiments in CalcR-Cre+TetTox and MC4R-Cre+TetTox mice also demonstrated a normal anorectic response to MTII, suggesting that potentially enough MC4R^{PVH} neurons remained unsilenced and thus able to communicate downstream (Figure 4.3 B,C). Overall, these findings indicate that removal of MC4R expression in CalcR cells does not influence energy expenditure nor the ability of mice to respond to MTII.

Discussion

MC4R expression in the PVH is crucial to maintain energy homeostasis through food intake regulation.[18,20] Through our previous investigation of the CalcR^{PVH} neurons, we determined that they are both sufficient and necessary to regulate body weight and

food intake and our in situ hybridization studies indicate that they overlap with nearly half of the $MC4R^{PVH}$ neurons. When comparing silencing of $CalcR^{PVH}$ neurons to $MC4R^{PVH}$ neurons in mice, we determined that the body weight gain in the $CalcR^{PVH}$ silenced mice (Figure 3.6 C) was half that which was observed in the $MC4R^{PVH}$ silenced mice (Figure 3.7 D).[23] This potentially indicates that the obesity observed in mice with $CalcR^{PVH}$ neurons silenced may be due to loss of signaling of the MC4R expressing subpopulation. To investigate this, we used Cre-loxP mediated deletion of MC4Rs from all CalcR-expressing cells, which leads to profound hyperphagic obesity in both male and female rodents. Loss of MC4Rs from CalcR neurons is associated with an increase in lean mass and overall body length, a distinct feature of MC4R knockout mediated obesity.[18]

The lack of change in energy expenditure measurements in $CalcR^{\Delta MC4R}$ mice is not surprising, as it has been determined that the deletion of MC4R expression from the PVH produces hyperphagic obesity without perturbing energy expenditure.[18,20] The unaffected anorectic behavior produced by MTII in $CalcR^{\Delta MC4R}$ mice suggests that potentially other regions with neurons that express MC4R and not CalcR are still responding to MTII and are suppressing feeding behavior. Further, over half of the $MC4R^{PVH}$ neurons do not express CalcR, and thus are unaffected by the Cre/lox mediated deletion of MC4R, allowing for continued melanocortin signaling downstream. Because the anorectic behavior of MTII is maintained in mice with $MC4R^{PVH}$ neurons silenced by tetanus toxin, this may support the idea that other brain regions expressing MC4R are responsible for suppressing food intake behavior through MTII action. It is also possible that not enough of the $MC4R^{PVH}$ neurons expressed the virus and

therefore were not silenced. Alternatively, the tetanus toxin may not completely silence downstream communication and perhaps enough signal is able to be released to maintain the anorectic behavior produced by MTII.

There are a few potential issues in the study that should be considered, first of which is the potential compensation that may have occurred during development. The deletion of MC4R expression from CalcR cells happens very early in development and therefore it is possible that some compensatory changes may have occurred to combat the partial loss of MC4R expression. As such, it is possible that loss of MC4R expression from CalcR cells later in development would produce a variation on the phenotypes observed. Further, it is important to note that CalcR-cre expression is not confined to the PVH and the loss of MC4Rs from non-PVH CalcR-expressing cells likely also contributes to this obesity phenotype. We have conducted IHC studies identifying brain regions which consist of both CalcR and MC4R neurons, many of which are in regions important for the regulation of energy homeostasis, such as the ARC, ventromedial nucleus of the hypothalamus, PBN and solitary nucleus to name just a few (Table 4.1). While this only serves to suggest the potential existence of neurons with overlapping expression of MC4R and CalcR in the regions identified, it will be necessary to confirm and quantify this overlapping expression. Future experiments examining the overlap of CalcR and MC4R transcripts outside the PVH will be necessary to ascertain the contribution of non-PVH CalcR-expressing cells in central melanocortin action.

References:

1. Morton GJ, Meek TH, Schwartz MW. Neurobiology of food intake in health and disease. *Nat Rev Neurosci.* 2014;15(6):367-378.
2. Kishi T, Aschkenasi CJ, Lee CE, Mountjoy KG, Saper CB, Elmquist JK. Expression of melanocortin 4 receptor mRNA in the central nervous system of the rat. *J Comp Neurol.* 2003;457(3):213-235.
3. Mountjoy KG, Mortrud MT, Low MJ, Simerly RB, Cone RD. Localization of the melanocortin-4 receptor (MC4-R) in neuroendocrine and autonomic control circuits in the brain. *Mol Endocrinol.* 1994;8(10):1298-1308.
4. Huszar D, Lynch CA, Fairchild-Huntress V, et al. Targeted disruption of the melanocortin-4 receptor results in obesity in mice. *Cell.* 1997;88(1):131-141.
5. Vaisse C, Clement K, Guy-Grand B, Froguel P. A frameshift mutation in human MC4R is associated with a dominant form of obesity. *Nat Genet.* 1998;20(2):113-114.
6. Yeo GS, Farooqi IS, Aminian S, Halsall DJ, Stanhope RG, O'Rahilly S. A frameshift mutation in MC4R associated with dominantly inherited human obesity. *Nat Genet.* 1998;20(2):111-112.
7. Chen AS, Marsh DJ, Trumbauer ME, et al. Inactivation of the mouse melanocortin-3 receptor results in increased fat mass and reduced lean body mass. *Nat Genet.* 2000;26(1):97-102.
8. Ste Marie L, Miura GI, Marsh DJ, Yagaloff K, Palmiter RD. A metabolic defect promotes obesity in mice lacking melanocortin-4 receptors. *Proc Natl Acad Sci U S A.* 2000;97(22):12339-12344.
9. Siljee JE, Unmehopa UA, Kalsbeek A, Swaab DF, Fliers E, Alkemade A. Melanocortin 4 receptor distribution in the human hypothalamus. *Eur J Endocrinol.* 2013;168(3):361-369.
10. Harris M, Aschkenasi C, Elias CF, et al. Transcriptional regulation of the thyrotropin-releasing hormone gene by leptin and melanocortin signaling. *J Clin Invest.* 2001;107(1):111-120.
11. Liu H, Kishi T, Roseberry AG, et al. Transgenic mice expressing green fluorescent protein under the control of the melanocortin-4 receptor promoter. *J Neurosci.* 2003;23(18):7143-7154.
12. Xi D, Gandhi N, Lai M, Kublaoui BM. Ablation of Sim1 neurons causes obesity through hyperphagia and reduced energy expenditure. *PLoS One.* 2012;7(4):e36453.
13. Bagnol D, Lu XY, Kaelin CB, et al. Anatomy of an endogenous antagonist: relationship between Agouti-related protein and proopiomelanocortin in brain. *J Neurosci.* 1999;19(18):RC26.
14. Cowley MA, Pronchuk N, Fan W, Dinulescu DM, Colmers WF, Cone RD. Integration of NPY, AGRP, and melanocortin signals in the hypothalamic paraventricular nucleus: evidence of a cellular basis for the adipostat. *Neuron.* 1999;24(1):155-163.
15. Giraudo SQ, Billington CJ, Levine AS. Feeding effects of hypothalamic injection of melanocortin 4 receptor ligands. *Brain Res.* 1998;809(2):302-306.

16. Kask A, Schioth HB. Tonic inhibition of food intake during inactive phase is reversed by the injection of the melanocortin receptor antagonist into the paraventricular nucleus of the hypothalamus and central amygdala of the rat. *Brain Res.* 2000;887(2):460-464.
17. Garfield AS, Li C, Madara JC, et al. A neural basis for melanocortin-4 receptor-regulated appetite. *Nat Neurosci.* 2015;18(6):863-871.
18. Shah BP, Vong L, Olson DP, et al. MC4R-expressing glutamatergic neurons in the paraventricular hypothalamus regulate feeding and are synaptically connected to the parabrachial nucleus. *Proc Natl Acad Sci U S A.* 2014;111(36):13193-13198.
19. Xu Y, Wu Z, Sun H, et al. Glutamate mediates the function of melanocortin receptor 4 on Sim1 neurons in body weight regulation. *Cell Metab.* 2013;18(6):860-870.
20. Balthasar N, Dalgaard LT, Lee CE, et al. Divergence of melanocortin pathways in the control of food intake and energy expenditure. *Cell.* 2005;123(3):493-505.
21. Marsh DJ, Hollopeter G, Huszar D, et al. Response of melanocortin-4 receptor-deficient mice to anorectic and orexigenic peptides. *Nat Genet.* 1999;21(1):119-122.
22. Krashes MJ, Lowell BB, Garfield AS. Melanocortin-4 receptor-regulated energy homeostasis. *Nat Neurosci.* 2016;19(2):206-219.
23. Gonzalez IE, Ramirez-Matias J, Lu C, et al. Paraventricular Calcitonin Receptor-Expressing Neurons Modulate Energy Homeostasis in Male Mice. *Endocrinology.* 2021;162(6).
24. Pan W, Adams JM, Allison MB, et al. Essential Role for Hypothalamic Calcitonin ReceptorExpressing Neurons in the Control of Food Intake by Leptin. *Endocrinology.* 2018;159(4):1860-1872.
25. Li C, Navarrete J, Liang-Guallpa J, et al. Defined Paraventricular Hypothalamic Populations Exhibit Differential Responses to Food Contingent on Caloric State. *Cell Metab.* 2019;29(3):681-694 e685.

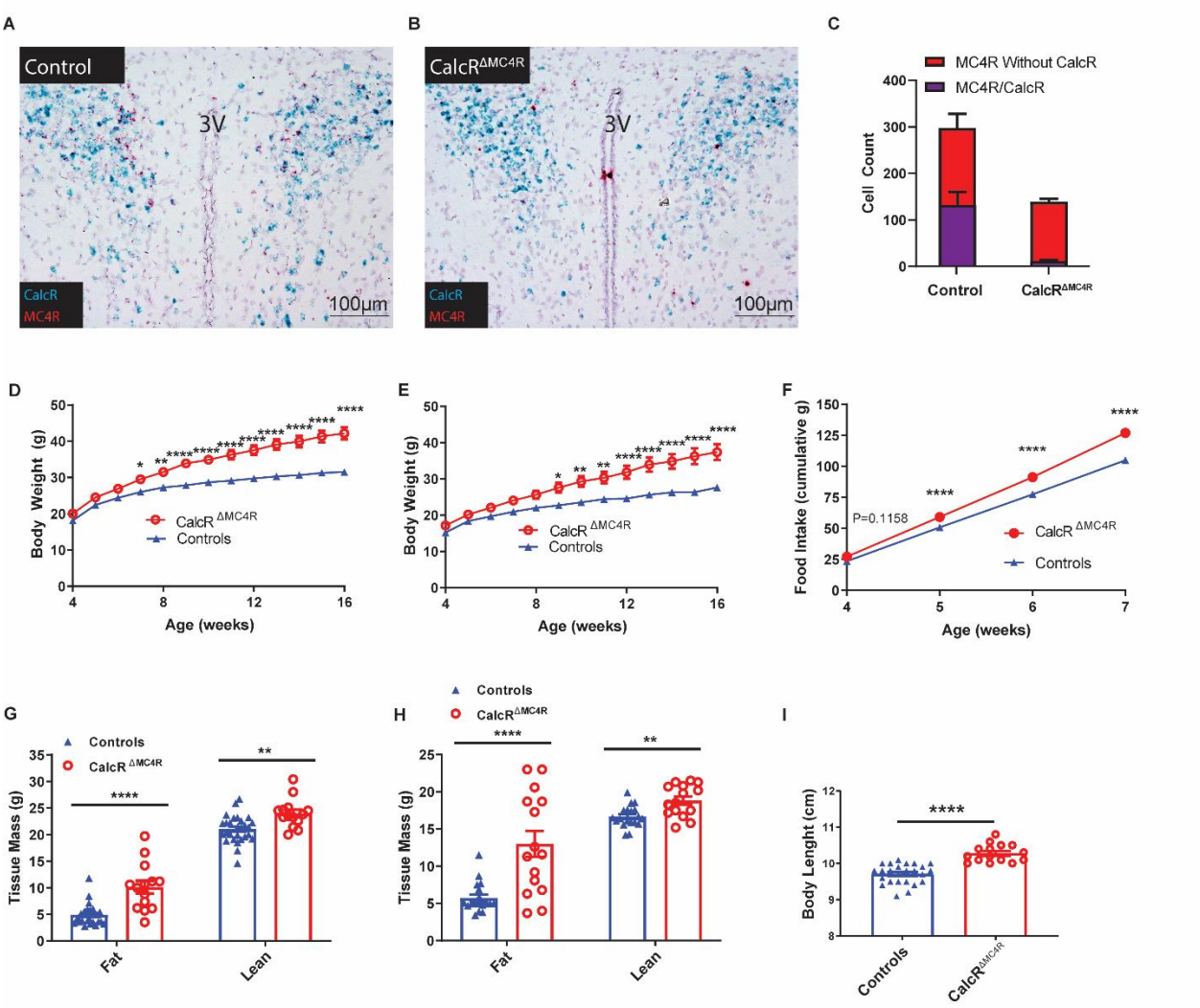

Figure 4.1: MC4Rs in CalcR-expressing neurons are required for body weight regulation. In situ hybridization of control (A) and CalcR$^{\Delta MC4R}$ (B) mice for Calcr (blue) and Mc4r RNAs (red). Quantification of Mc4r and Calcr co-expression in both CalcRΔ^{MC4R} and WT groups (C). Longitudinal body weight for males (D) and females (E). Cumulative food intake for CalcR$^{\Delta MC4R}$ and control male mice was taken between 4 and 7 weeks of age (F). Fat mass and lean mass in males (G) and females (H) were measured at 16-18 weeks of age. Body length was conducted at 22 weeks of age (I).

Average values ± SEM are shown; for male BW and body composition: N=14-28/group, for female BW and body composition: N=15-19/group; for cumulative food intake of males: N=16-25/group; for body length: N=15-25/group. P values for BW, cumulative food intake were determined via 2-way ANOVA followed by Sidak's multiple comparisons test, and for body composition an unpaired t test was used. * $p<0.05$, ** $p<0.01$, **** $p<0.0001$.

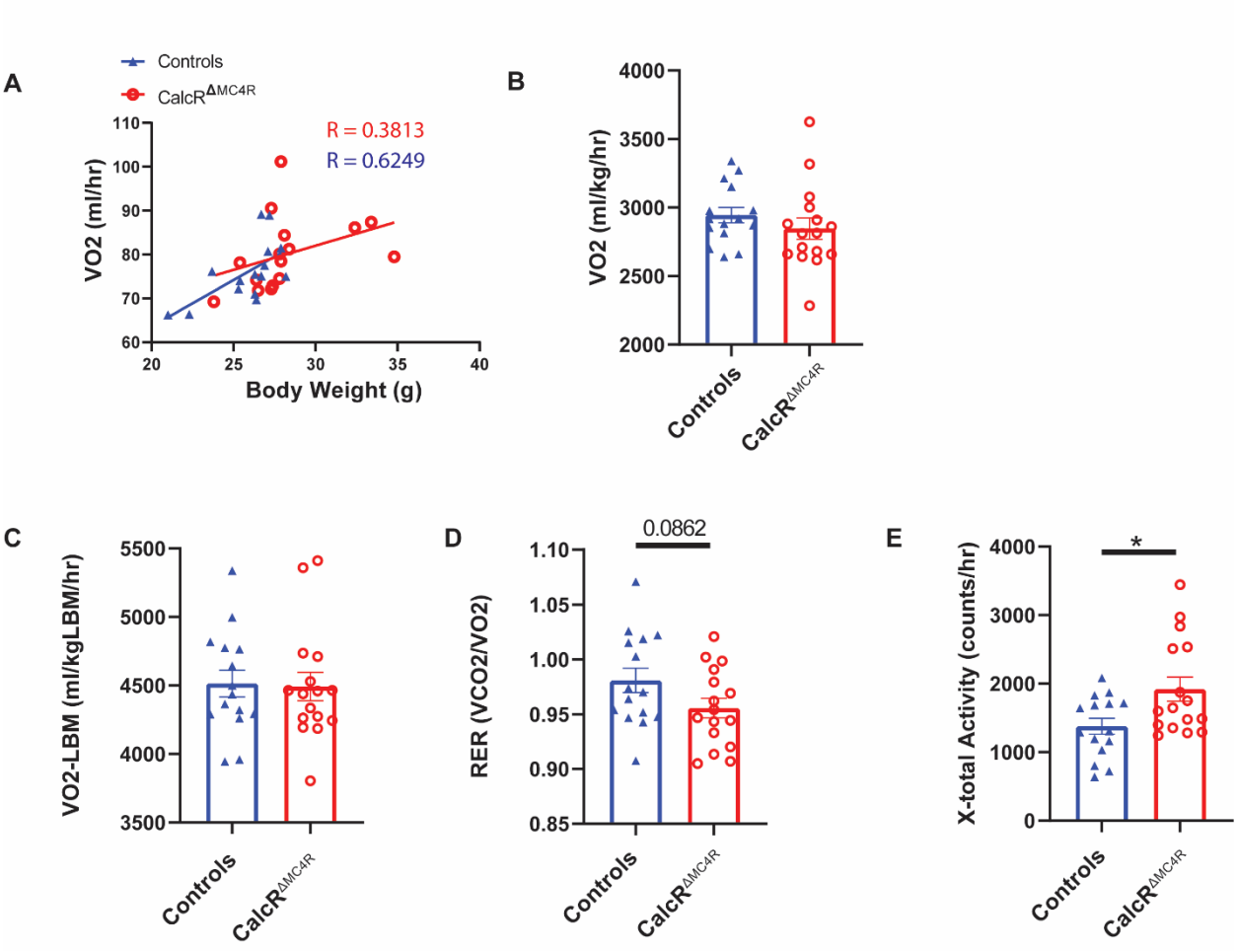

Figure 4.2: Deletion of MC4Rs in CalcR-expressing neurons has minimal effects on energy expenditure. The mice were placed in CLAMS at 8-10 weeks of age. Raw VO2 consumption over a 24 hour period was compared to their respective body weights (A). VO2 consumption adjusted to total body mass (B), VO2 consumption adjusted to LBM (C), RER (D) and X-total activity (E) were also measured. Average values ± SEM are shown, for CLAMS measurements: N=15-16/group. P values for body length and CLAMS measurements, unpaired t tests were used. For the Raw VO2 consumption over a 24 hr period comparison, a simple linear regression and correlation analysis was used to determine the Pearson correlation (R) values. * p<0.05, ****p<0.0001.

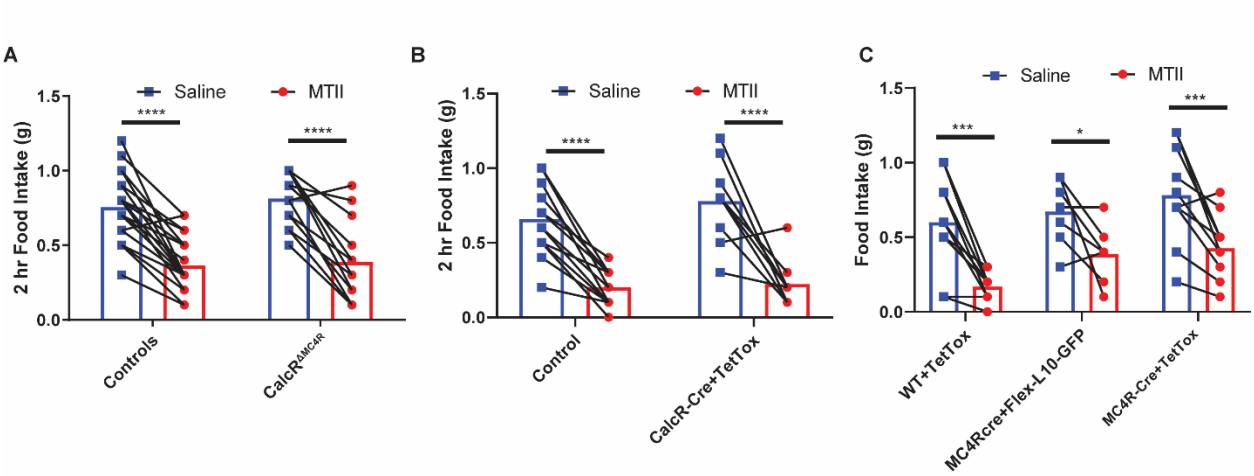

Figure 4.3: Anorectic effect of melanocortin agonist in mice with the deletion of MC4R from CalcR cells or with silenced CalcR^{PVH} neurons. Two-hour food intake was measured following the i.p. injection of the MC4R agonist MTII (150 ug/mouse) for CalcR$^{\Delta MC4R}$ (A), CalcR-Cre+TetTox (B) and MC4R-Cre+TetTox (C) mice. Average values ± SEM are shown; for the deletion experiment: N=15-25/group, for the CalcR^{PVH} silencing experiment: N=9-20/group, and for the MC4R^{PVH} silencing experiment: N=6-11/group. P values were determined via paired t-tests. * p<0.05, **p<0.01, ***p<0.001, ****p<0.0001.

Regions of MC4R and CalcR Overlap	Bregma (Start)	Bregma (End)
STLV/STMV/STMA/STMPL/Stmpi/STMPM	0.73mm	0.61mm
AVPe	0.37mm	0.25mm
MPOM/MPOL/MPA	0.01mm	-0.11mm
STHY	-0.35mm	
AHA/AHP/AHC	-0.47mm	
LA	-0.47mm	
PaV/PaMM/PaMP/PaLM/PaDC	-0.59mm	-0.95mm
RChL	-0.95mm	
Aco	-1.07mm	-1.23mm
BMA	-1.07mm	-1.23mm
Mtu	-1.43mm	-1.67mm
ArcL/ArcM/ArcMP	-1.67mm	-2.27mm
DM/DMD	-1.67mm	-1.79mm
LH	-1.67mm	
VMHVL	-1.67mm	
MePD/MePV	-1.67mm	-2.15mm
PH	-2.03mm	
PMV	-2.27mm	
LPAG/DMPAG/DLPAG/VLPAG	-3.79mm	-5.19mm
PnO	-4.03mm	
DRD/DRL	-4.71mm	
LPB/LPBV/LPBC/LPBI	-5.19mm	-5.51mm
MPB	-5.19mm	-5.51mm
RMg	-5.63mm	
Rpa	-5.91mm	-5.99mm
MVePC	-6.23mm	-6.83mm
PCRtA	-6.23mm	-6.59mm
IRT	-6.23mm	-6.83mm
SolC/SOLIM/SOLV/SOIDL/SOIVL/SOLM/SOLDM/SolL	-6.35mm	7.83mm
10N	-6.35mm	7.83mm
AP	-7.43mm	-7.67mm

Table 4.1: Brain regions that abundantly express MC4R and CalcR neurons. IHC was conducted on MC4R-Cre mice that expressed a Cre-dependent TdTomato reporter and on CalcR-Cre mice that expressed a Cre-dependent GFP reporter. Images were taken between Bregma 0.85mm and Bregma -8.15mm (coordinates obtained from the atlas Paxinos and Franklin's the Mouse Brain in Stereotaxic Coordinates 4th Edition) and regions were recorded based on the degree of expression of either MC4R or

CalcR. The regions listed are those in which both CalcR and MC4R neurons were found in abundance and the rostral (start) to caudal (end) coordinate range is listed for each region. STLV= bed nucleus of the stria terminalis, lateral division, ventral part; STMV= bed nucleus of the stria terminalis, medial division, ventral part; STMA= bed nucleus of the stria terminalis, medial division, anterolateral part; STMPL= bed nucleus of the stria terminalis, medial division, posterolateral part; stmpi= bed nucleus of the stria terminalis, medial division, posterointermediate part; STMPM= bed nucleus of the stria terminalis, medial division, posteromedial part; AVPe= anteroventral periventricular nucleus; MPOM= medial preoptic nucleus, medial part; MPOL= medial preoptic nucleus, lateral part; MPA= medial preoptic area; STHY= striohypothalamic nucleus; AHA= anterior hypothalamic area, anterior part; AHP= anterior hypothalamic area, posterior part; AHC= anterior hypothalamic area, central part; LA= lateroanterior hypothalamic nucleus; PaV= paraventricular hypothalamic nucleus, ventral part; PaMM= paraventricular hypothalamic nucleus, medial magnocellular part; PaMP= paraventricular hypothalamic nucleus, medial parvicellular part; PaLM= paraventricular hypothalamic nucleus, lateral magnocellular part; PaDC= paraventricular hypothalamic nucleus, dorsal cap; RChL= retrochiasmatic area, lateral part; Aco= anterior cortical amygdaloid nucleus; BMA= basomedial amygdaloid nucleus, anterior part; Mtu= medial tuberal nucleus; ArcL= arcuate hypothalamic nucleus, lateral part; ArcM= arcuate hypothalamic nucleus, medial part; ArcMP= arcuate hypothalamic nucleus, medial posterior part; DM= dorsomedial hypothalamic nucleus; DMD= dorsomedial hypothalamic nucleus, dorsal part; LH= lateral hypothalamus; VMHVL= ventromedial hypothalamic nucleus, ventrolateral part; MePD= medial amygdaloid nucleus,

posterodorsal part; MePV= medial amygdaloid nucleus, posteroventral part; PH= posterior hypothalamic nucleus; PMV= premamillary nucleus, ventral part; LPAG= lateral periaqueductal gray; DMPAG= dorsomedial periaqueductal gray; DLPAG= dorsolateral periaqueductal gray; VLPAG= ventrolateral periaqueductal gray; PnO= pontine reticular nucleus, oral part; DRD= dorsal raphe nucleus, dorsal part; DRL= dorsal raphe nucleus, lateral part; LPB= lateral parabrachial nucleus; LPBV= lateral parabrachial nucleus, ventral part; LPBC= lateral parabrachial nucleus, central part; LPBl= lateral parabrachial nucleus, internal part; MPB= medial parabrachial nucleus; RMg= raphe magnus nucleus; Rpa= raphe pallidus nucleus; MVePC= medial vestibular nucleus, parvicellular part; PCRtA= parvicellular reticular nucleus, alpha part; IRT= intermediate reticular nucleus; SolC= solitary nucleus, commissural part; SOLIM= solitary nucleus, intermediate part; SOLV= solitary nucleus, ventral part; SOlDL= solitary nucleus, dorsolateral part; SOlVL= solitary nucleus, ventrolateral part; SOLM= solitary nucleus, medial part; SOLDM= solitary nucleus, dorsomedial part, SolL= solitary nucleus, lateral part; 10N= vagus nerve nucleus; AP= area postrema

Chapter 5

Discussion: Delineating Physiologic Roles of PVH Neurons with an Anatomical Approach

PVH neurons differentially regulate energy balance depending on their downstream projection targets

The previously described projects served to identify novel neuronal populations in the PVH responsible for regulating energy homeostasis. However, these studies lacked the capability to identify the role these neurons specifically play through their downstream projection targets, as our activation and inhibition of these neurons influence all outputs rather than those that target a particular region. This distinction is crucial to understanding energy balance circuitry, as the downstream regions these neurons project to in the hindbrain have been found to regulate different aspects of energy balance through their own neuronal subpopulations.

As a subpopulation of the $Sim1^{PVH}$ neurons, we have previously determined that $NOS1^{PVH}$ neurons project to regions of the hindbrain (PBN and NTS) and the upper thoracic spinal cord that are important in the regulation of food intake and energy expenditure.[1] Further, chemogenetic activation of $NOS1^{PVH}$ neurons suppresses food intake in a similar manner to $Sim1^{PVH}$ neurons and increases energy expenditure.[1] In

comparison, the OXT^{PVH} neurons, as a subpopulation of the NOS1 neurons, send projections to the ChAT neurons of the IML but do not send dense projections to the PBN or NTS. OXT^{PVH} neurons do increase energy expenditure when chemogenetically activated, although to a lesser degree than the $NOS1^{PVH}$ or $Sim1^{PVH}$ neurons, but do not influence feeding behavior when activated.[1] This study makes it clear that subpopulations of the $Sim1^{PVH}$ neurons regulate different aspects of energy homeostasis, and highlights the variability of the physiological roles specific PVH neurons play in regulating energy homeostasis through their downstream projection targets. The studies presented here concerning the $IRS4^{PVH}$ and $CalcR^{PVH}$ neurons were made in an attempt to parse out the different ways in which the PVH regulates food intake and energy expenditure.[2,3] However, they do not paint a complete picture and only hint to their downstream influences on energy balance, failing to discern which regions are responsible for feeding and energy expenditure regulation through the PVH. As such, studies which use chemogenetic activation of specific neuronal populations of the PVH gives the overall physiological effects generated by these neurons through all their downstream projection targets. This creates a problem in trying to determine the specific contributions of neural circuits targeting specific brain regions. Because the $IRS4^{PVH}$, $CalcR^{PVH}$ and $NOS1^{PVH}$ neurons project to both the PBN and NTS, we are unable to discern the physiological effects associated with specific projections to the PBN or to the NTS alone.[1-3]

Determining how these brain regions contribute to the physiological effects produced by the PVH will require the use of methods that either selectively manipulate PVH cells based on their projection targets or through activating specific PVH neurons

at their axon terminals. For the latter, it has been found that optogenetic activation of $MC4R^{PVH}$ neurons at their projection terminals in the PBN suppresses food intake without producing an aversive response.[4] Stimulating $MC4R^{PVH}$ neurons at their terminals in the PBN in hungry mice promoted place preference, indicating that activating $MC4R^{PVH}$ neurons that project to the PBN produces an appealing or pleasant response.[4] Termination of feeding is often associated with either a pleasant feeling of fullness (non-aversive) or with an unpleasant feeling of visceral illness (aversive). It is important to distinguish between anorectic treatments that produce non-aversive vs aversive responses, as therapeutic methods tend to favor those that produce non-aversive responses.[4,5] While projections from the PVH to PBN have suggested involvement in food intake regulation, there is little evidence to suggest that the PBN is involved in regulating energy expenditure.

The NTS integrates satiety signals from the central nervous system, as well as hormonal signals from the peripheral system.[6-10] The NTS contains both neuronal populations that suppress food intake in an aversive and non-aversive manner when activated.[5] Optogenetic activation of CCK^{NTS} neurons that project to the PBN suppresses food intake behavior in an aversive manner, while activating CCK^{NTS} neurons that project to the PVH suppresses feeding non-aversively. Conversely, NTS projections to the PBN have been determined to suppress feeding through an aversive response.[5] The NTS closely associates with the spinal cord and may serve to modulate the sympathetic nervous system through this interaction. The NTS also serves as an integrator of metabolic signals from regions of the forebrain and brainstem, potentially regulating BAT activity downstream.[8] Several neuronal populations of the PVH send

projections to the NTS, and it is through these projections that the PVH may influence sympathetic output and energy expenditure.[11-15]

Investigation of the contribution of PVH projections to specific hindbrain regions in energy homeostasis

Given that the PBN and NTS regions are known to regulate energy homeostasis, it would be valuable to determine the contribution of PVH projections to these two regions to further clarify their role in energy homeostatic circuitry. We hypothesize that PVH to PBN projections would regulate food intake behavior but not energy expenditure while PVH to NTS projections could potentially influence feeding as well as energy expenditure. To investigate this, we have used retrograde viral methods to determine the contribution of PVH to PBN projecting cells vs PVH to NTS projecting cells in the regulation of energy balance. We used a novel Cre virus that is transported in a retrograde fashion (Retro-Cre) to transduce projection terminals and induce expression of Cre in the cell bodies of PVH neurons, allowing us to manipulate them with Cre-dependent viruses.[16] Optogenetics is typically the method of choice to investigate the activation of the projection terminals of specific neuronal populations, as it allows for immediate and direct stimulation of the desired pathway. This is not always feasible, as there are cases where an optic fiber cannot be easily implemented without skull coverage, such as caudal areas of the hindbrain or the spinal cord. In these instances, injection of a Retro-Cre virus would be the preferable method.

To determine the sufficiency of PVH neurons projecting to the PBN or NTS in modulating food intake and energy expenditure, we stereotaxically injected an AAV Retro-Cre virus bilaterally into the PBN (coordinates relative to bregma: A/P= -5.400, M/L=+/- 1.200, D/V= -2.900; 50 nL/side) or NTS (D/V= -0.500; 50 nL/side) of adult male mice between the ages of 8-12 weeks to induce Cre expression in neurons that project to either region. This allowed us to utilize a Cre-dependent AAV-FLEX hM3Dq-mCherry DREADD virus injected bilaterally into the PVH (coordinates relative to bregma: A/P= -.500, M/L= +/- .200, D/V= -4.77; 50nL/side) to selectively activate PVH neurons that project to the PBN or NTS. The mice were given at least two weeks to recover from the surgeries and to allow for sufficient viral expression before running any experiments. To investigate the role of PVH to PBN (PVH>PBN) or PVH to NTS (PVH>NTS) circuitry in the regulation of food intake circuitry, several food intake experiments were conducted.

For the mice with Retro-Cre injected into the PBN and hM3Dq injected into the PVH (PVH^{hM3Dq}>$PBN^{Retro\text{-}Cre}$), they were singly housed and injected IP with saline for three consecutive days prior to the food intake experiment to acclimate them to receiving injections (Figure 5.1 A-C). On the day of the experiment, food was removed from the cages and the animals were fasted for 8 hours. At the start of the dark cycle, either saline or CNO (0.3 mg/kg) was IP injected into the mice (N=6). Food pellets were weighed and placed into the cages, with measurements being taken 2, 4 and 16 hours after the injection to determine food intake. The treatments were then reversed the following week to compare the food intake between the CNO and saline treatments. For the PVH^{hM3Dq}>$PBN^{Retro\text{-}Cre}$ mice, we determined that 2 hours after injection, food intake was suppressed due to CNO activation of the PVH neurons that project to the PBN

(Figure 5.1 D). This finding supports the previously discussed optogenetic experiment in which $MC4R^{PVH}$ neurons were stimulated at the axon terminals in the PBN, which resulted in a trend towards significant reduction in food intake (significance determined using a paired t-test).[4] PVH neurons projecting to the PBN are therefore sufficient to suppress food intake acutely.

For the mice with Retro-Cre injected into the NTS and hM3Dq injected into the PVH (PVH^{hM3Dq}>$NTS^{Retro\text{-}Cre}$), we conducted the same food intake experiment described previously and found that food intake was unaffected by CNO induced activation of the PVH>NTS neurons (N=4) (Figure 5.2 A-D). Additionally, we conducted a longer-term experiment in which we injected the PVH^{hM3Dq}>$NTS^{Retro\text{-}Cre}$ mice with either CNO or saline twice daily (once at 8:00AM and again at 5:30PM) over the course of three days and found that while food intake was unaffected by the CNO activation, body weight was significantly reduced on the second day of injections (Figure 5.2 E-F). This difference in body weight was less on the third day and may have been due to a compensatory mechanism to maintain body weight (Figure 5.2 F). This suggested that while PVH>NTS neurons did not influence neurons responsible for regulating food intake in the NTS, they may have played a role in regulating energy expenditure.

For our energy expenditure experiments, the PVH^{hM3Dq}>$NTS^{Retro\text{-}Cre}$ mice were placed in a Comprehensive Laboratory Animal Monitoring System (CLAMS, Columbus Instruments) which is managed by the University of Michigan Small Animal Phenotyping Core. The PVH^{hM3Dq}>$NTS^{Retro\text{-}Cre}$ mice were given a day to acclimate to the CLAMS chamber and on the second day, food was removed at 9:00AM. Just prior to 12:00PM, the mice were then injected with either CNO or saline (N=4) and measurements were

taken over the next 4 hours and at 5PM the mice were refed. This was repeated on the fourth day, with the CNO and saline treatments switched. From our CLAMS measurements, we found that while RER remained unaffected, energy expenditure, oxygen consumption and ambulatory activity significant increased four hours after the injection of CNO (significance determined using a paired t-test) (Figure 5.2 G-J). This supports our pervious findings, as the weight loss experienced may have been due to the increase in energy expenditure as a result of CNO activation of PVH>NTS neurons. This strongly suggests that the PVH engages the sympathetic nervous system through the NTS to regulate energy expenditure.[11-15]

Not yet conducted, but still of interest are experiments that test whether activating PVH>PBN or PVH>NTS neurons result in an aversive or non-aversive response. To test whether stimulation of these neurons is aversive, we would run a conditioned taste aversion (CTA) assay.[17] The PVH^{hM3Dq}>$PBN^{Retro\text{-}Cre}$ or PVH^{hM3Dq}>$NTS^{Retro\text{-}Cre}$ mice would be singly housed with cages receiving water from two water bottles. With a three-day acclimation period, followed by a 7-day routine of timed water-restriction, mice would receive access to two water bottles for two 1-hour sessions each day. This serves to habituate the mice to consuming water only during these two periods of time. For the conditioning day, the mice will receive two water bottles, one of which contains 0.15% saccharin during the morning session. Groups of mice will then receive subcutaneous injections of either saline, CNO or lithium chloride (0.3M), with lithium chloride serving as a positive control for inducing an aversive response.[18] For the afternoon session and the sessions the following day, the mice can be rehydrated with regular water. The next day, the mice will have access to two bottles

in the morning, with one containing saccharin and the other with water. The water and saccharin volumes ingested during that hour will be measured and a preference ratio will be determined as the volume of saccharin consumed divided by the total volume of liquid consumed. A lower preference ratio for saccharin will be interpreted as an aversive response.[17]

In contrast to the previous experiment, if we find that activation of PVH>PBN or PVH>NTS neurons is non-aversive, we would also want to conduct a conditioned place preference (CPP) assay, to determine if activation of PVH>PBN or PVH>NTS neurons is associated with positive valence. For this experiment, the mice would be placed individually into a two chambered apparatus and undergo 30 minute sessions over 3 days to freely habituate to the apparatus and remove its novelty. For each mouse during these sessions, we will determine which chamber is designated as “preferred” or “not preferred”. The mice will then receive six days of conditioning, during which they will be given IP injections of CNO or saline followed by containment in the “not preferred” chamber for 30 minutes. For the test day, the mice will be placed in the chamber and allowed to travel between them freely. We will then determine the percentage of time the mouse spends in each chamber. A high percentage of time spent in the “not preferred” chamber would be interpreted as the mouse showing preference and would therefore be an indication of positive valence. The treatments would then be switched and the assay repeated.[4,19]

Our preliminary findings support much of what we have learned concerning the downstream projection targets of the PVH in the hindbrain.[1,7,20] Previous studies have demonstrated that many neuronal populations of the PVH that regulate feeding send

projections to the PBN and optogenetics studies have demonstrated that activating axon terminals of specific PVH neurons in the PBN suppresses food intake.[4] Our preliminary studies using chemogenetics have reinforced this finding. While the NTS serves as an integrator of satiety signals primarily from the periphery, we have demonstrated that stimulating PVH neurons that project to the NTS do not suppress feeding. However, stimulating PVH neurons projecting to the NTS does promote increased energy expenditure and increased oxygen consumption, potentially due to its sympathetic output to brown adipose tissue as well as other peripheral sites influenced by the sympathetic nervous system.[11-14] We do not expect that the PBN would influence energy expenditure, but this is an experiment that has yet to be conducted.[4] Additional future experiments include those of the CTA and CPP assays. We expect that activating PVH neurons that project to the PBN would produce an appetitive response without aversion, as this was found to be true of optogenetic stimulation of $MC4R^{PVH}$ neurons that project to the PBN.[4] In contrast, stimulating PVH neurons that project to the NTS could be aversive, as cell types such as the CCK^{NTS} neurons that project to PBN suppress feeding through associated aversion when activated.[5]

Further considerations and future directions for the investigation of PVH neurons

While the Retro-Cre virus is a useful tool, there are a few considerations and limitations that need to be addressed. The most concerning issues is that it appears that the PVH contains neurons that send collateral projections to both the PBN and NTS. For our experiment in which we injected Retro-Cre into the PBN and hM3Dq into the PVH, we conducted a DAB stain for mCherry (a reporter for hM3Dq expression) (Figure

5.3 A). As expected, we found expression in the PVH (Figure 5.3 B) and found signal at the neuronal terminals in the PBN (Figure 5.3 C). We also found mCherry expression in the NTS, indicating that at least some of the PVH>PBN neurons also project to the NTS (Figure 5.3 D). This could confound our attempts to parse out the specific role the PBN and NTS play in PVH mediated energy homeostasis. As this data is preliminary, we can more definitively confirm and quantify this overlap through the use of two differently labeled retrograde viruses applied to the PBN and NTS.

Optogenetics would be a viable alternative to our studies using Retro-Cre and hm3Dq, as we could stimulate the axon terminals of all PVH neurons that project to the PBN. This method becomes less viable when investigating the physiological role of the PVH to NTS circuitry. Implanting the fiberoptic into the NTS would be difficult, as its location is so caudal that the skull would not be present to anchor it in place. Another issue to consider is that the PVH neurons that project to either the PBN or NTS may be composed of both aversive and non-aversive subpopulations. This could result in opposing responses that cancel each other out and therefore other genetic tools might need to be developed to manipulate specific PVH neuronal populations that project to these downstream regions.

Fortunately, the Olson laboratory is developing such tools in the form of viral systems that require the expression of both Cre and flippase (Flp) recombinase. Flp recombinase recognizes flippase recognition target (FRT) sites in a similar manner in which Cre recognizes LoxP sites.[21] We could generate a hM3Dq or hM4Di (inhibitory DREADD) virus that requires the excision of a STOP cassette flanked by FRT sites and a STOP cassette flanked by LoxP sites in order for hM3Dq/hM4Di to be expressed. The

problem with a method that uses several STOP cassettes is that STOP cassette sequences are rather large and are not likely to fit within the limits of a viral capsid.[22] Alternatively, we could use an INTronic Recombinase Sites Enabling Combinatorial Targeting (INTRSECT) system to reduce sequence size. INTERSECT can be used to produce viruses that have inverted Cre dependent and Flp dependent domains that require the expression of both Cre and Flp to be converted to the proper orientation and express the desired sequence.[23] This virus could then be placed in the PVH of a mouse that expresses Flp in conjunction with the desired genetic marker, such as CalcR or IRS4. With the cells of the PVH transduced with a Cre/Flp dependent virus, we could then inject a retrograde Cre virus into a downstream projection target of the PVH, such as the PBN or NTS. With Cre expression traveling back to the cell bodies of the PVH, we would now have Cre expressed in PVH cells that project to our region of interest, and Flp expressed in our PVH neuronal subpopulation of interest. This combination would result in expression of hM3Dq/hM4Di in the desired cell type that projects to the desired location, allowing us to activate $CalcR^{PVH}$ neurons that project only to the NTS as an example. This technique would allow us to selectively activate or inhibit neuronal subpopulations of neurons in the CNS that project to specific downstream targets, making it easier to identify the activity of specific circuits.

Overview

Many regions of the hypothalamus and hindbrain receive peripheral signals that indicate the energy and nutrient demands of the body.[6] These peripheral signals are

then converted to neuronal outputs that project centrally to integrative nodes within the CNS. The PVH is one such node, which in turn produces outputs that regulate feeding, energy expenditure, glucose regulation and the neuroendocrine system through projections to the forebrain, hindbrain, pituitary and spinal cord.[24] Such integration within a singular node is important, as it takes into account the summation or negation of various signals to maintain a homeostatic system, which has been evolutionarily honed to support survival. This could be furthered by the potential interconnectivity and crosstalk between several neurons within the PVH.[25,26] This suggests the PVH may regulate various aspects of energy balance as well as other physiological processes through interconnected circuits, with the combination of signal inputs modulating a given physiological process. It is also interesting that the PVH contains several neuronal populations that regulate energy balance through similar means, such as feeding behavior, but are non-overlapping.[27] This suggest that there may be redundancies in the regulation of feeding circuitry, which would be crucial as maintaining energy balance is essential to survival. Under conditions in which one of these pathways are altered, one of these redundant systems could compensate for impaired function. This redundancy creates a rigid yet malleable system of homeostatic control, allowing for internal changes in response to environmental pressures, but still maintaining a level of stability. Through therapeutic techniques, we may be able manipulate these alternative pathways, shifting a faulty system towards a healthy energy balance and compensating for the impairment.

The PVH is composed of diverse neuronal populations that have been defined in part through their expression of various neuropeptides, enzymes and cell surface

receptors. Many of these neuronal subgroups within the PVH manipulate energy homeostasis differently based on their downstream projection targets, engaging in circuitry that influences aversive and non-aversive food intake behavior, as well as energy expenditure through sympathetic output or the neuroendocrine system.[1-4,24] The body engages with each of these energy homeostatic neurocircuits based on the current need, whether through engaging aversive feeding circuitry to deter consumption of a potentially harmful substance or through burning energy through BAT to aid in thermoregulation.[1,6] Identifying and mapping the neuronal subgroups of the PVH that engage in particular aspects of energy balance will allow us to develop therapeutics that target desired means of energy balance, such as drugs that activate appetitive pathways with positive valence or activating neurons that promote passive energy expenditure.

Our laboratory and others have investigated the unique roles of the various PVH cell types in energy homeostasis with an ongoing goal to better understand energy balance circuitry. IRS4 is highly expressed in the PVH and acts synergistically with IRS2 in the hypothalamus to preserve regular body weight and thus became a neuronal population of interest in the PVH.[28] We have determined that activation of IRS4^{PVH} neurons suppresses food intake and increases energy expenditure, while silencing these neurons results in obesity.[3] These IRS4^{PVH} neurons are distinct from OXT^{PVH} and NOS1^{PVH} neuronal populations and project to the hindbrain regions PBN and NTS, as well as the median eminence and the ChAT neurons of the IML of the spinal cord.[3] This study demonstrates that IRS4^{PVH} neurons are a valuable component of energy homeostatic circuitry. It is still unclear, however, through which mechanism these

IRS4^{PVH} neurons maintain energy balance via endogenous systems. Whole body deletion of IRS4 alone does not perturb food intake or the ability to maintain body weight, but hyperphagic obesity results when coupled with the deletion of IRS2.[28] It would therefore be interesting to assess whether this synergy exists in the PVH, perhaps through the duel deletion of IRS4 and IRS2 expression in Sim1 expressing neurons. Additionally, we observed MC4R expression in a population of the IRS4^{PVH} neurons, presenting another possible means through which feeding behavior is regulated through the IRS4^{PVH} neurons. It would therefore be interesting to investigate the effects of deleting MC4R from IRS4 neurons on feeding behavior and body weight. The PDYN subset of the IRS4^{PVH} neurons may also contribute to the regulation of feeding behavior observed.[27] Finally, IRS4^{PVH} neurons overlap with TRH^{PVH} neurons and may influence energy expenditure through the autonomic nervous system or via the pituitary-thyroid axis.[3]

Because calcitonin and amylin suppress food intake when applied peripherally and centrally, we investigated CalcR expression in the PVH through the deletion of CalcR expression from Sim1 neurons, which are heavily expressed in the PVH.[29-32] Our findings indicated that CalcR expression in the PVH and other regions that express Sim1 is dispensable in maintaining energy homeostasis and its deletion does not influence the anorectic effects of sCT.[33] Although deletion of CalcR expression from the PVH did not produce a notable difference in energy homeostasis, it would be valuable to investigate other potential physiological process that may have been influenced by the deletion of CalcR from the PVH. While deletion of CalcR from the PVH did not appear to influence energy balance, we investigated CalcR neurons as a subpopulation

of the PVH and their role in regulating energy homeostasis. We found that activating CalcR^{PVH} neurons suppressed feeding and promoted ambulatory activity, while silencing these neurons produces increased feeding and weight gain, although to a lesser extent than when the MC4R^{PVH} neurons were silenced.[2] Similar to the IRS4^{PVH} neurons, the CalcR^{PVH} neurons project to the PBN and NTS as well as the median eminence. When investigating the overlap of CalcR^{PVH} neurons with other neurons in the PVH, we found that CalcR neurons most notably expressed MC4R and CRH.[2] As CalcR^{PVH} neurons project to the pituitary, this suggests that the CRH expressing subpopulation may influence the neuroendocrine release through the release of CRH. It would be worthwhile to investigate the influences CalcR^{PVH} neurons have on corticosterone and glucose levels due to their potential interaction with the hypothalamic-pituitary-adrenal axis.[34] Due to the overlap between CalcR and MC4R neurons in the PVH, we deleted MC4R expression from CalcR cells to determine if MC4R expression is necessary for the regulation of energy balance. Through our studies, we found that deletion of MC4R from CalcR neurons caused hyperphagic obesity in male and female mice without influencing the anorectic effects of MTII. While compelling, we determined that our method of deletion potentially deleted MC4R from CalcR neurons beyond the PVH, as there are many regions of potential overlap in the hypothalamus and hindbrain. It is for this reason that further investigation of the overlap of these neurons in other regions through in situ hybridization or other means would be necessary.

We have done much to characterize the neuronal populations of the PVH and their roles in energy homeostasis, however there are many neuronal populations in this

diverse nucleus that have yet to be explored or thoroughly defined. Further, as the PVH is an integrator of signaling within the central nervous system, and in turn exerts influence on many downstream regions in the hindbrain and hypothalamus through its projections, more studies need to be done to delineate the contribution of these downstream projections to the regulation of energy homeostasis. In doing so, we improve our understanding of the physiological roles of defined PVH cell types and the neural circuitries in which they operate. Characterizing neuronal populations of the PVH that play a known role in regulating energy homeostasis could aid in the identification of receptors that could be targeted by specific synthetic ligands as well as identify sites downstream that can be characterized and targeted. As we unravel the cellular and neurobiological mechanisms used by subpopulations of the PVH to regulate energy balance, we further our efforts to identify therapeutic targets to help manage obesity and its comorbid diseases.

References:

1. Sutton AK, Pei H, Burnett KH, Myers MG, Jr., Rhodes CJ, Olson DP. Control of food intake and energy expenditure by Nos1 neurons of the paraventricular hypothalamus. *J Neurosci.* 2014;34(46):15306-15318.
2. Gonzalez IE, Ramirez-Matias J, Lu C, et al. Paraventricular Calcitonin Receptor-Expressing Neurons Modulate Energy Homeostasis in Male Mice. *Endocrinology.* 2021;162(6).
3. Sutton AK, Gonzalez IE, Sadagurski M, et al. Paraventricular, subparaventricular and periventricular hypothalamic IRS4-expressing neurons are required for normal energy balance. *Sci Rep.* 2020;10(1):5546.
4. Garfield AS, Li C, Madara JC, et al. A neural basis for melanocortin-4 receptor-regulated appetite. *Nat Neurosci.* 2015;18(6):863-871.
5. Roman CW, Sloat SR, Palmiter RD. A tale of two circuits: CCK(NTS) neuron stimulation controls appetite and induces opposing motivational states by projections to distinct brain regions. *Neuroscience.* 2017;358:316-324.
6. Morton GJ, Meek TH, Schwartz MW. Neurobiology of food intake in health and disease. *Nat Rev Neurosci.* 2014;15(6):367-378.
7. Geerling JC, Shin JW, Chimenti PC, Loewy AD. Paraventricular hypothalamic nucleus: axonal projections to the brainstem. *J Comp Neurol.* 2010;518(9):1460-1499.
8. Grill HJ, Hayes MR. Hindbrain neurons as an essential hub in the neuroanatomically distributed control of energy balance. *Cell Metab.* 2012;16(3):296-309.
9. Gibbs J, Young RC, Smith GP. Cholecystokinin decreases food intake in rats. 1973. *Obes Res.* 1997;5(3):284-290.
10. Grill HJ, Schwartz MW, Kaplan JM, Foxhall JS, Breininger J, Baskin DG. Evidence that the caudal brainstem is a target for the inhibitory effect of leptin on food intake. *Endocrinology.* 2002;143(1):239-246.
11. Bamshad M, Song CK, Bartness TJ. CNS origins of the sympathetic nervous system outflow to brown adipose tissue. *Am J Physiol.* 1999;276(6):R1569-1578.
12. Caverson MM, Ciriello J, Calaresu FR. Paraventricular nucleus of the hypothalamus: an electrophysiological investigation of neurons projecting directly to intermediolateral nucleus in the cat. *Brain Res.* 1984;305(2):380-383.
13. Cao WH, Madden CJ, Morrison SF. Inhibition of brown adipose tissue thermogenesis by neurons in the ventrolateral medulla and in the nucleus tractus solitarius. *Am J Physiol Regul Integr Comp Physiol.* 2010;299(1):R277-290.
14. Fyda DM, Cooper KE, Veale WL. Modulation of brown adipose tissue-mediated thermogenesis by lesions to the nucleus tractus solitarius in the rat. *Brain Res.* 1991;546(2):203-210.
15. Madden CJ, Morrison SF. Neurons in the paraventricular nucleus of the hypothalamus inhibit sympathetic outflow to brown adipose tissue. *Am J Physiol Regul Integr Comp Physiol.* 2009;296(3):R831-843.
16. Tervo DG, Hwang BY, Viswanathan S, et al. A Designer AAV Variant Permits Efficient Retrograde Access to Projection Neurons. *Neuron.* 2016;92(2):372-382.

17. Adams JM, Pei H, Sandoval DA, et al. Liraglutide Modulates Appetite and Body Weight Through Glucagon-Like Peptide 1 Receptor-Expressing Glutamatergic Neurons. *Diabetes.* 2018;67(8):1538-1548.
18. Arias C, Pautassi RM, Molina JC, Spear NE. A comparison between taste avoidance and conditioned disgust reactions induced by ethanol and lithium chloride in preweanling rats. *Dev Psychobiol.* 2010;52(6):545-557.
19. Huston JP, Silva MA, Topic B, Muller CP. What's conditioned in conditioned place preference? *Trends Pharmacol Sci.* 2013;34(3):162-166.
20. Shah BP, Vong L, Olson DP, et al. MC4R-expressing glutamatergic neurons in the paraventricular hypothalamus regulate feeding and are synaptically connected to the parabrachial nucleus. *Proc Natl Acad Sci U S A.* 2014;111(36):13193-13198.
21. Turan S, Kuehle J, Schambach A, Baum C, Bode J. Multiplexing RMCE: versatile extensions of the Flp-recombinase-mediated cassette-exchange technology. *J Mol Biol.* 2010;402(1):52-69.
22. Yizhar O, Fenno LE, Davidson TJ, Mogri M, Deisseroth K. Optogenetics in neural systems. *Neuron.* 2011;71(1):9-34.
23. Fenno LE, Mattis J, Ramakrishnan C, et al. Targeting cells with single vectors using multiple-feature Boolean logic. *Nat Methods.* 2014;11(7):763-772.
24. Sutton AK, Myers MG, Jr., Olson DP. The Role of PVH Circuits in Leptin Action and Energy Balance. *Annu Rev Physiol.* 2016;78:207-221.
25. Boudaba C, Schrader LA, Tasker JG. Physiological evidence for local excitatory synaptic circuits in the rat hypothalamus. *J Neurophysiol.* 1997;77(6):3396-3400.
26. Ziegler DR, Herman JP. Local integration of glutamate signaling in the hypothalamic paraventricular region: regulation of glucocorticoid stress responses. *Endocrinology.* 2000;141(12):4801-4804.
27. Li MM, Madara JC, Steger JS, et al. The Paraventricular Hypothalamus Regulates Satiety and Prevents Obesity via Two Genetically Distinct Circuits. *Neuron.* 2019;102(3):653-667 e656.
28. Sadagurski M, Dong XC, Myers MG, Jr., White MF. Irs2 and Irs4 synergize in non-LepRb neurons to control energy balance and glucose homeostasis. *Mol Metab.* 2014;3(1):55-63.
29. Lutz TA, Tschudy S, Rushing PA, Scharrer E. Amylin receptors mediate the anorectic action of salmon calcitonin (sCT). *Peptides.* 2000;21(2):233-238.
30. Chait A, Suaudeau C, De Beaurepaire R. Extensive brain mapping of calcitonin-induced anorexia. *Brain Res Bull.* 1995;36(5):467-472.
31. Xi D, Gandhi N, Lai M, Kublaoui BM. Ablation of Sim1 neurons causes obesity through hyperphagia and reduced energy expenditure. *PLoS One.* 2012;7(4):e36453.
32. Balthasar N, Dalgaard LT, Lee CE, et al. Divergence of melanocortin pathways in the control of food intake and energy expenditure. *Cell.* 2005;123(3):493-505.
33. Cheng W, Gonzalez I, Pan W, et al. Calcitonin Receptor Neurons in the Mouse Nucleus Tractus Solitarius Control Energy Balance via the Non-aversive Suppression of Feeding. *Cell Metab.* 2020;31(2):301-312 e305.

34. Smith SM, Vale WW. The role of the hypothalamic-pituitary-adrenal axis in neuroendocrine responses to stress. *Dialogues Clin Neurosci.* 2006;8(4):383-395.

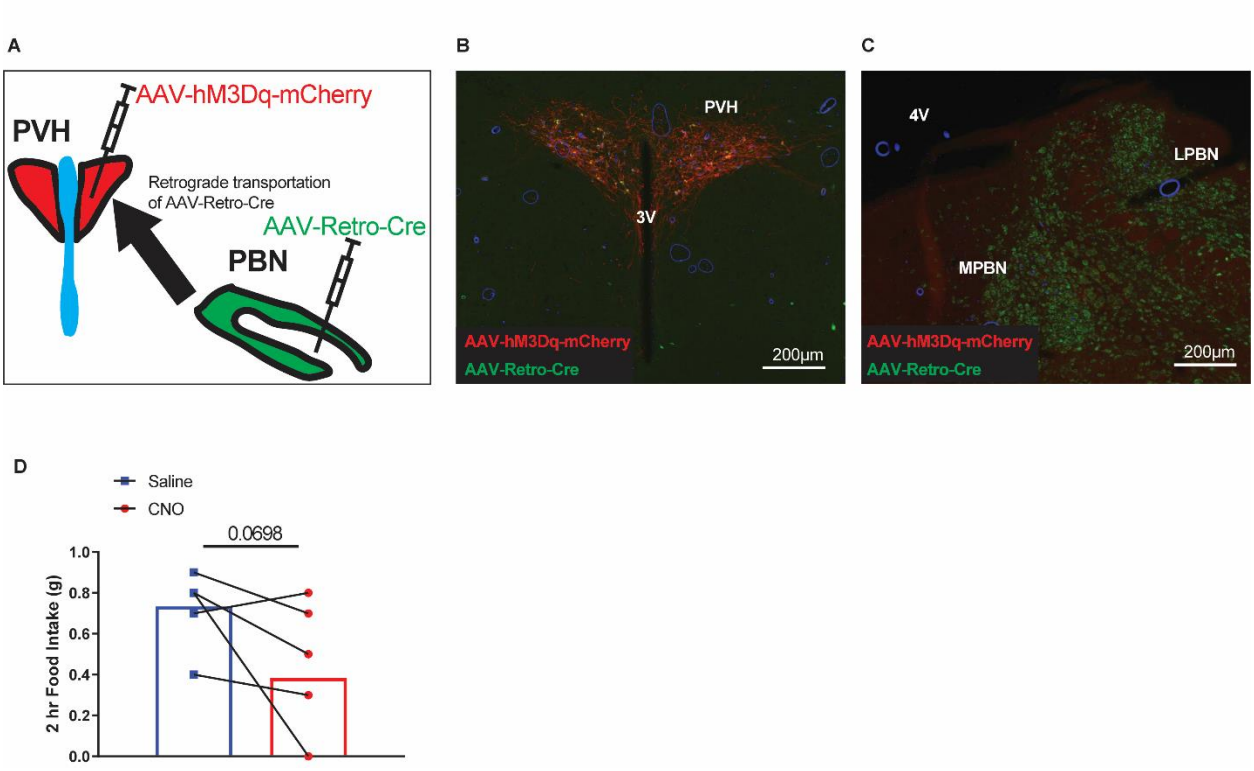

Figure 5.1: Effect of acute activation of PVH>PBN neurons using DREADDs on food intake. A) Diagram depicting simultaneous injection of AAV-Retro-Cre into the PBN and AAV-hM3Dq-mCherry into the PVH of mice expressing a Cre dependent GFP. The AAV-Retro-Cre was taken up by the PVH axons that project to the PBN. IHC was used to detect expression of AAV-hM3Dq-mCherry bilaterally injected into the PVH (B) and AAV-Retro-Cre bilaterally injected bilaterally into the PBN (C) of mice. D) Two-hour food intake following i.p. injection of CNO (0.3 mg/kg) at start of the dark cycle. Average values ± SEM are shown. P values for feeding behavior (N=6) was determined by a paired-t-test. PVH=paraventricular nucleus of the hypothalamus, 3V=third ventricle, LPBN=lateral parabrachial nucleus, MPBN=medial parabrachial nucleus, 4V=fourth ventricle.

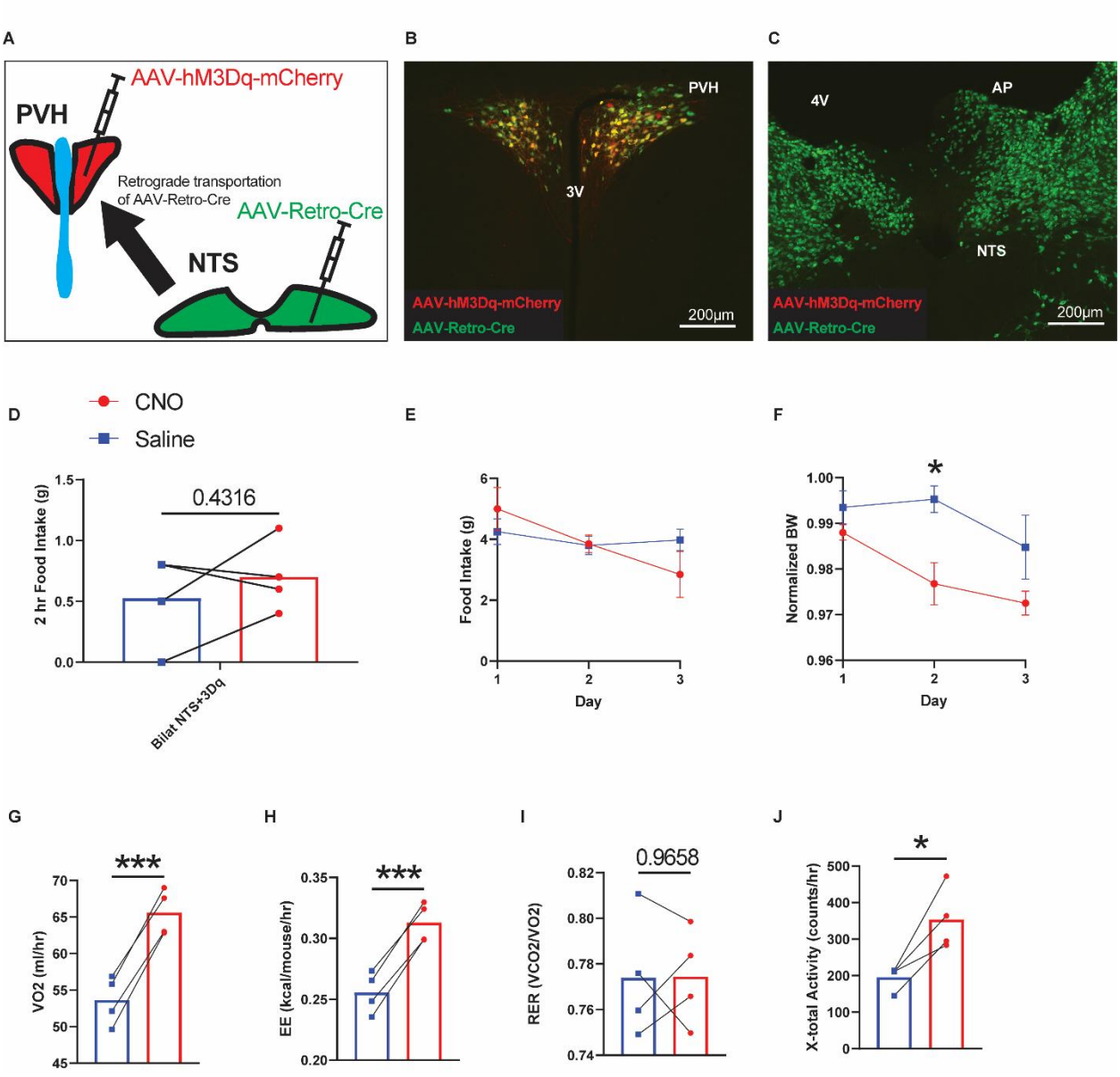

Figure 5.2: Effect of acute activation of PVH>NTS neurons using DREADDs on food intake and energy expenditure. A) Diagram depicting simultaneous injection of AAV-Retro-Cre into the NTS and AAV-hM3Dq-mCherry into the PVH of mice expressing a Cre dependent GFP. The AAV-Retro-Cre was taken up by the PVH axons that project to the NTS. IHC was used to detect expression of AAV-hM3Dq-mCherry bilaterally injected into the PVH (B) and AAV-Retro-Cre bilaterally injected into the NTS

(C) of mice. D) Two-hour food intake following i.p. injection of CNO (0.3 mg/kg) at start of the dark cycle. Long-term feeding (E) and body weight (F) experiments in which CNO was injected twice daily for three days. CLAMS measurements of VO_2 consumption (G), energy expenditure (H), the respiratory exchange ratio (I) and total X-activity (J) 4 hours following DREADD-mediated activation of PVH>NTS neurons. Average values ± SEM are shown. P values for feeding behavior and CLAMS measurements (N=4) were determined by a paired-t-test; P values for long-term feeding and body weight experiments (N=4) were determined using a 2-way ANOVA followed by Tukey's multiple comparisons test. *p<0.05, ***p<0.001, PVH=paraventricular nucleus of the hypothalamus, 3V=third ventricle, NTS=solitary nucleus, AP=area postrema, 4V=fourth ventricle.

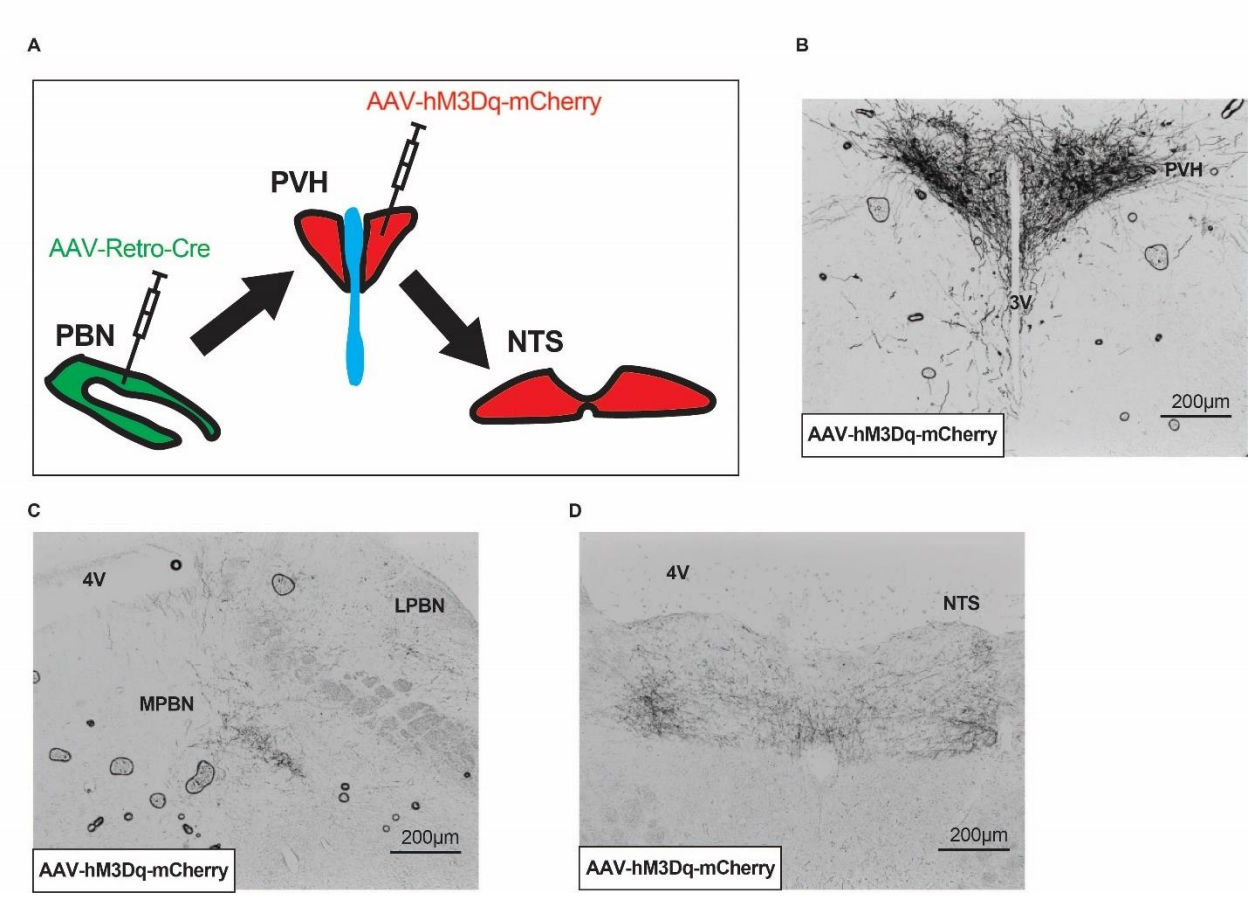

Figure 5.3: A subset of PVH>PBN neurons also project to the NTS. A) Diagram depicting simultaneous injection of AAV-Retro-Cre into the PBN and AAV-hM3Dq-mCherry into the PVH of mice expressing a Cre dependent GFP. The AAV-Retro-Cre was taken up by the PVH axons that project to the PBN and hM3Dq-mCherry expression was induced in the PVH. hM3Dq-mCherry terminals were found in both the PBN and NTS. DAB immunohistochemistry staining was used to detect expression of AAV-hM3Dq-mCherry in the bilaterally injected PVH (B) and hM3Dq-mCherry terminals were detected in the PBN (C) and NTS (D).